THE COMPLEXATION CHEMISTRY OF DISSOLVED MANGANESE(III) IN THE OCEAN AND ITS ROLE IN THE COUPLED CYCLES OF CARBON, IRON AND SULFUR

by

Véronique E. Oldham

A dissertation submitted to the Faculty of the University of Delaware in partial fulfillment of the requirements for the degree of Doctor of Philosophy in Oceanography

Spring 2017

THE COMPLEXATION CHEMISTRY OF DISSOLVED MANGANESE(III) IN THE OCEAN AND ITS ROLE IN THE COUPLED CYCLES OF CARBON, IRON AND SULFUR

by

Véronique E. Oldham

Approved: _____
Mark A. Moline, Ph.D.
Director of School of Marine Science and Policy

Approved: _____
Mohsen Badiey, Ph.D.
Acting Dean of the College of Earth, Ocean, and Environment

Approved: _____
Ann L. Ardis, Ph.D.
Senior Vice Provost for Graduate and Professional Education

I certify that I have read this dissertation and that in my opinion it meets the academic and professional standard required by the University as a dissertation for the degree of Doctor of Philosophy.

Signed: _____

George W. Luther III, Ph.D.
Professor in charge of dissertation

I certify that I have read this dissertation and that in my opinion it meets the academic and professional standard required by the University as a dissertation for the degree of Doctor of Philosophy.

Signed: _____

Bradley M. Tebo, Ph.D.
Member of dissertation committee

I certify that I have read this dissertation and that in my opinion it meets the academic and professional standard required by the University as a dissertation for the degree of Doctor of Philosophy.

Signed: _____

Katharina Billups, Ph.D.
Member of dissertation committee

I certify that I have read this dissertation and that in my opinion it meets the academic and professional standard required by the University as a dissertation for the degree of Doctor of Philosophy.

Signed: _____

Thomas E. Hanson, Ph.D.
Member of dissertation committee

ACKNOWLEDGMENTS

I would like to first thank George Luther for his unwavering support of my growth as both a researcher and person. You were there whenever I needed you, unconditionally, with insight and for discussion. Thank you for all your guidance and for the independence to pursue research I truly found rewarding. You have been a constant inspiration for me to work diligently and with purpose. I will be forever grateful for the many experiences you have guided me through; from well-organized and fascinating research cruises, to workshops and conferences across the country. You went above and beyond to make sure I received a complete experience as a graduate student and researcher.

Thanks also to my committee for helpful discussions and feedback throughout the course of my dissertation. Dr. Tebo, you opened my mind to a different perspective on Mn chemistry, especially in light of the organisms that alter Mn chemistry. Our times together in the lab on cruises are some of my most treasured memories from this project. Dr. Billups, thank you for helping me with personal growth and writing, your thoughtful discussions have helped guide me beyond my dissertation project. Dr. Hanson, thank you for your enthusiasm and your insight into the world of microbiology, an area that was previously foreign to me.

Collaborating with Dr. Alfonso Mucci for cruises in the St. Lawrence Estuary, was a highlight of my time working on this project. Your organization, enthusiasm and vast knowledge were instrumental to understanding the importance of this work in the St. Lawrence.

Thanks to my lab members for their advice and collaborative work: Dan MacDonald, Matt Siebecker and Alyssa Findlay. I also want to thank the many summer interns who assisted me with my research: Shannon Owings, Gabriel Browning, Laramie Jensen, Megan Miller, Kristen Burk, Chris Chambers and Nicole Coffey. Your help, collecting and analyzing samples from the Broadkill River and Chesapeake Bay, was integral to the success of this project. Thank you to Dr. Matthew R. Jones and Dr. Mitch Wright from the Tebo lab, who conducted most of the solid phase Mn assays, and whose company was always a pleasure on research cruises.

Thank you also to the CEOE community: my friends come and gone, Connie Edwards, Carol Kitchen, Luci Coumatos, Lisa Dorey, Joe Schudlark, and Marcia Pettay. Special thanks to Janis Lopez for the countless discussions and sage advice, as well as Mark Moline for his professional support and conversations.

I would also like to thank my faraway friends and family from Canada and beyond, who have kept me going and have been wonderful sources of positivity and encouragement. Robin, thank you for your words of advice, your friendship kept me sane. A huge thank you to my parents, Mike and Mireille Oldham, and my brother Robi, for your continued support in everything I do. Your unwavering enthusiasm for my work has been a constant motivation. Finally, Andrew: thank you for being loving, positive, calm, and especially for always being able to make me laugh.

This work was supported by grants from the Chemical Oceanography program of the National Science Foundation (OCE-1558738 and OCE-1155385 to GWL; OCE-1558692 and OCE-1154307 to BMT). Thanks to the University of Delaware for receipt of a Marian R. Okie Fellowship, University of Delaware Graduate Fellowship, and University of Delaware Dissertation Fellowship.

TABLE OF CONTENTS

LIST OF TABLES

LIST OF FIGURES

ABSTRACT

Manganese (Mn) speciation is dominated by dissolved Mn(II), Mn(III) and solid Mn(III/IV) oxides in seawater. Soluble Mn (dMn_T) speciation has been re-evaluated in the last decade to include Mn(III)-L in low O_2 environments. The same ligands that bind iron(III) [Fe(III)] can also bind Mn(III). Therefore, in the marine environment, Mn(III) may have a profound impact on the bioavailability of dissolved Fe, which often requires organic complexation for uptake. In oxic waters, dMn_T speciation is still thought to be dominated by dMn(II), and the presence of Mn(III)-L has not yet been assessed in oxic environments because of current detection limits for dMn speciation (50 nM).

Speciation assays were performed in contrasting redox environments: the Chesapeake Bay (seasonally anoxic bottom waters), the St. Lawrence Estuary (SLE) (air saturated O_2 in surface waters, decreasing to 55 μM at the sediment-water interface), and a coastal waterway in Delaware, bordered by wetlands (air saturated O_2 in surface waters). These systems provide unique O_2 gradients to examine Mn biogeochemistry and its role in the cycles of C, Fe and S. I show that Mn(III)-L complexes are ubiquitous in the oxic marine environment (up to 99.9% of dMn_T), much like their Fe(III)-L analogs, which dominate dFe speciation. I measured dMn

speciation and Mn(III)-L conditional stability constants (K_{cond}), by competition with an added porphyrin ligand, where weak complexes are outcompeted by the added porphyrin ($logK_{cond}$<13.2) and strong complexes require reduction before detection ($logK_{cond}$>13.2).

In the Chesapeake Bay, I show that strong Mn(III)-L complexes make up to 80% of dMn_T in areas of low/no oxygen, and in the presence of equimolar concentrations of a reducing agent, H_2S. The reductive dissolution of MnO_x produces Mn(III)-L in this system, and chemical reduction (by HS^-) or ligand-promoted reduction may be responsible. In low O_2 regimes, the stabilization of dMn(III) is favorable, thus, the increase in oxygen minimum zones due to changing climate regimes could lead to greater stabilization, cycling and transport of Mn(III)-L. I show that the suboxic portion of the water column in the Chesapeake Bay is an intense zone of Mn cycling, where Mn oxides can form at non-detectable dissolved O_2 concentrations, and where Mn oxidizers and reducers may coexist.

I found that Mn(III)-L complexes made up to 99.9% of dMn_T in the surface waters of the Broadkill River, DE and up to 86% in the SLE, indicating, for the first time, that Mn(III)-L complexes are also stable in oxygenated waters. In the SLE, dMn fluxed out of the sediments as dMn(II) (0.43 mmol m^{-2} day^{-1}) and oxidation processes dominate Mn(III)-L production in the water column. The vertical profile of dMn_T was 20-80% higher in the lower SLE than in 1974, corresponding to lower dO_2 in the system. Here, dMn_T was much higher in bottom waters (~2 µM), with Mn(III)-L stabilized 50 m above the sediment water interface (200 nM, 60% of dMn_T). However,

in the nearby Saguenay fjord, Mn(III)-L was not only entering via sediment flux and subsequent stabilization by ligands, but also through surface waters (60 nM Mn(III)-L, 65 % of dMn_T), indicating that terrestrial ligands stabilize Mn(III).

Terrestrial-type ligands were also found to stabilize Mn(III)-L in the surface samples of dMn along a salinity gradient in the Broadkill River, a coastal waterway bordered by salt marshes. Here, high Mn(III)-L corresponded to high humic material, as indicated by characteristic UV absorption peaks. Additionally, an assay of ligand character was made after precipitating humic matter, and confirmed that Mn(III)-L complexes had ligands of humic character. Thus, humic material serves to bind Mn(III), which transports both Mn(III) and organic matter to the coastal ocean, indicating that *estuarine export, rather than removal* may be dominating these types of systems.

Chapter 1

AN INTRODUCTION TO MANGANESE SPECIATION AND CYCLING

1.1 Introduction

Manganese (Mn) is an essential trace nutrient in the environment, and its many oxidation states allow it to partake in a host of reactions and processes. Manganese is ubiquitous in the global ocean, and exists in three oxidation states: Mn(II), Mn(III) and Mn(IV). In marine environments, Mn plays a role in diverse metallo-enzymes - most notably as the redox active center of photosystem II for photosynthetic organisms. Mn also plays a role in the bacterial decomposition of organic matter (Froelich et al, 1979); solid Mn(III/IV) oxides are important scavengers in seawater (Goldberg et al, 1954); and finally, Mn(III/IV) oxides are some of the strongest natural oxidants in the ocean (Tebo et al, 2004). Because of its many natural oxidation states, Mn participates in a wide range of redox reactions with inorganic and organic chemical species (Stumm and Morgan, 1996). The reactivity and speciation of Mn is pH and Eh dependent, thus are variable in differing oceanic environments (Stumm and Morgan, 1996), particularly along different oxygen gradients.

The aim of this research is to elucidate the processes underlying the biogeochemical cycling of and speciation of Mn in seawater, and to shed light on the impact of Mn speciation on coupled elemental cycles - notably: iron (Fe), carbon (C) and sulfur (S). In the research discussed herein, I will present my findings surrounding the chemical speciation of Mn in three systems with different oxygen regimes and

describe the chemical reactions surrounding the formation of soluble Mn(III)-L complexes.

The chemical speciation of an element refers to its binding and oxidation state. Broadly, for metals in the water column, chemical speciation can be operationally defined by filtration (e.g. Schlosser et al, 2013): soluble (< 20 nm), colloidal (between 20 nm and 200 nm) and insoluble species (>200 nm). Soluble species include free hydrated species, or hexa-aquo complexes ($M^{n+}\cdot 6H_2O$); inorganic complexes (i.e. metal hydroxides, carbonates, silicates and chlorides); and organically (L) complexed species (M^{n+}-L). Trace metals in these forms exist in a variety of oxidations states in seawater, and many metals, like Fe(III), have been found to be largely complexed to organic ligands (Stumm and Morgan, 1996). The speciation of these metals plays an important role in metal kinetic lability, reactivity, solubility, and hence, bioavailability. For metals that exist in multiple oxidation states in seawater, redox transformations are important for biological availability (especially for Fe, Cu, Mn and Co) because redox state will affect solubility, ligand-exchange kinetics and acid-base chemistry. For example, arguably the most important biologically relevant metal in seawater, Fe, is largely found complexed to organic ligands as Fe(III), but it can be photochemically reduced to Fe(II), which has fast ligand-exchange kinetics, and is more biologically available than Fe(III). The Fe(II) is rapidly reoxidized to Fe(III) and the cycling between the two states increases the biological availability of Fe (Anderson and Morel, 1982). Until the last decade, it was thought that soluble Mn was predominantly found as free-hydrated Mn(II) in seawater. However, Mn(III)-L complexes have been found to make up a major, if not the major, component of soluble Mn species in low oxygen environments (Trouwborst et al, 2006; Yakushev et al, 2007, 2009; Madison et al, 2011, 2013;

Dellwig et al, 2012; Oldham et al, 2015). Because Mn(III)-L complexes can donate or accept electrons, their presence in the water column is critical when determining organic carbon budgets, oxidation capacity, and reducing capacity of a system. Additionally, Mn(III) can bind to the same ligands as Fe(III) (Duckworth and Sposito, 2005, 2007; Parker et al., 2007; Luther et al., 2015), and thus, the presence of Mn(III) could disrupt Fe uptake in regions where Fe uptake is facilitated by binding to organic ligands.

1.1.1 Manganese in Seawater

To my knowledge, there is currently no global oceanic model for manganese (Mn) redox cycling. This is likely because Mn concentrations, speciation, and fluxes have not yet been determined for all of the oceanic basins with a high degree of certainty, and many *processes* underlying the role of Mn in seawater are not well described. This is in part because low-level detection of Mn speciation is notoriously difficult due to low open ocean soluble Mn concentrations, ranging from 0.1 nM to 3 nM (Landing and Bruland, 1987; Martin and Gordon, 1988). In addition, Mn has many different chemical species in seawater, many of which are not well defined. As such, studies often report only total dissolved Mn, which is not sufficient to accurately describe its role in biogeochemical cycling.

The primary **sources** of Mn to the ocean are fluvial input, atmospheric input (primarily crustal, anthropogenic sources are not as significant), and input from hydrothermal vents (Chester and Jickells, 2012). The main Mn **sinks** in the ocean occur via adsorption of Mn to sinking particles, where Mn is deposited to estuarine, coastal shelf or deep ocean sediments (Chester and Jickells, 2012). Finally, the main **processes** to consider are redox cycling, sediment diagenesis, uptake by biomass, remineralization,

scavenging, deep ocean mixing by advection/diffusion, and lateral fluxes (i.e. along a salinity or oxygen gradient). Mn speciation is sensitive to changes in O_2 concentrations, so changes in an oceanic basin with a transition from oxic to anoxic waters will have different Mn chemistry than a fully oxygenated water column.

The main processes that govern the redox cycling of Mn, in *an oceanic basin with a vertical transition from oxic to anoxic conditions*, are (1) the oxidation of reduced forms when they are resupplied to the upper water column, and (2) the dissolution of the oxidized forms of Mn in suboxic and anoxic waters. These two processes are described in detail in the sections 1.1.3 and 1.1.4, respectively.

The vertical structure of Mn speciation in a typical *oxygenated oceanic water column profile* has different features, with high concentrations of dissolved Mn in surface waters due to photochemical dissolution of Mn oxides (described in section 1.1.4), and higher Mn oxide concentrations below the photic zone. Regions of the ocean with mid-water oxygen minimum zones (OMZs) may also experience dissolution of Mn oxides and a mid-depth soluble Mn maximum (Landing and Bruland, 1987). The vertical structure of the Mn profile is thought to be largely controlled by oxygen availability. This can be seen in particular in sediment pore waters where the oxidation of organic matter is governed by available electron acceptors which change with depth, usually in the order O_2>NO_3~MnO_x>Fe (hydr)oxides>SO_4>CH_4 (Froelich et al, 1979).

The extent of Mn release from *sediment diagenesis* is then also governed by oxygen concentration. Sundby and Silverberg (1985) observed the release of Mn from sediments in a benthic flux-chamber experiment when the oxygen concentration of the water decreased, but no release when the oxygen concentration was constant. Thus, the release of Mn(II) from oceanic sediments is variable; higher in anoxic conditions and

lower in oxic sediments. Despite this seemingly high rate of release of Mn from sediments, Sundby and Silverberg (1985) found that, in the Laurentian shelf sediments, most of the dissolved Mn produced by sediment diagenesis did not escape but rather re-precipitated (71-87%). They also found that increased rates of biological mixing corresponded to increased rates of Mn release, so perhaps more shallow oxic sediments with bioturbation could see a higher Mn release due to mixing. However, I predict that precipitation of Mn will dominate in most coastal sediments, resulting in a net loss of Mn as it gets transported from the coast to the open ocean. This prediction fits with what is observed for shelf versus ocean concentrations. Shiller (1997) compiled 494 data points to construct a surface map of Mn concentrations in the Atlantic Ocean and found that in coastal surface waters, the concentration of dissolved Mn ranged from 5-25 nM, versus the open ocean, which was below 5 nM.

1.1.2 The Contrasting Biogeochemistry of Fe and Mn

Periodic table neighbors Mn and Fe can partake in similar chemical reactions in seawater (i.e. Formation of metal oxides, complexation to organic matter), however, their different fluxes and reactivity change how they are used in the environment, and likely shaped how the ocean evolved to be the way it is today. The vertical profiles of dMn and dFe are fairly different. Dissolved Fe follows a much more traditional nutrient-like profile with depletion at the surface, a subsurface maximum and gradual decrease towards the bottom (e.g. Rue and Bruland, 1995). In contrast, dissolved Mn follows a more scavenged-type profile. Soluble Mn is enriched at the surface, with a subsurface minimum, and in some places another smaller maximum in low oxygen environments, decreasing towards the bottom (Landing and Bruland, 1980).

In a fully oxygenated environment, at seawater pH (~8), Mn should exist predominantly in the form of Mn(IV) as solid Mn oxides. The Mn(IV) oxides [and mixed valence Mn(III/IV) oxides] in seawater have crystal structure featuring large gaps, capable of containing many other cations within their crystal lattices. These oxides also have high surface areas with negative charges, contributing to their high adsorption capacity. However, surface ocean contains Mn(II) as high as 25 nM, and a portion of this is the result of aeolian dust deposition which contains Mn in the +2 oxidation state (Guieu et al, 1994). However, a more important process that maintains Mn(II) in the upper water column is the photoreduction of Mn oxides (Sunda et al, 1983). In contrast, the thermally stable oxidation state of Fe is Fe(III), which is relatively insoluble in seawater and precipitates rapidly, limiting its concentration in seawater (Rose and Waite, 2002). The high atmospheric deposition of Fe helps to maintain its concentration in surface seawater, but dissolved Fe is still depleted in the surface due to biological uptake.

Although the crustal abundance of Fe is greater than that of Mn, the abiotic oxidation of Fe proceeds more rapidly than that of Mn (Grassian et al, 2005). Thus, Fe is lost more rapidly than Mn during riverine transport, with 50-95% of riverine Fe deposited to the sediments, and only a small fraction of the dissolved Fe actually transported from the coast to the global ocean (Boyle et al., 1977; Sholkovitz et al., 1978). Most riverine Fe is in small colloids (20 – 200 nm), which flocculate and are removed (Sholkovitz, 1976). In contrast, only 25-45 % of Mn is deposited (Sholkovitz et al, 1978), indicating that Mn is more labile during estuarine mixing.

Aside from riverine inputs, the primary inputs of Mn and Fe are atmospheric deposition, ice input, and hydrothermal input. For these three sources, the input of iron is more significant than Mn, due to greater crustal abundance of Fe relative to Mn.

The primary removal mechanism of both Mn and Fe is particulate scavenging. Landing and Bruland (1987) compared the residence times of Mn and Fe particles, and found that they were shorter for Fe, which results in greater export of Fe. Sediment diagenesis is more significant for Mn than for Fe because Mn oxides are preferred as electron acceptors to Fe(hydr)oxides, and so would be reduced and released to the water column higher in the sediments than Fehydr(oxides) (Madison et al., 2013).

Manganese requirement is second only to Fe for marine phytoplankton. Sunda and Hunstman (1996) conducted experiments to show that it was possible to limit the growth of marine organisms, by lowering the concentration of Mn(II) in the medium of marine diatom *Thalassiosira pseudonana*. However, the conditions from their experiment do not represent oceanic concentrations of dissolved Mn. Compared to other trace elements, dissolved Mn concentrations are high in surface waters, largely due to the photoreduction of Mn oxides (Sunda et al, 1983; Millero, 1996). As such, the concentration of dissolved Mn in seawater is in excess of its biological requirement. Perhaps as a result, the affinity for Mn is low in most phytoplankton (Sunda and Hunstman, 1998); that is, it is so readily available that the uptake system is less specialized than other uptake systems for other elements like Fe, zinc (Zn) or copper (Cu). Sunda and Hunstman (1998) showed that high levels of Cu(II) and Zn(II) inhibited the uptake of Mn(II) in the coastal green alga *Chlamydomonas sp.* by blocking the Mn(II) binding site, indicating that these metals had a higher affinity for the non-specific uptake system of Mn(II). Therefore, in some areas of the ocean, Mn limitation

is possible but unlikely. Such areas could include anthropogenically-polluted areas such as estuaries, harbors, and areas where industrial runoff is high, and metal pollution is significant. Cu and Zn concentrations are often high in harbors as a result of their use in anti-fouling boat paint. In contrast, natural input of Mn exceeds anthropogenic input (Chester and Jickells, 2012), and so in heavily polluted environments, it is possible that metals like Cu and Zn could effectively outcompete Mn for uptake by marine organisms.

In contrast to Mn, Fe is a limiting nutrient in many environments. In situations where iron is limited, like the Southern Ocean, some phytoplankton have adapted strategies to uptake iron and to reduce cellular iron requirements (Strzepek et al, 2011). Most dissolved Fe in the ocean is up to 99.9% complexed to organic ligands in seawater, as Fe(III)-L (Rue and Bruland, 1995; Witter and Luther, 1998) and some microorganisms have been shown to use Fe(III)-L by reducing Fe(III) bound to organic ligands on their cell surface with a ferric reductase enzyme (Maldonato and Price, 2000; 2001). Because very few Fe(III)-binding ligands have been characterized in the marine environment, it is difficult to assess the importance of *in situ* ligand production in facilitating Fe(III) uptake, but siderophores have been produced by marine bacteria under laboratory conditions where soluble Fe was limited (Haygood et al, 1993). Another mechanism by which some organisms have adapted to Fe limitation is by metal replacement. For example, in Fe limited environments, some diatoms have been observed to use Mn instead of Fe (Peers and Price, 2004). The main difference in the bioavailability of Mn compared to that of Fe is due to their different distributions and chemical speciation in seawater. In particular, the relative abundance of Mn(III) relative to Fe(III) is important for understanding the potential for Mn(III) to inhibit Fe(III)

bioavailability. In order to better understand this potential competition, the formation mechanisms of Mn(III)-L complexes need to be examined. These formation mechanisms have not previously been reviewed or studied concurrently, and therefore in sections 1.1.3 and 1.1.4, I will provide a review of potential oxidative and reductive formation pathways for Mn(III)-L complexes in seawater.

1.1.3 Formation Pathways of Mn(III)-L: Oxidation of Mn(II)

The oxidative pathways of Mn(III)-L formation are summarized in Table 1.1, and the mechanisms for each pathway are briefly described herein. These are discussed in more detail in Chapters 2-5 of this dissertation. Not listed is the abiotic oxidation of Mn(II) to Mn(IV)O_2. At seawater pH, the oxidation of Mn(II) to MnO_x by O_2 has been shown to be orders of magnitude slower in the laboratory than in the environment (Morgan, 1967; Emerson et al, 1982; Tebo, 1991). Thus, catalytic processes in the environment must dominate the oxidation of Mn(II).

Table 1.1 Oxidative formation pathways for Mn(III)-L, given as unbalanced reactions.

Pathway	Unbalanced reaction
1. Surface catalyzed oxidation	$Mn(II) + \text{surface} + O_2 \xrightarrow{L} Mn(III) - L$
2. Bacterial oxidation	$Mn(II) + O_2 + bacteria \xrightarrow{L} Mn(III) - L$
3. Superoxide-promoted oxidation	$Mn(II) + O_2^- + 2H^+ \xrightarrow{L} Mn(III) - L + H_2O_2$
4. Ligand-promoted oxidation	$Mn(II) + L_{ox} \rightarrow Mn(III) - L$

The surface-catalyzed oxidation of Mn(II) occurs on metal oxide surfaces (Table 1.1, **Pathway #1**), which are often terminated by hydroxyl (OH) groups that bind Mn(II). The following reactions describe this process and end in products like >Mn(IV)O_2 or >MnOOH where ">" denotes a surface:

$$> OH^+ + Mn^{2+} \xrightarrow{fast} > 0 - Mn^{2+} + H^+ \quad 1.1$$

$$> 0 - Mn^{2+} + O_2 \rightarrow > 0 - Mn^{2+} - O_2 \quad 1.2$$

$$> 0 - Mn^{2+} - O_2 \rightarrow > 0 - Mn^{3+} - O_2^- \quad 1.3$$

Upon adsorption of Mn(II), an inner sphere surface complex is formed and rapid oxidation can occur. The catalysis can occur autocalytically (e.g. Mn(II) on >MnOOH) or on foreign metal oxides (e.g. Mn(II) on FeOOH). The oxidation of Mn(II) by oxygen alone is symmetry forbidden at seawater pH because the donating molecular orbital of Mn(II) is a σ orbital, which does not favorably overlap with the π accepting orbital on O_2 (Luther, 2010). The hydroxyl site on a metal oxide surface replaces OH^- as a π donor ligand via surface complexation of the Mn(II) which allows for the electron transfer from Mn(II) to O_2.

Bacterial Mn(II) oxidation (Table 1.1, **Pathway #2**) is thought to be the predominant mechanism of oxidation in seawater as rates of Mn(II) oxidation by bacterial catalysis are reported as ~5 orders of magnitude higher than surface catalyzed reactions (Tebo et al, 2004). Some functions for Mn(II) oxidation have been proposed (reviewed by Tebo et al, 2004) and include that Mn oxidation may be energetically favorable, with energy conservation gained via the coupling of ATP synthesis to Mn(II) oxidation (Erlich and Salerno, 1990), or that the formation of Mn oxides facilitates the breakdown of complex organic matter (Sunda and Kieber, 1994). Webb et al (2005) showed that the enzymatic bacterial oxidation of Mn(II) resulted in an Mn(III)

intermediate, by trapping the intermediate with an addition of Mn(III)-binding ligand pyrophosphate (PP). Thus, microbial oxidation of Mn(II) may act as a source of Mn(III)-L to seawater. However, when the kinetics of the oxidation pathway for Mn(II) to MnO_x were examined, it was found that the Mn(II)→Mn(III) step was rate-limiting, 30 times slower than the electron transfer from Mn(III)→Mn(IV) (Webb et al, 2005). This result is not surprising given that the transfer from the d^5 ($t^2g^3eg^2$) molecular orbital configuration of Mn(II) to a d^4 ($t^2g^3eg^1$) configuration means going from a more stable to less stable state ($\Delta G° = 67$ kJ mol^{-1}, Webb et al, 2005) versus the d^4 to d^3 transition, which means going from a Jahn-Teller stabilized d^4 state to the very stable inert d^3 (t^2g^3) state ($\Delta G° = -134$ kJ mol^{-1}, Webb et al, 2005). Therefore, in the two-step oxidation pathway, the Mn(III)→MnO_2 reaction is more energetically favorable for the organism during Mn oxidation. Thus, if the Mn(II)→Mn(III) step is rate limiting, the presence of Mn(III) in seawater would be a useful electron donor for a Mn-oxidizing organism.

The third oxidation pathway of Mn(II) given in Table 1.1 is the oxidation of Mn(II) via reactive oxygen species (ROS). This pathway has been demonstrated in seawater, even at nanomolar concentrations of ROS (Hansard et al, 2011; Wuttig et al, 2013). The reaction of the ROS superoxide with Mn(II) produces Mn(III), and hydrogen peroxide:

$$Mn(II) + O_2^{\cdot -} + 2\,H^+ \rightarrow Mn(III) + H_2O_2 \qquad 1.4$$

The resulting Mn(III) may be reduced by the hydrogen peroxide to Mn(II), or it can be trapped as a Mn(III)-L species in the presence of an Mn(III)-binding ligand as the following Mn(III)-L formation pathway:

$$Mn(II) + O_2^- + 2H^+ + L \rightarrow Mn(III) - L + H_2O_2 \qquad 1.5$$

Learman et al (2013) examined the oxidation of Mn(II) via abiotically produced superoxide, and found that in the absence of an ambient ligand the Mn(III) produced via reaction 1.5 was reduced by hydrogen peroxide. However, in the presence of pyrophosphate or citrate (Mn(III)-binding ligands), Mn oxides (predominantly disordered colloidal hexagonal birnessite) were produced via formation of Mn(III)-L complexes, and some of these complexes were also stabilized in solution.

Another oxidation process that may be important for Mn is oxidation by ambient ligands (Table 1.1, **Pathway #4**). Of the oxidation pathways described thus far, oxidation by ambient ligands is the least well understood. The mechanism involves the oxidation of an ambient ligand, and subsequent oxidation of Mn(II) by the oxidized ligand.

$$L + oxidizer \rightarrow L_{ox} \quad 1.6$$

$$Mn(II) + L_{ox} \rightarrow Mn(III) - L \quad 1.7$$

Laboratory experiments indicate that ligand promoted oxidation of Mn(II) by the strong Mn(III)-binding ligand desferrioxamine-B (DFOB) is possible with O_2 as the oxidant (Duckworth and Sposito, 2005), but there are no direct studies of Mn(II) oxidation by natural organic matter. Ligand-promoted oxidation of Fe(II) by natural organic matter has been shown to enhance the oxidation of Fe(II) by nitrite under anoxic conditions (Kopf et al, 2013). Additionally, Rose and Waite (2002) compared the kinetics of Fe(II) oxidation in oxic waters, with and without natural organic matter, and found that the presence of Fe(III) binding ligands significantly increased the rate of Fe(II) oxidation by O_2, further suggesting that oxidation of reduced metals can be ligand-promoted.

1.1.4 Formation Pathways of Mn(III)-L: Reductive and Non-reductive MnO_x Dissolution

The discussion below reviews potential pathways of Mn(III)-L formation via the dissolution of Mn(III/IV) oxides. Table 1.2 provides a summary of these pathways, and their mechanisms are described in the section below.

Table 1.2 Reductive formation pathways for Mn(III)-L, given as unbalanced reactions. ">" denotes a surficial particle.

Pathway	Unbalanced reaction
1R. Photo-enhanced ligand-promoted reductive dissolution	$> Mn^{4+}O_x + L \xrightarrow{hv}$ new particle surface $+ Mn(III) - L$
2R. ROS-promoted reductive dissolution	$> Mn^{4+}O_x + O_2^- + L \rightarrow$ new particle surface $+ Mn(III) - L$ OR $> Mn^{4+}O_x + H_2O_2 + L \rightarrow$ new particle surface $+ Mn(III) - L$
3R. Ligand-promoted reductive dissolution	$> Mn^{4+}O_x + L \rightarrow$ new particle surface $+ Mn(III) - L$
4R. Chemical reductive dissolution where red=HS^-, Fe(II), or NO_2^-	$> Mn^{4+}O_x + \text{red} + L \rightarrow$ new particle surface $+ Mn(III) - L$
5R. Direct bacterially-catalyzed reductive dissolution	$> Mn^{4+}O_2 + L \xrightarrow{bacteria}$ new particle surface $+ Mn(III) - L$

Thermodynamics predict that Mn should exist in oxic waters as solid $Mn(IV)O_2$, however most surface waters also contain soluble Mn (Landing and Bruland, 1980). Unlike most transition metals, soluble Mn actually exhibits a surface maximum (Landing and Bruland, 1980), which corresponds to a MnO_x minimum, thereby suggesting that particulate scavenging rates must be low in these surface waters and/or that dissolution of MnO_x dominates in surface waters. The persistence of relatively high soluble Mn concentrations in surface seawater is partially due to slow abiotic Mn(II)

oxidation by O_2, but can be better explained by a number of inorganic and organic reductive processes, which can be both directly and indirectly microbially mediated. In surface waters, most of the soluble Mn is thought to persist due to photoassisted reductive dissolution of manganese(IV) oxide phases (Mn(IV)O_x + OM + photons) (e.g. Sunda et al, 1983) and light inhibition of microbial Mn(II) oxidation (Sunda and Huntsman, 1988).

The mechanism of Mn(IV) oxide photoreduction in seawater is not known, but may result from light-enhanced ligand-to-metal charge transfer between organic molecules and particulate Mn (Waite et al., 1988), as in the simplified, unbalanced reaction below, where ">" denotes a particle (Table 1.2, **Pathway #1R)**.

$$> Mn^{4+}O_2 + \mathrm{L} \rightarrow Mn^{2+} + L^{+} + H_2O \qquad 1.8$$

This reaction pathway involves intermediate reactions, including adsorption of the reductant to the Mn(IV) oxide surface, which would result in a precursor colloid-type complex, ligand to metal electron transfer within the complex, followed by breakdown of the complex through ligand substitution (with water) and release of the products. The product is written as Mn(II) in equation 1.8, but this same process could equally result in the formation of Mn(III)-L complexes via a similar mechanism, described in equations 1.9-1.11 below:

$$> Mn^{4+}O_2 + \mathrm{L} \xrightarrow{\text{adsorption}} > Mn^{4+} - \mathrm{L} + H_2O \qquad 1.9$$

$$> Mn^{4+} - \mathrm{L} + Mn^{4+}OH \xrightarrow{\text{electron transfer}} > Mn^{4+}\mathrm{O}Mn^{3+} - L^{+} + H^{+} \qquad 1.10$$

$$> Mn^{4+}\mathrm{O}Mn^{3+} - L^{+} + H^{+} \xrightarrow{\text{dissociation}} > Mn^{4+}\mathrm{OH} + Mn^{3+} - L^{+} \qquad 1.11$$

In the mechanism above, reaction 1.10 should be rate limiting, and will depend on the nature of the particulate surface. We expect that a particle defect in the Mn-oxide structure would result in favorable adsorption of a ligand. For example, an exposed

Mn(IV) atom, would readily accept electrons from a ligand, allowing reactions 1.10 and 1.11 to proceed. If the particle defect was an exposed Mn(III), this would proceed even more rapidly, and be considered *non-reductive* Mn oxide dissolution. The average oxidation state of Mn(III,IV) oxides in sediments overlain by oxic waters has been, with O/Mn ratios of 1.9 – 2.0 (Murray et al., 1985), indicating that most Mn in Mn oxide structures is in the form of Mn(IV), but Mn(III) is also expected because as Mn oxides age, more Mn(III) is formed within the lattice, leading to greater stability. Thus, we predict that reductive dissolution and non-reductive dissolution of Mn(III/IV) oxides via ligand-to-metal charge transfer are important processes in the formation of Mn(III)-L complexes, particularly in surface waters where this process is light enhanced (Sunda et al, 1983).

The sunlight-induced production of reducing reactive oxygen species (ROS) like superoxide (O_2^-) and hydrogen peroxide (H_2O_2) may also be an important mechanism in reducing Mn oxides (Table 1.2, **Pathway #2R**). Both of these ROS are major photochemical products in seawater with superoxide concentrations in sunlit waters of 10 nM (Petasne and Zika, 1987), and H_2O_2 persisting longer with concentrations of 10-200nM (Cooper et al., 1988). In Section 1.1.3, ROS were listed as potential Mn(II) oxidizers, but these can also act as reductants (Baral et al, 1985), and result in the formation of Mn(III)-L, as in Table 1.2. Thus, the cycling of Mn with ROS species superoxide and hydrogen peroxide is complex to track, and the formation of Mn(III)-L in this cycling is likely via both oxidative and reductive pathways.

The dissolution of MnO_x can also be achieved in the absence of photo-induced pathways. As in Section 1.1.3, superoxide species can be produced extracellularly, in the absence of light (Learman et al., 2013). Additionally, the dissolution of MnO_x by

ligand-promoted reductive dissolution can also be achieved in the absence of light (Table 1.2, **Pathway #3R**). Duckworth and Sposito (2007) examined the dissolution of three types of Mn oxides by siderophore desferrioxamine-B (DFOB) in freshwater: biogenic MnO_x, mixed valence (Mn(III)/Mn(IV)) oxides and δ-Mn(IV)O_2. They found that dissolution was faster for mixed valence and biogenic Mn oxides, and that at pH = 7 – 9, the product was Mn(III)-DFOB for all three Mn oxide types. They proposed that the formation of a surface complex catalyzes the reductive dissolution in all cases, followed by a rapid redox reaction and subsequent detachment of the surface complex – which they assume to be the rate limiting step. Thus, the reaction mechanism proceeds as in reactions 1.9 – 1.11. In this process, the electron-accepting ligand removes electron density between the metal atom and the oxygen atom in the mineral oxide lattice which decreases the energy barrier for the mineral dissolution (Stumm and Morgan, 1996).

The chemical reduction of MnO_x has also been documented in seawater, notably by strong reducing agents like sulfide (HS^-) and Fe(II) (Table 1.2, **Pathway #4R**). The disappearance of MnO_x at oxic-anoxic interfaces in the marine environment is well documented (Spencer and Brewer, 1971; Burdige and Nealson, 1986; Lewis and Landing, 1991; Canfield et al., 1993; Trouwborst et al., 2006; Yakushev et al., 2007, 2009; Dellwig et al., 2012; Oldham et al., 2015). Herzage and dos Santos Afonso (2003) showed that the dissolution of MnO_2 is surface controlled. Mn(III) is stabilized at the mineral surface during the reaction with sulfide, and thus in the presence of a strong organic ligand, Mn(III)-L could be released. Nico and Zasoski (2000) observed a decrease in Cr(III) oxidation by δ-MnO_2 in the presence of pyrophosphate, a Mn(III)-binding ligand, suggesting that Mn(III)-L complexation at mineral surfaces is occurring.

Thus, in environmental systems, MnO_x reduction by sulfide should lead to the formation of Mn(III)-L complexes if organic ligand concentrations are high enough to kinetically stabilize the Mn(III)-L complexes against further reduction by sulfide.

In addition to chemical reduction by sulfide in anoxic zones, the chemical reduction of MnO_2 by Fe(II) (Postma and Appelo, 2000; Siebecker et al., 2015), and nitrite (Luther and Popp, 2002) can also occur in aquatic systems. The resulting products are Fe(III) and NO_3^- respectively, with Mn(III) stabilized as a potential product in the presence of strong organic ligands. The kinetics of Fe(II) reduction are approximately one order of magnitude greater than those for sulfide, which are greater than an order of magnitude for nitrite [k_2= 4338 M^{-1} s^{-1} for Fe(II) (Siebecker et al., 2015); k_2 = 436 M^{-1} s^{-1} for sulfide (Yao and Millero, 1993); k_2 = 8.2 M^{-1} s^{-1} for nitrite (Luther and Popp, 2002)]. These reactions are particularly favorable at lower pH. Chemical reductants sulfide and nitrite are negatively charged ions, and at higher pH MnO_2 also becomes negatively charged, thus repulsion between the two species may kinetically hinder the reaction. Therefore, microbial reduction of MnO_x species may be more important than abiotic pathways at seawater pH (~8.0).

The microbial reduction of Mn oxides can be achieved *directly* by bacteria (Myers and Nealson, 1988; Lovley and Phillips, 1988) or *indirectly* by microbial metabolites like sulfide from sulfate-reducing bacteria in the *Desulfovibrio* group (Burdige and Nealson, 1986), with these reducing reactions coupled to metabolism in the oxidation of organic matter. Indirect reduction may be particularly important in suboxic zones, where sulfate reduction and bacterial denitrification/nitrate reduction occur, and where MnO_x could be an important electron acceptor in the absence of O_2. It has been suggested that at interfaces where O_2 and H_2S overlap, that most of the

Mn(IV) reduction is mediated indirectly via sulfate reducers (Nealson and Myers, 1992).

Direct catalysis (Table 1.2, **Pathway #5R**) has been documented for *Shewanella putrefaciens*, a facultative anaerobe and obligate respirer (Myers and Nealson, 1988), which can use Mn(IV), Fe(III), or O_2 as an electron acceptor for growth. This adaptation may be favorable in conditions where redox gradients shift with time, like seasonally stratified basins. Nealson and Myers (1992) suggest that Mn(IV)-reducing organisms are widespread and abundant, having isolated more than 200 strains of manganese reducers. In a study by Lin et al., (2012), the Mn(IV)→Mn(III) and Mn(III)→Mn(II) reduction steps by *Shewanella oneidensis* were examined. They showed that both reductive steps occurred on the cell surface, the first Mn(IV)→Mn(III) step required an initial solubilization, but only the second Mn(III)→Mn(II) step generated energy. If this is the case in many systems, then Mn(III)-L may be a preferable electron acceptor to MnO_2 because it may be easier to reduce Mn(III)-L complexes than to reductively dissolve MnO_2.

1.1.5 The Complexation Chemistry of Soluble Manganese

Dissolved trace metals in seawater have a strong bonding affinity for organic ligands in seawater, which are ubiquitous in marine environments. The composition of organic ligands in seawater is not well known, though they have been found to include degradation products of organic matter like humics and biogenically produced siderophores. Metals form complexes with natural organic ligands, which can stabilize metals in solution, and maintain certain oxidation states. As such, ligands can act to govern metal speciation. Where M denotes a metal and L an organic ligand, we find:

$$M + nL \rightarrow M(L)_n \qquad 1.12$$

As seawater is a highly electrolytic solution, corrections to stability constants, K, need to be made to account for the complexation of a metal to inorganic ligands like Cl^-, SO_4^{2-}, OH^-, carbonate species, etc., which can bind the metal in addition to an organic ligand. This inorganic complexation makes less free metal available for complexation, and their side reactions are grouped as a side reaction coefficient α_M'. The conditional stability constant (K_{cond}) can then be described, where the metal side reaction coefficient is known, $M' = \alpha_M'[M]_{free}$, but the side reaction coefficient is not known for L. In this work, I give K as a conditional constant, uncorrected for M and L side reactions, which can tell how strongly metal-ligand complexes are bound:

$$K^{cond}_{ML,\,M^{n+}} = \frac{[ML]}{[M]_{free}[L']} \qquad 1.13$$

Organic ligands in seawater are thus typically characterized by binding strength into two or more classes: the L_1 class corresponds to the strongest binding ligand class (high $K^{cond}_{ML,\,M^{n+}}$) then L_2, L_3, and so on to reflect correspondingly weaker binding ligands. Until recently, Mn(III)-L complexation was not considered because at high pH (>9), Mn(III) forms the solid manganite (MnOOH) (Murray et al., 1985) whereas in the absence of strong complexing agents, and at lower pH, free Mn^{3+} is unstable in seawater and rapidly disproportionates:

$$2Mn^{3+} + 2H_2O \rightarrow Mn^{2+} + MnO_2 + 4H^+ \qquad 1.14$$

However, because the donating and accepting orbitals of Mn(IV) and Mn(II) are spatially distinct, the reduction or oxidation between Mn(IV) and Mn(II) must be the result of one electron transfer processes, with Mn(III) acting as an intermediate (Luther, 2005). Therefore, Mn(III), though perhaps transient, can be isolated in solution and stabilized in the right conditions.

Based on the work presented in this dissertation, and in previous work in suboxic (Madison et al., 2011, 2013) and anoxic (Trouwborst et al., 2006; Yakushev, 2007, 2009; Dellwig et al., 2012) seawater systems, the stabilization of dissolved Mn(III) by ambient ligands in seawater is now thought to control the fractionation of dissolved Mn between Mn(II) and Mn(III). As Mn(III) has a higher electrostatic charge and smaller cationic radius than Mn(II), it is predicted to form more stable complexes with organic ligands. Because analogous dissolved Fe(III) in seawater is up to 99.9% complexed to strong binding ligands in seawater (van den Berg, 1995; Rue and Bruland, 1995, 1997; Wu and Luther, 1996), and Mn(III) binds to the same lifands as Fe(III), it is likely that the impact of Mn(III) complexation seawater has been underestimated.

1.2 Determination of Soluble Mn Speciation in Seawater

Historically, the speciation of soluble Mn has not been investigated, as Mn speciation was determined operationally by filtration, where soluble Mn passed through a 0.2 μm or 0.4 μm filter, and the filter retained insoluble Mn(III/IV) oxides. Soluble Mn determination was subsequently determined using ICP-MS, ammonium pyrrolidine extraction (e.g. Yeats et al, 1979) or the formaldoxime method (Spencer and Brewer, 1971). Trouwborst et al. (2006) developed a voltammetric method for soluble Mn detection, which led to the first measurements of Mn(III)-L in the environment, in the suboxic zones of the Black Sea and Chesapeake Bay. Subsequently, a few studies have measured soluble Mn(III)-L in the environment (Yakushev et al, 2007, 2009; Dellwig et al, 2011) including work from Madison et al. (2011, 2013), whose method using a soluble porphyrin addition to complex Mn is presented and updated in this dissertation. The use of this method to determine conditional stability constants is described in

section 1.2.1, below, and has been modified in this work for lower-level speciation, as described in section 1.2.2.

1.2.1 Soluble Mn Speciation and Determination of K_{cond} for Mn(III)-L_{weak}

Conditional stability constants and corresponding ligand classes have not been determined for natural Mn(III)-binding ligands in seawater - a major gap in our understanding of Mn cycling. A kinetic approach has been proven effective for assessing conditional stability constants other metals by Wu and Luther (1996) and Witter and Luther (1998) where the formation and dissociation constants (k_f and k_d) are used to describe K_{cond} (uncorrected for side reaction coefficients of M and L):

$$K_{cond}=k_f/k_d \quad 1.14$$

In the work of Madison et al., (2011; 2013), a weak ligand class was demonstrated by the kinetics of the reaction of the ambient ligands with the added porphyrin ligand α, β, γ, δ-tetrakis(4-carboxyphenyl)porphine (T(4-CP)P). In this method, seawater samples were filtered through a 0.2 µm filter, and the dissolved fraction analyzed by UV/Vis spectroscopy. The addition of soluble porphyrin, T(4-CP)P, rapidly complexes any dissolved Mn(II) in solution as Mn(II)-T(4-CP)P, and oxygen in solution rapidly oxidizes this to Mn(III)-T(4-CP)P, which has a sharp absorption peak at 468 nm. The reaction is allowed to proceed for 15 minutes and, for Mn(II), the curve generated shows an exponential rise to a maximum, with a single two-parameter solution:

$$y = a(1 - e^{-k_1 x}) \quad 1.15$$

Where "a" is the concentration of Mn(II) and k_1 is the rate constant for the Mn(II) growth curve. However, when Mn(III) is present and bound to weak ambient ligands, the rise to a maximum has a four-parameter solution:

$$y = a\left(1 - e^{k_1 x}\right) + b(1 - e^{k_2 x}) \quad 1.16$$

Where "b" is the concentration of Mn(III) and k_2 is the rate constant for the Mn(III) growth curve. In Madison et al (2013), the unknown ligands had slower kinetics than Mn(III) bound to pyrophosphate and faster kinetics than Mn(III) bound to desferrioxamine-B. The kinetic data from this study and additional laboratory experiments indicate that the conditional stability constants for Mn(III)-L are similar to or higher than those for Fe(III)-L complexes in organic matter decomposition zones (Luther et al, 2015), and thus Mn(III) may compete with Fe(III) for ambient ligands. The relevant chemical reactions for eqs. 1.15 and 1.16 are eqs. 1.17 and 1.18, respectively.

$$Mn^{2+} + T(4-CP)P \rightarrow Mn(II)T(4-CP)P + O_2 \xrightarrow{fast, k_1} Mn(III)T(4-CP)P \quad 1.17$$

$$Mn(III) - L + T(4-CP)P \overset{k_2}{\leftrightarrow} Mn(III)T(4-CP)P + L \quad 1.18$$

Reaction 1.17 proceeds rapidly to the right, and the Mn(III) ligand substitution reaction 1.18 proceeds more slowly. In the presence of strong ambient ligands, reaction 1.18 does not proceed forward. A strong reducing agent, H_2S or hydroxylamine, needs to be added to reduce any Mn(III)-L for the total dissolved Mn to be measured (Oldham et al, 2015). The concentration of Mn(III)-L can be calculated by subtracting the measured [Mn(II)] from this total. In this way, we can designate strong and weak binding ligands for dissolved Mn(III), by categorizing them as one of the following (illustrated in Figure 1.1):

(1) A sample with weak binding ligands will exhibit a rise to a maximum with a four-parameter solution (eqs. 1.15 and 1.37).

(2) A sample with no Mn(III) will show a simple two-parameter rise to a maximum with no increase in Mn detection upon addition of excess strong reducing agent (eqs. 1.14 and 1.16).

(3) A sample with strong binding ligands will show a simple two-parameter rise to a maximum, with an increase in Mn detection upon addition of excess strong reducing agent.

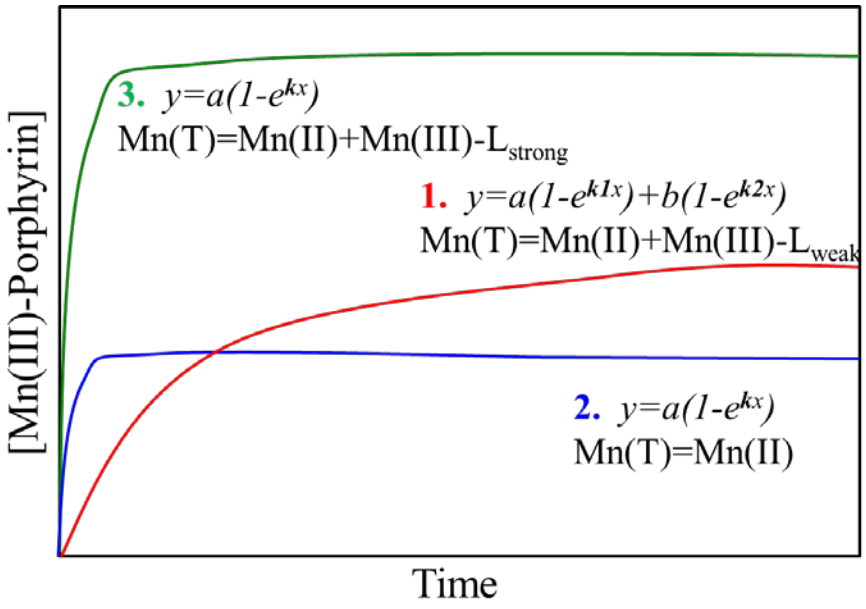

Figure 1.1 Schematic of three kinetic curves for each one of the three ligand scenarios outlined by the kinetics of the porphyrin complex formation with time, as would be seen on a UV/Vis spectrophotometer scan.

1.2.2 Low-Level Mn Speciation

Because the method described above is only suitable for concentrations above 50 nM, a modification is required to achieve lower level speciation. As detailed in Chapter 4, I have employed the spectrophotometric method previously optimized for the detection of total soluble Mn, with a detection limit of 50 nM (Madison et al., 2011), coupled with the addition of a strong reducing agent for Mn speciation, as described in section 1.2.1 to achieve a sample detection limit of 3 nM. The detection limit was lowered by increasing the pathlength cell length from 1 cm to 100 cm. Given the Beer-Lambert law (where A = absorbance, ε = molar absorptivity coefficient, b= pathlength and c = concentration):

$$A = \varepsilon bc \qquad 1.19$$

Thus, by increasing the cell length from 1 cm to 100 cm, the previous detection limit (Madison et al, 2011) is theoretically increased 100-fold. Since the absorbance is proportional to pathlength, for low levels of Mn, the reagents were diluted 100-fold to fit into the analytical window of detection. The rate of reaction is proportional to the concentration of reactants, and at these low levels, the reaction is slow. In this modified method, a 1 hour heating step, in a 90 °C bath, prior to analysis is employed to increase the reaction kinetics. Thus, the ability to kinetically assess Mn(III)-L_{weak} is lost and we can only speciate Mn(II) (and presumably some Mn(III)-L_{weak} reacted during the heating step) from Mn(III)-L_{strong} which are determined by the addition of an excess of a strong reducing agent, hydroxylamine. Samples are analyzed first without hydroxylamine, for dissolved Mn(II) and then with the addition of hydroxylamine for total Mn (Mn(II) + Mn(III)).

Figure 1.2 shows the results from a five-point calibration for the low-level Mn speciation method described above. Standards were measured in triplicate, and the

molar absorptivity calculated from the Beer-Lambert Law fell within one standard deviation of the known molar absorptivity (E= 95,4000 M^{-1} cm^{-1}) for all data points. I will detail the application of the low-level method in Chapters 3 and 4, along with details on the UV/Vis spectrophotometric setup.

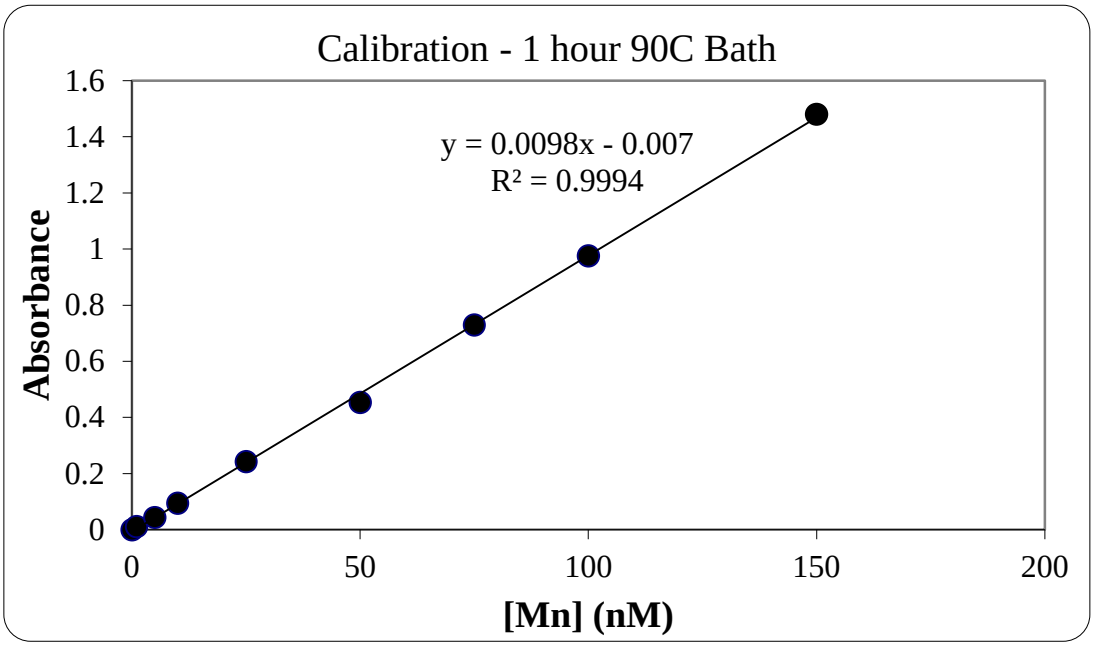

Figure 1.2 Linear regression from a 9 point calibration curve, and the resulting R^2 value.

1.3 Study Sites

Three study sites were selected for this study based on differing oxygen gradients. The Chesapeake Bay, which exhibits seasonal anoxia in its bottom waters; the St. Lawrence Estuary, where both a fjord and a hemipelagic site were studied; and

an oxygenated wetland river system, bordered by salt marshes, that empties into the Delaware Bay.

1.3.1 The Chesapeake Bay

The Chesapeake Bay is located on the mid-Atlantic coast of the United States, and is the largest estuary in the United States. Thus, it plays a significant role in the biogeochemical transformations of many nutrients at the interface of land and ocean. This site is characterized by high productivity, and seasonal oxygen depletion. The first reports of episodic oxygen depletion in the Chesapeake Bay were made in the 1930s (Newcombe and Horn, 1938), and the extent of this oxygen depletion has increased both spatially and temporally over the last several decades (Officer et al, 1984). The decrease in oxygen is predominantly the result of anthropogenic nutrient discharge within the watershed (Breitburg et al, 2001; Kemp et al, 2005; Kaushal et al, 2008). In the spring, riverine export of nutrient-rich freshwater is high, which stimulates phytoplankton productivity that subsequently sinks to deeper water and sustains oxygen-consuming metabolism. This is enhanced by the co-occurrence of increased stratification due to the influx of fresher water atop heavier saline water, leading to seasonal anoxia in bottom waters. Generally, the vertical salinity gradient is the dominating contribution to seasonal density stratification in the Chesapeake Bay (>90%, Goodrich et al, 1987), and once this stratification is set-up in the spring, the bottom water dissolved oxygen concentrations decline steadily as a result of nutrient enrichment. This large volume of anoxic water has important ecological implications, creating unsuitable habitat for many organisms, but also has many biogeochemical implications. Non-detectable oxygen levels in bottom waters allow for the release of reduced sulfur, which is a strong reducing agent, which can reduce many oxidized metal

species. Thus, seasonal anoxia results in a change of many biogeochemical cycles in a system.

Our study site was located in a 30 m depression on the eastern side and near the Chesapeake Bay Bridge. In the summer months, dissolved Mn concentrations can exceed 18 µM (Troubworst et al, 2006), thereby making it an ideal site for studying Mn cycling in changing oxygenic regimes. In anoxic waters, where chemical species that can accept or donate electrons are limited, the presence of Mn(III) would have important implications for other coupled redox reactions, like those with Fe, O, and S.

1.3.2 The St. Lawrence Estuary

The St. Lawrence Estuary is the largest estuary in the world, and the outlet of the Great Lakes to the Atlantic Ocean through the Cabot Strait and the Strait of Belle Isle. The Lower St. Lawrence Estuary (LSLE) is a long continuous trough over 300 m deep, extending 1250 km from the continental shelf. The circulation of the estuary is controlled by tides, exchange with the atmosphere, riverine inputs, seasonal ice cover and inflow from its bounding straits. In the summer months, the LSLE has a three-layered structure. Surface waters are fresher due to sea-ice melt and continental runoff, and this surface water flows towards the Atlantic. Below (30-150 m deep) is a permanent pycnocline of colder water known as the cold intermediate layer (CIL). Cold (-1.8 to 0ºC; Galbraith, 2006), saline Labrador shelf water currents flow into the estuary, resulting in the formation of the CIL. Below the CIL, waters are slightly warmer (2 to 6 ºC) and more saline (32.5 – 35) waters, flowing landward. Long-term changes in circulation patterns have led to changes in the properties of the St. Lawrence deep waters (Bugden, 1991), including decreased dissolved oxygen concentrations (Gilbert et al., 2005). Gilbert et al. (2005) showed that O_2 concentrations have

decreased from ~130 μM in the 1930s to 60 μM at present, and indicated that 50-66% of this decrease in oxygen could be attributed to a 1.7ºC warming of the bottom waters in the estuary from the 1930s to the 1990s, with the remaining change potentially attributable to increased nutrient loading from land sources.

The two study sites in this study were station Saguenay 30, in the Saguenay Fjord, and Station 23, in the LSLE. Few studies have examined soluble metals in the water column of the St. Lawrence Estuary (Yeats et al., 1979; Yeats and Bewers, 1982; Cossa et al., 1990; Lum et al., 1991; Quemerais et al., 1992). However, studies in the sediments at Station 23 have indicated that Mn is a dominant redox species in the upper sediment with MnO_x concentrations exceeding 100 μmol g^{-1} of sediment (Anschutz et al., 2000; Madison et al., 2013).

1.3.3 Delaware Salt Marsh – the Great Marsh

The study sites in the Delaware salt marsh were located along the Broadkill River, a waterway which drains into the Delaware Bay and is bordered by salt marshes in the Great Marsh, Delaware. The Broadkill River has surface water salinities ranging from 0-30 and is oxygen saturated during the day. The marsh is dominated by the cord grass *Spartina alterniflora*, and is only inundated during spring tides and storm surges. During spring and summer months, productivity increases in the marsh, and in the late summer and fall, plant degradation products are highest in concentration.

1.4 Dissertation Structure

Current chemical cycling of Mn in seawater does not consider soluble Mn(III) an important chemical species. However, its detection in suboxic and anoxic marine environments demonstrates that this exclusion of Mn(III) renders previous models of

Mn cycling incomplete. Thus, to fully incorporate Mn(III) into present-day Mn cycling, soluble Mn speciation must be addressed in the water column. In particular, the reactivity of Mn(III) and its formation pathways need to be determined. In this dissertation, the first measurements of Mn(III) in oxygenated systems are presented and include measurements in three distinctly different marine environments.

In Chapter 2, I show that Mn(III) is stable in areas of low/no oxygen, in the anoxic bottom waters of the Chesapeake Bay. The presence of Mn(III) in such environments allows for potential pathways for metabolism by microorganisms, and for an electron acceptor/donor to drive reactions with other elements. In particular, I showed that Mn(III)-L complexes are kinetically stabilized against reduction in the presence of H_2S. Using laboratory experiments, I was also able to confirm that reductive dissolution of Mn oxides by organic ligands and H_2S may be important sources of Mn(III)-L to systems like the Chesapeake Bay. These data are now published (Oldham et al., 2015).

In Chapter 3, I expand on the work from Chapter 2 in the Chesapeake Bay to show that Mn(III)-L complexes are stable in the entire water column of the Chesapeake Bay – not just in the anoxic bottom waters. In particular, I expand on the potential formation pathways of Mn(III) in the context of the Mn cycle. Using pump-profiling for better spatial resolution (10 cm), and a low-level spectrophotometric modification of the UV/Vis method used in Chapter 2, I indicate that MnO_x is formed in the suboxic zone in the absence of detectable oxygen. This MnO_x is reduced at the suboxic-anoxic interface to form Mn(III)-L complexes. The Mn(III)-L complexes are also detected in the upper oxic waters, but their formation processes appear distinct from the processes happening in the suboxic and anoxic layers. The results at this site highlight that the

redox cycling of Mn is happening at least daily and that several physical, chemical and biological processes are at play, concurrently.

In Chapter 4, I show that Mn(III)-L complexes are ubiquitous in the St. Lawrence Estuary of Quebec Canada regardless of the O_2 concentration. In particular, I show that these Mn(III)-L complexes are precipitated with humic material, and thus, humic binding may play an important role in dissolved Mn stabilization and transport in estuaries. Additionally, I discuss that the Mn(III)-L complexes are non-colloidal (a size fraction between 20 and 200 nm), unlike analogous Fe(III)-L complexes. I evaluate potential production pathways of Mn(III)-L complexes at this site by examining the profiles of Mn species at two sites in the St. Lawrence Estuary: the Saguenay Fjord and Station 23. The Saguenay Fjord represents a more terrestrial site, whereas Station 23 is more hemipelagic, and I indicate different potential pathways at each site based on their respective water column properties. This work is now published (Oldham et al., 2017).

Where Chapters 2-4 focus on the ubiquity of Mn(III)-L complexes using water column profiles with depth, Chapter 5 focuses on the transport and fate of Mn(III)-L complexes by looking at a surface transect of Mn speciation along a salinity gradient in the Broadkill River. I found that Mn(III) was stabilized by humic-type ligands coming off of the Great Marsh. The work in this chapter highlights the importance of Mn(III) in systems like the Great Marsh, which dominate the East Coast of North America. I find that this humic material may be responsible for binding up to 99 % of the dissolved Mn in these systems, and since these complexes have not been accounted for in the past, metal transport from estuaries to the coastal ocean may need to be reevaluated.

Chapter 6 reviews the main findings from this study, presents general conclusions and recommends areas for future study.

REFERENCES

Anschutz, P., Sundby, B., Lefrancois, L., Luther, G.W. and Mucci, A. (2000). Interactions between metal oxides and species of nitrogen and iodine in bioturbated marine sediments. *Geochim. Cosmochim. Acta.* 64, 2751-2763.

Baral, D., Lume-Pereira, C., Janata, A. and Henglein, A. (1985). Chemistry of colloidal manganese dioxide. 2. Reaction with superoxide anion (O_2^-) and hydrogen peroxide (pulse radiolysis and stop flow studies). *J. Phys. Chem.* 89, 5779-5783.

Boyle, E. A., Edmond, J.M., and Sholkovitz, E.R. (1977). The mechanism of iron removal in estuaries. *Geochim. Cosmochim. Acta.* 41, 1313-1324.

Breitburg, D.L., Pihl, L., and Kolesar, S.E. (2001) Effects of low dissolved oxygen on the behavior ecology and harvest of fishes, a comparison of the Chesapeake Bay and Baltic-Kattegat systems. In, Rabalais NN, Turner RE (eds) Coastal hypoxia, consequences for living resources and ecosystems. American Geophysical Union, Washington, DC, pp 241–268

Bugden, G.L. (1991). Changes in the temperature–salinity characteristics of the deeper waters of the Gulf of St. Lawrence over the past few decades. In The Gulf of St. Lawrence, small ocean or big estuary? Edited by J.-C. Therriault. *Publ. spéc. can. sci. halieut. aquat*. 113, 139–147.

Burdige, D. J. and Nealson, K. H. (1986). Chemical and microbiological studies of sulfide-mediated manganese reduction. *Geomicrobio. J.* 4, 361-387.

Canfield, D. E., Thamdrup, B. and Hassen, J. W. (1993). The anaerobic degradation of organic matter in Danish coastal sediments, iron reduction, manganese reduction and sulfate reduction. *Geochim. Cosmochim. Acta.* 57, 3867-3883.

Chester, R., and Jickells, T. (2012). Marine Geochemistry (3rd Ed.). Wiley-Blackwell, West Sussex, UK, 411 pp.

Cooper, W.J., Zika, R.G., Petasne, R.G., and Plane, J.M.C. (1988). Photochemical formation of H_2O_2 in natural waters exposed to sunlight. *Environ. Sci. Technol.* 22, 1156-1160.

Cossa, D., Tremblay, G.H., and Gobeil, C. (1990). Seasonality in iron and manganese concentrations of the St. Lawrence River. *Sci. Total. Environ.* 98, 185-190.

Dellwig, O., B. Schnetger, H. J. Brumsack, H. P. Grossart, and L. Umlauf. (2012). Dissolved reactive manganese at pelagic redoxclines (part II), Hydrodynamic conditions for accumulation. *J. Mar. Syst.* 90, 31–41.

Duckworth O. W. and Sposito G. (2005). Siderophore-manganese(III) interactions I. Manganite dissolution promoted by desferrioxamine-B. *Environ. Sci. Technol.* 39, 6045-6051

Duckworth, O.W., and Sposito, G. (2007) Siderophore-promoted dissolution of synthetic and biogenic layer type Mn oxides. *Chem. Geol.* 242, 497-508.

Ehrlich, H.L., Salerno, .J.C. (1990). Energy coupling in Mn^{2+} oxidation by a marine bacterium. *Arch. Microbiol.* 154, 12–17.

Emerson, S., Kalhorn, S., Jacobs, L., Tebo, B.M., Nealson, K.H., and Rosson, R.A. (1982). Environmental oxidation rates of Mn(II), bacterial catalysis. *Geochim. Cosmochim. Acta.* 46, 1073-1079.

Froelich, P.N., Klinkhammer, G.P., Bender, M.L., Luedtke, N.A., Heath, G.R., Cullen, D., Dauphin, P., Hammond, D., Hartman, B., and Maynard, V. (1979). Early oxidation of organic matter in pelagic sediments of the eastern equatorial Atlantic, suboxic diagenesis. *Geochim. Cosmochim. Acta*. 43, 1075–1090.

Galbraith, P.S. (2006). Winter water masses in the Gulf of St. Lawrence. *J. Geophys. Res. C, Oceans.* 111, C06022.

Gilbert, D., Sundby, B., Gobeil, C., Mucci, A., and Tremblay, G.–H. (2005). A seventy–two–year record of diminishing deep–water oxygen in the St. Lawrence Estuary, the northwest Atlantic connection. *Limnol. Oceanogr*. 50, 1654–1666.

Goldberg, E. (1954). Marine Geochemistry 1. Chemical Scavengers of the Sea. *J. Geolog.* 62, 249-265.

Goodrich, E., Boicourt, W., Hamilton, P., and Pritchard, D. (1987) Wind-induced destratification in Chesapeake Bay. *J. Phy. Oceanogr*. 17, 2232–2240.

Grassian, V. (2005). Environmental Catalysis. CRC Press, pp.64-76.

Guieu, C., Duce, R. and Arimoto, R., (1994). Dissolved Input of Manganese to the Ocean - Aerosol Source. *J. Geophys. Res. Atmos.* 99, 18789- 18800.

Hansard, S. P., Easter, H. D., and Voelker, B. M. (2011). Rapid reaction of nanomolar Mn(II) with superoxide radical in seawater and simulated freshwater. *Environ. Sci. Technol.* 45, 2811−2817.

Hastings, D. and Emerson, S. (1986). Oxidation of manganese by spores of a marine Bacillus, kinetic and thermodynamic considerations. *Geochim. Cosmochim. Acta*. 50, 1819-1824.

Haygood, M.G., Holt, P.D. and Butler, A. (1993). Aerobactin Production by a Planktonic Marine Vibrio Sp. *Limnol. Oceanogr.* 38, 1091-1097.

Herzage, J., and dos Santos Afonso, M. (2003). Mechanism of hydrogen sulfide oxidation by manganese(IV) oxide in aqueous solutions. *Langmuir*. 19, 9684-9692.

Kaushal, S.S., Groffman, P.M., Band, L.E. et al (2008). Interaction between urbanization and climate variability amplifies watershed nitrate export in Maryland. *Environ. Sci. Tech.* 42, 5872–5878.

Kemp, W.M., Boynton, W.R., Adolf, J.E. et al (2005) Eutrophication of Chesapeake Bay, historical trends and ecological interactions. *Mar. Ecol. Prog. Ser.* 303, 1–29.

Kopf, S. H., Henny, C., and Newman, D. K. (2013). Ligand-Enhanced Abiotic Iron Oxidation and the Effects of Chemical versus Biological Iron Cycling in Anoxic Environments. *Environ. Sci. Technol*. 47, 2602–2611.

Landing, W.M., and Bruland, K.W. (1980). Manganese in the North Atlantic. *Earth, planet. Sci. Lett.* 49, 45-56.

Landing, W.M., and Bruland, K.W. (1987). The contrasting biogeochemistry of iron and manganese in the Pacific Ocean. *Geochim. Cosmochim. Acta.* 51, 29-43.

Learman, D.R., B.M. Voelker, A.S. Madden and C.M. Hansel (2013). Constraints on superoxide mediated formation of manganese oxides. *Frontiers Microbiol.* 4, 1-11.

Lewis B. L. and Landing W. M. (1991) The biogeochemistry of manganese and iron in the Black Sea. *Deep-Sea Res.* 38, S773-S803.

Lin, H., Szeinbaum, N.H., DiChristina, T.J., and Taillefert, M. (2012). Microbial Mn(IV) reduction requires an initial one-electron reductive solubilization step. *Geochim. Cosmochim. Acta.* 99, 179-192.

Lovely, D.R., and Phillip, E.J.P. (1988). Novel mode of microbial energy metabolism, organic carbon oxidation coupled to dissimilatory reduction of iron or manganese. *Appl. Environ. Microbiol.* 54, 1472-1480.

Luther, G.W., and Popp, J.I. (2002) Kinetics of the abiotic reduction of polymeric manganese dioxide by nitrite, an anaerobic nitrification reaction. *Aquat. Geochm.* 8, 15-36.

Luther, G.W. III, A.S. Madison, A. Mucci, B. Sundby and V. E. Oldham. (2015). A kinetic approach to assess the strengths of ligands bound to soluble Mn(III). *Mar. Chem.* 173, 93-99.

Lum, K.R., Kaiser, K.L.E. and Jaskot, C. (1991). Distribution and fluxes of metals in the St. Lawrence River from the outflow of Lake Ontario to Quebec City. *Aquat. Sci.* 53, 1-19.

Madison, A.S., Tebo, B.M., Luther, G.W. (2011) Simultaneous determination of soluble manganese(III), manganese(II) and total manganese in natural (pore)waters. *Talanta.* 84, 374-381.

Madison, A.S., Tebo, B.M., Mucci, A., Sundby, B., and Luther, G.W. (2013). Abundant porewater Mn(III) is a major component of the sedimentary redox system. *Science.* 341, 875-878.

Maldonato M.T., and Price, N.M. (2000). Nitrate regulation of Fe reduction and transport by Fe-limited Thalassiosira oceanica. *Limnol. Oceanogr.* 45, 814-826.

Maldonato, M.T., and Price, N.M. (2001). Reduction and transport of organically bound iron by *Thalassiosira oceanica*. *J. Phycol.* 37, 298-309.

Martin, J.H. and Gordon, R.M. (1988). Northeast Pacific iron distributions in relation to phytoplankton productivity. *Deep-Sea Res.* 35, 177-196.

Morgan, J.J. (1967). Chemical equilibria and kinetic properties of manganese in natural waters. In Principles and Applications of Water Chemistry, pp. 561-623. John Wiley and Sons, Inc.

Millero, F. J. (1996). Chemical Oceanography (2nd Ed.). CRC Press, Boca Raton, 469 pp.

Murray J.W., J.G. Dillard, R. Giovanoli, H. Moers and W. Stum. (1985). Oxidation of Mn(II): Initial mineralogy, oxidation state and aging. *Geochim. Cosmochim. Acta.* 49, 463-470

Myers, C.R., and Nealson, K.H. (1988). Bacterial manganese reduction and growth with manganese oxide as the sole electron acceptor. *Science.* 240, 1319-1321.

Nealson, K.H., and Myers, C.R. (1992). Microbial reduction of manganese and iron, New approaches to carbon cycling. *Appl. Environ. Microbio.* 58, 439-443.

Newcombe C.L., and Horn, W.A. (1938) Oxygen poor waters of the Chesapeake Bay. *Science.* 88,80–81.

Nico, P.W., and Zasoski, R.J. (2000). Importance of Mn(III) availability on the rate of Cr(III) oxidation on δ-MnO_2. *Environ. Sci. Technol.* 34, 3363-3367.

Officer, C.B., Biggs, R.B., Taft, J.L., Cronin, E. Tyler, M.A. and Boynton, W.R.. (1984). Chesapeake Bay anoxia, origin, development and significance. *Science.* 223, 22–27.

Oldham, V.E., Owings, S. M., Jones, M., Tebo, B.M., and Luther, G.W. (2015). Evidence for the presence of strong Mn(III)-binding ligands in the water column of the Chesapeake Bay. *Mar. Chem.* 171, 58-66.

Oldham, V.E., Mucci, A., Tebo, B.M., Luther, G.W. (2017). Soluble Mn(III)-L complexes are abundant in oxygenated waters and stabilized by humic ligands. *Geochim. Cosmochim. Acta.* 199, 238-246.

Parker D.L., Takami M., Mylene L., Mozafarzadeh R.V., McCarthy J.K., Tebo B.M. 2007. Inter-Relationships of MnO2 Precipitation, siderophore–Mn(III) Complex Formation, Siderophore Degradation, and Iron Limitation in Mn(II)-Oxidizing Bacterial Cultures. *Geochim. Cosmochim. Acta.* 71, 5672-83.

Peers, G., and Price, N.M. (2004). A role for manganese in superoxide dismutases and growth of iron-deficient diatoms. *Limnol. Oceanogr*. 49,1774-1783.

Petasne, R.G., and Zika, R.G. (1987). Fate of superoxide in coastal seawater. *Nature.* 325, 516-518.

Postma, D., and Appelo, C. A. J. (2000). Reduction of Mn-oxides by ferrous iron in a flow system, column experiment and reactive transport modeling. *Geochim. Cosmochim. Acta* 64, 1237-1247.

Quémerais, B., Lum, K.R. and Lemieux, C. (1996). Concentrations and transport of trace metals in the St. Lawrence River. *Aqu. Sci.* 58, 52-68.

Rose, A.L., and Waite, T.D. (2002). Kinetic model for Fe(II) oxidation in seawater in the absence and presence of natural organic matter. *Environ. Sci. Technol.* 26, 433-444.

Rue, E.L., and Bruland, K.W. (1995). Complexation of iron(III) by natural organic ligands in the Central North Pacific as determined by a new competitive ligand equilibration/adsorptive cathodic stripping voltammetric method. *Mar. Chem.* 50, 117-138.

Schlosser C., Streu P. and Croot P.L. (2013) Vivaspin ultrafiltration, A new approach for high resolution measurements of colloidal and soluble iron species. *Limnol. Oceanog. Methods*. 11, 187-201.

Shiller, A.M. (1997). Manganese in surface waters of the Atlantic. *Geophys. Res. Let.* 24, 1495-1498.

Sholkovitz, E.R. (1976). Flocculation of dissolved organic and inorganic matter during the mixing of river water and seawater. *Geochom. Cosmochim. Acta*. 40, 831-845.

Sholkovitz, E.R.(1978) The flocculation of dissolved Fe, Mn, Al, Cu, Ni, CO and Cd during estuarine mixing. *Earth Planet. Sci. Lett.* 41, 77-86.

Siebecker, M. G., Madison, A. S. and Luther, G. W. (2015). Reduction Kinetics of Polymeric (Soluble) Manganese (IV) Oxide (MnO_2) by Ferrous Iron (Fe^{2+}). *Aqu. Geochem.* 21,143–158.

Spencer, D.W. and Brewer, P.G. (1971). Vertical advection diffusion and redox potentials as controls on the distribution of manganese and other trace metals dissolved in waters of the Black Sea. *J. Geophys. Res.* 76, 5877-5892.

Strzepek, R.F., Maldonato, M.T., Hunter, K.A., Frew, R.D., and Boyd, P.W. (2011). Adaptive strategies by Southern Ocean phytoplankton to lessen iron limitation, Uptake of organically complexed iron ad reduced cellular iron requirements. *Limnol. Oceanogr.* 56, 1983-2002.

Stumm, W. and Morgan, J.J. (1996.) Aquatic Chemistry. Wiley-Interscience, New York, 1022 pp.

Sunda, W.G., Huntsman, S.A. and Harvey, G.R., (1983). Photoreduction of manganese oxides in seawater and its geochemical and biological implications. *Nature.* 301, 234- 236.

Sunda, W.G., and Huntsman, S.A. (1988). Effect of sunlight on redox cycles of manganese. *Deep-Sea Res.* 35, 1297-1317.

Sunda, W.G., and Hunstman, S.A. (1996). Antagonisms between cadmium and zinc toxicity and manganese limitation in a coastal diatom. *Limnol. Oceanogr.* 40, 1404-1417.

Sunda, W.G., and Hunstman, S.A. (1998). Interactions among Cu2+, Zn2+, and Mn2+ in controlling cellular Mn, Zn and growth rate in the coastal alga Chlamydomonas. *Limnol. Oceanogr.* 43, 1055-1064.

Sunda, W.G., and Kieber, D.J. (1994) Oxidation of humic substances by manganese oxides yields low molecular-weight organic substrates. *Nature*. 367,62–64

Tebo, B. M. (1991). Manganese(II) oxidation in the suboxic zone of the Black Sea. *Deep-Sea Res.*. 38(Suppl. 2), S883-S905.

Tebo, B.M., Bargar J.R., Clement, B.G., Dick, G.J., Murray, K.J., Parker, D., Verity, R., Webb, S.M. (2004). Biogenic manganese oxides, properties and mechanisms of formation. *Ann. Rev. Earth Planet. Sci*. 32, 287-328.

Trouwborst, R. E., Clement, B. G., Tebo, B. M., Glazer, B. T. and Luther, G. W. (2006). Soluble Mn(III) in suboxic zones. *Science.* 313, 1955-1957.

van den Berg, C.M.G. (1995) Evidence for organic complexation of iron in seawater. *Mar. Chem.* 50, 139-157.

Waite, T.D., Wrigley, I.C. and Szymczack, R. (1988). Photoassisted dissolution of a colloidal manganese oxide in the presence of fulvic acid. *Environ. Sci. Technol*. 22, 778-785.

Webb, S. M., Dick, G. J., Bargar, J. R., and Tebo, B. M. (2005). Evidence for the presence of Mn(III) intermediates in the bacterial oxidation of Mn(II). *Proc. Nat. Acad. Sci.* 102, 5558–5563.

Witter, A.E., and Luther, G.W. (1998). Variation in Fe-organic complexation with depth in the Northwestern Atlantic Ocean as determined using a kinetic approach. *Mar. Chem.* 62, 241-258.

Wu, J. and Luther III, G.W. (1996). Spatial and temporal distribution of iron in the surface water of the northwestern Atlantic Ocean. *Geochim. Cosmochim. Acta*. 60, 2729-2742.

Wuttig, K., Heller, M.I., and Croot, P. (2013). Reactivity of inorganic Mn and Mn Desfrerrioxamine B with O_2, O_2^-, and H_2O_2 in seawater. *Environ. Sci. Technol.* 47, 10257-10265.

Yakushev,E., Pakhomova, S., Sørenson, K., and Skei, J. (2009). Importance of the different manganese species in the formation of water column redox zones: Observations and modeling. *Mar. Chem.* 117, 59-70.

Yakushev, E.V., F. Pollehne, G. Jost, I. Kuznetsov, B. Schneider and L. Umlauf. (2007). Analysis of the water column oxic/anoxic interface in the Black and Baltic seas with a numerical model. *Mar. Chem.* 107, 388-410.

Yao W. and Millero, F.J. (1993). The rate of sulfide oxidation by MnO2 in seawater. *Geochim. Cosmochim. Acta* 57, 3359-3365.

Yeats P.A., Sundby B. and Bewers J.M. (1979) Manganese recycling in coastal waters. *Mar. Chem.* 8, 43-55.

Yeats, E A. and Bewers, J.M. (1982). Discharge of metals from the St. Lawrence River. *Can. J. Earth Sci.* 19, 982- 992.

Chapter 2

EVIDENCE FOR THE PRESENCE OF STRONG MANGANESE(III)-BINDING LIGANDS IN THE WATER COLUMN OF THE CHESAPEAKE BAY[1]

Abstract

Soluble manganese speciation was determined in suboxic and anoxic waters of the Chesapeake Bay using a water soluble porphyrin ligand as spectrophotometric reagent. Initial addition of the reagent detected only Mn(II); on addition of 100 μM H_2S (excess of the expected total dissolved Mn concentration) an increase in Mn occurred, indicating a reduction of Mn(III). Mn(III) comprised up to 54.21 ± 2.71 % of the total dissolved Mn pool. Samples with low H_2S (4.82 ± 0.80 μM) had high Mn(III) (6.98 ± 0.63 μM) whereas those with high H_2S (38.37 ± 1.70 μM) had low Mn(III) (1.12 ± 0.17 μM) indicating Mn(III) is kinetically stabilized *in situ* by strong ligands so reduction to Mn(II) is not complete. Assays for MnOx particles showed these were negligible or not detected except near the oxic-anoxic interface, and Mn(III) depth profiles showed peaks below the oxic-anoxic interface. Sulfidic sediments were not a source of Mn(III) to overlying waters as no Mn(III) was detected in overlying waters. These Mn(III) profiles likely result from the one electron reductive dissolution of solid MnO_2 particles formed at the oxic-anoxic interface, which then fall into the anoxic hydrogen sulfide rich zone.

---

[1] *Chapter 2 published in Marine Chemistry:* Oldham, V.E., Owings, S. M., Jones, M., Tebo, B.M., and Luther, G.W. (2015). Evidence for the presence of strong Mn(III)-binding ligands in the water column of the Chesapeake Bay. Mar. Chem. 171, 58-66.

Laboratory experiments with known ligands bound to Mn(III) confirm that Mn(III)-L complexes do not completely react with H_2S as these are concentration dependent reactions under kinetic control.

2.1 Introduction

The oxidation states of Mn render it important in a host of reduction and oxidation reactions as a trace nutrient and indirectly in the cycles of other biologically significant redox active elements. In seawater, Mn is important in photosynthetic organisms as the metal redox center of Photosystem II, where the splitting of water occurs (Dismukes, 1986). In this role, Mn is responsible for the accumulation of oxygen in the atmosphere, and for much of the primary production of the ocean. Though the importance of Mn to biogeochemical systems is well known, its cycling is not completely described. This disjoint is largely the result of an incomplete understanding of the speciation of manganese.

Until recently, the speciation of Mn has been operationally defined by filtration, where the fraction passed through a 0.2 μm or 0.45 μm filter was deemed the dissolved fraction, dominated by Mn(II), and the unfiltered fraction was characterized as particulate Mn(IV)/(III) as MnO_x. The importance of soluble Mn(III) was previously neglected because it was presumed thermodynamically unstable, and disproportionates to Mn(II) and Mn(IV) (Stumm and Morgan, 1996) or hydrolyzes and precipitates as Mn(III) oxides (Klewicki and Morgan, 1998). However, Mn(III) is an important component in the environment for one electron transfer reactions (Luther, 2005; 2010). Since the orbitals (σ, e_g*) of Mn(IV) and Mn(II) that accept and donate electrons are spatially distinct, the reduction or oxidation between these two species must be the result of one electron transfer processes, with Mn(III) acting as the intermediate

(Luther, 2005). In the presence of ligands, Mn(III) can be stabilized in solution as Mn(III) complexes are much more stable than Mn(II) complexes, due to a smaller atomic radius and higher electrostatic charge. Additionally, Mn(III) has a strong affinity for ligands that also bind Fe(III); thus, Mn(III) could compete for siderophores and disrupt Fe(III) uptake (Duckworth et al., 2009), since siderophores act to increase Fe(III) bioavailability for microbes and plants (Kraemer, 2004).

Recent work in the suboxic water column of the Black Sea, Chesapeake Bay and Baltic Sea as well as the pore-waters of the St. Lawrence River has shown that Mn(III)-ligand (Mn(III)-L) complexes make up to 100 % of the total dissolved Mn species in suboxic and anoxic waters, and sediment pore-waters (Madison et al., 2011, 2013; Trouwborst et al., 2006; Yakushev, 2007, 2009). In the St. Lawrence river, dissolved Mn(III) was deemed an important component of diagenetic processes because Mn(III)-L complexes constituted up to 90 % of the total dissolved Mn pool in suboxic marine sediments (Madison et al., 2013). Dissolved Mn(III) has also been detected as an intermediate in bacterial MnO_2 reduction (Lin et al., 2012) and in the oxidation of Mn(II) (Webb et al., 2005). In the Chesapeake Bay, dissolved Mn(III)-L complexes were detected in 2003 when the suboxic zone was well developed, but not in 2002 when the suboxic zone was poorly developed (Troubworst et al., 2006).

The nature of these Mn(III)-L complexes is only beginning to be described (Luther et al, 2015). For many metal-ligand complexes in seawater, Fe and Cu for example, ligand classes have been designated based on conditional stability constants (K_{cond}). For Mn, $K_{cond} = K_{Mn'L}$ where Mn′ represents all dissolved inorganic forms (aquated ions and complexes with Cl^-, OH^-, etc.) in seawater at ambient pH. Equations 2.1 and 2.1a describe the equilibrium reaction and equilibrium expression, respectively.

The rate constant for formation of Mn′L is k_f (our adopted value is 10^9 $M^{-1}s^{-1}$ based on Jahn-Teller distortion of Mn(III) and its water exchange rate), and the dissociation rate constant for Mn′L is k_d. In Saint Lawrence estuary porewaters $K_{Mn'L}$ was found to range from 1.39 to 4.35 x 10^{11} M^{-1}. $K_{Mn'L}$ values were determined from the actual k_d values and the adopted k_f.

$$Mn' + L \underset{k_d}{\overset{k_f}{\rightleftarrows}} Mn'L \qquad 2.1$$

$$where\ K_{cond} = K_{Mn'L} = \frac{Mn'L}{[Mn'][L]} = \frac{k_f}{k_d} \qquad 2.1a$$

Higher conditional stability constants correspond to a strong-binding L_1 ligand class, and lower conditional stability constants to correspondingly weaker classes: L_2, L_3, and so on. In the work of Madison et al., (2011 and 2013), a weak ligand class was demonstrated by the kinetics of the reaction of the ambient ligands with the added porphyrin ligand α, β, γ, δ-tetrakis(4-carboxyphenyl)porphine (T(4-CP)P). In this method, seawater samples were filtered through a 0.2 µm filter, and the filtrate was analyzed by UV/Vis spectroscopy. The addition of soluble porphyrin, T(4-CP)P, rapidly complexes any dissolved Mn(II) in solution as Mn(II)-T(4-CP)P, and oxygen in solution rapidly oxidizes this to Mn(III)-T(4-CP)P, which has a sharp absorption peak at 468 nm. The reaction is allowed to proceed for 15 minutes, and for Mn(II), the curve generated shows an exponential rise to a maximum, with a single two-parameter solution:

$$y = a(1 - e^{-k_1 x}) \qquad 2.2$$

Here, a is the concentration of Mn(II) and k_1 is the rate constant for the Mn(II) formation curve. However, when Mn(III) is present and bound to weak ambient ligands, the rise to a maximum has a four-parameter solution (eq. 2):

$$y = a\left(1 - e^{k_1 x}\right) + b(1 - e^{k_2 x}) \quad 2.3$$

Here, b is the concentration of Mn(III) and k_2 is the rate constant for the Mn(III) formation curve. In Madison et al (2013), the unknown ligands had slower kinetics than Mn(III) bound to pyrophosphate and faster kinetics than Mn(III) bound to desferrioxamine-B. Using the steady state approximation, Luther et al. (in press) showed that k_2 is the dissociation rate constant, k_d, for the Mn′L complex (reverse of eq. 1). The kinetic data from this study indicate that the conditional stability constants for Mn(III)-L ($K_{Mn'L}$) are similar to or higher than those for the formation of Fe(III)-L complexes in organic matter decomposition zones (Luther et al., in press). The relevant chemical reactions for eqs. 2.2 and 2.3 are eqs. 2. 4 and 2.5, respectively.

$$Mn^{2+} + T(4-CP)P \xrightarrow{k_1} Mn(II)T(4-CP)P + O_2 \xrightarrow{fast, k_1} Mn(III)T(4-CP)P \quad 2.4$$

$$Mn(III) - L + T(4-CP)P \overset{k_2}{\leftrightarrow} Mn(III)T(4-CP)P + L \quad 2.5$$

Reaction (2.4) proceeds rapidly to the right, and the Mn(III) substitution reaction (2.4) proceeds more slowly, in the presence of weak binding ligands. In the presence of strong ambient ligands, reaction (2.5) does not proceed forward. A strong reducing agent, H2S or hydroxylamine, needs to be added to reduce any Mn(III)-L for the total dissolved Mn to be measured. The concentration of Mn(III)-L can be calculated by subtracting the measured [Mn(II)] from this total. In this way, it is now possible to designate strong and weak binding ligands for dissolved Mn(III) based on the following distinct measurements:

(i) A sample with weak binding ligands will exhibit a rise to a maximum with a four-parameter solution (eqs. 2.3 and 2.5).

(ii) A sample with strong binding ligands will show a simple two-parameter rise to a maximum, with an increase in Mn detection upon addition of excess strong reducing agent.

(iii) A sample with no Mn(III) will show a simple two-parameter rise to a maximum with no increase in Mn detection upon addition of excess strong reducing agent (eqs. 2.2 and 2.4).

In this study, this principle is demonstrated using known Mn(III)-binding ligands in the laboratory and unknown ligands from the environment. We find that unknown strong binding ligands bind more strongly to Mn(III) than the siderophore desferrioxamine-B; that NH_2 functional groups reduce Mn(III), including desferrioxamine which binds Mn(III) at a 1:1 ratio through the hydroxamate groups; and that unknown weaker binding ligands are more similar to pyrophosphate. This measurement approach of strong and weak Mn ligands was applied to natural samples in the Chesapeake Bay.

The Chesapeake Bay exhibits seasonal anoxia as a result of intense productivity (Boynton et al., 1982) and in the suboxic and anoxic zones, dissolved Mn concentrations can be greater than 18 µM (Trouwborst, 2006). In suboxic and anoxic waters, where chemical species that can accept or donate electrons are limited, the presence of Mn(III) would have important implications for other coupled redox reactions, like those with Fe, O_2, and S.

In this study, the water column above a 30 m deep hole in the Chesapeake Bay was sampled during August 9-13, 2013. In addition to Mn speciation, concentrations of hydrogen sulfide (H_2S defined as the sum of H_2S, HS^-, S_x^{2-}, and S_8) and O_2 were determined by *in situ* voltammetry (Brendel and Luther, 1995; Rozan et al., 2000;

Konovalov et al., 2003); dissolved O_2 was also measured during casts using the shipboard CTD system. The results from this study demonstrate *in situ* H_2S reduction of Mn(III)-L complexes over time as well as the first findings of strong Mn(III)-L complexes in the marine environment.

2.2 Methods:

2.2.1 Sample Collection

During a sampling campaign from August 9th to 13th, 2013 at a 30 m hole South of the Chesapeake Bay bridge (Station 848, 38^{0}58.54' N; 076^0 22.11' W), 27 seawater samples were collected from four depths in the suboxic and anoxic zones, and were analyzed for Mn speciation. Samples were collected into new, rinsed 50 mL falcon tubes (Fisher Scientific) at high and low tide (slack water) from a sampling CTD rosette system aboard the R/V *Hugh R. Sharp*. Sampling contamination was minimized by wearing gloves and by using clean tubing for sample collection. The exposure of the samples to oxygen was minimized by removing air bubbles in the tubing and in the head-space of the collection tubes by overfilling the tubes three times before capping. Samples were filtered within 15 minutes of collection through a 0.2 µm Millipore® syringe filter, in a glove bag with an argon atmosphere, to prevent oxygenation of the sample prior to analysis. In the laboratory, MnO_2 was filtered in this way, to ensure complete removal of MnO_x from samples, and indeed, no MnO_2 passed through the filters.

A sediment core using the multi-corer model MC-400 from Ocean Instruments, Inc. was taken on August 12th and the overlying water was sampled immediately upon recovery using a clean syringe. The sample was also filtered within 15 minutes of

collection through a 0.2 μm Millipore® syringe filter, in a glove bag with an argon atmosphere.

Conductivity, temperature, and salinity profiles were taken during the CTD casts, from the R/V *Sharp* rosette system.

2.2.2 Sulfide Measurements on Discrete Samples

Samples were filtered as above. Sulfide was then determined in triplicate using a DLK-60 electrochemical analyzer; the flow cell (Analytical Instrument Systems Inc.) was used in conjunction with 100 μM Au/Hg amalgam PEEK microelectrodes prepared according to Luther et al. (2008). Cyclic voltammetry ran from -0.1 V to -1.8 V, and back to -1.8 V at a scan rate of 2 V s-1 after conditioning at -0.9 V for 5 s then at -0.1 V for 2 s. These electrodes are capable of measuring an array of redox active species including oxygen, sulfide, thiosulfate, elemental sulfur, iron, and manganese (Luther et al., 2008). The detection limit of this method is 0.2 μM for sulfide and polysulfides and 3 μM for oxygen.

2.2.3 MnO_x Determination

Chesapeake Bay water was obtained directly from the CTD Niskin bottles in 50 mL centrifuge tubes. Known volumes of samples (usually 50 mL) were filtered through Whatman 0.2 μm track etched polycarbonate filters. Filters were subsequently transferred to 5 mL vials to which 20 μM of leucoberbelin blue dye (LBB, 65 %, Sigma-Aldrich) were added. The volumes of the sample and dye solution had a concentration factor of usually 12.5 or 16.7. The dye color formed on oxidation by particulate manganese or MnO_x was measured in a 1 cm cuvette at 620 nm using an Ocean Optics USB2000 spectrophotometer coupled to an HL-2000-FHSA halogen light

source. The method is refined from that published by Altmann (1972). The LBB (410.5 g mol^{-1}) stock solution is made by dissolving the crystals in Milli-Q water to a strength between 1 to 4 % (24 to 97 mM) and adding 40 μL of either 10 M sodium hydroxide (NaOH) or 21 % ammonium hydroxide (NH_4OH) per 10 mL of solution. This solution is stable for greater than 1 year. Working solutions involve diluting the stock into 1% acetic acid (made up in Mili-Q water), to a range between 0.01 to 0.04 % (240 to 970 μM). Over time a precipitate will form in the working solution. Thorough agitation through shaking, or sonicating, will help re-dissolve the precipitate, even when present there is no detrimental effect of this precipitate on the final measurement. Measurement of samples on filters involves a final dilution of the LBB working solution so that the maximum final concentration used is ~80 μM LBB.

Potassium permanganate is used to produce the calibration curves that range between 0.2 and 10 μM $KMnO_4$. MnO_x measurements are referred to as MnO_x equivalents for two reasons. The first is due to the calibration being a different species than the analyte as the oxidation of the LBB dye is directly proportional to the electrons provided from the manganese species. Mn(VII) will oxidize 5 LBB molecules during its reduction to Mn(II) whereas Mn(IV) only oxidizes 2 LBB molecules. To produce the equivalent LBB blue color at 620 nm, 2.5 times more Mn(IV) is required; i.e., 12.5 μM Mn(IV) produces an equivalent color to 5 μM $KMnO_4$. It is also probable that not all the particulate MnO_X exists as Mn(IV) because a small percentage will be as a Mn(III) oxide. LBB calibration curves in a 1 cm cell can become non-linear above 1 μM $KMnO_4$. Sample concentration was calculated using a non-linear calibration, with an r^2 ~ 1. The limit of detection (LoD) using a single linear calibration is around 0.085 μM $KMnO_4$ or 0.21 μM MnO_X (99% confidence limit using a MQ water blank); correcting

for the concentration factor (12.5) gives a LoD of ~ 0.017 µM MnO_X for natural samples. All sample filters were measured in the same media and with the same strength LBB as the $KMnO_4$ standards. On occasion, dissolved organic material can affect the underlying baseline of the LBB measurement. A correction was applied for samples where excess dissolved material conflicted with the sample signal, by calculating the underlying baseline signal at 620 nm from the slope between readings taken at 460 and 700 nm.

2.2.4 Fe Measurements on Discrete Samples

Triplicate Fe(II) and total iron measurements were made on filtered samples using the method of Stookey (1970) and the UV-Vis system described below. Samples were buffered in 2.5 M ammonium acetate prior to addition of the ferrozine reagent, which reacts with Fe(II) to produce an absorption at 562 nm. Hydroxylamine hydrochloride was added as a reducing agent to separate subsamples in order to measure total iron. The difference between the Fe total and the Fe(II) measurements is soluble Fe(III).

2.2.5 Mn(II) and Mn(III) Determination

Samples were analyzed ship-board, in duplicate, within two days of collection. Duplicates were within 0.005 absorbance units (AU) of each other, indicating high method precision. Some samples were analyzed immediately, and then reanalyzed two days later, and it was determined that the speciation did not change in the samples. Samples were kept capped and in the dark, in a clean van, between analyses to ensure no contamination. Samples were analyzed using the established method of a spectrophotometric ligand ([α, β, γ, δ-tetrakis(4-carboxyphenyl)porphine] or T(4-CP)P

(ε= 95,400 M^{-1} cm^{-1})) previously developed by Ishii et al., (1982) and modified by Madison et al., (2011) to determine dissolved Mn(II) and Mn(III). In this spectrophotometric method, the initial reagent mixture contains Cd-T(4-CP)P complex which is brought to a pH of 7.5 – 8.0 using an imidazole borate buffer. When a water sample, which contains Mn(II) or Mn(III), is added to the reagent mixture the Mn(II) outcompetes Cd(II) to form a Mn(II)-T(4-CP)P complex; this reaction is catalyzed by imidazole. The Mn(II) is rapidly oxidized to Mn(III) by dissolved oxygen, and the Mn(III)-T(4-CP)P exhibits an absorption peak at 468 nm by UV/Vis spectroscopy. This peak is measured over 15 minutes to extract kinetic data; however, only the first 150 s are used to produce an absorbance measurement when only Mn(II) and Mn(III) bound to weak ligands are present. The sample limit of detection for this method is 50 nM. The precision of the determination of both the Mn(II) with and without a reductant is typically better than 5%, as shown in Table 2.2. The addition of a strong reducing agent (in > tenfold excess of expected Mn concentration), such as hydroxylamine or hydrogen sulfide, prior to analysis reduces strong binding Mn(III)-L complexes in solution (see below); defined as complexes that do not react with the porphyrin ligand.

A Hewlett Packard 8452B diode array spectrophotometer was used, coupled with Olis. Inc. Globalworks software for all UV/Vis measurements (2 nm wavelength resolution). All reagents were made according to Madison et al., (2011) , and a standard calibration was performed prior to analysis with standards ranging from 50 nM to 10 μM, made from $MnCl_2$-$4H_2O$ (Fisher Scientific, 97.5 % purity) into deionized water (18.2 mΩ). Samples were analyzed for Mn(II) and Mn(III) bound to weak ligands using the method described by Madison et al., (2011). To ensure that total manganese was determined, a strong reducing agent, hydroxylamine (NH_2OH) (Fisher Scientific) was

added in excess (1.5 mM) to an aliquot of the seawater sample and was allowed to reach a maximum value (a minimum of 30 minutes equilibration time). The reactivity of the porphyrin was not found to be affected by the addition of hydroxylamine. Another separate aliquot of the seawater sample was amended with an excess of H_2S (final concentration of 100 µM) and was allowed to come to reach a maximum value (a minimum 30 minutes equilibration time). These reduced samples, with either hydroxylamine or H_2S, were also analyzed using the same spectrophotometric method.

We have found that HS^- is typically a more efficient reducing agent than hydroxylamine, except in the case of Mn(III)-porphyrin, which is reduced by hydroxylamine but not HS^-. The strong unknown Mn(III)-L complexes likely have 6 ligating atoms binding Mn(III), so the smaller HS^- is more efficient in reaching the Mn(III) center in an inner sphere one electron redox process (Luther, 2005). In the case of the Mn(III)-porphyrin, the superoxide bound to the Mn(III) center stabilizes the Mn(III), even in the presence of HS^-, whereas the neutral hydroxylamine can attack the superoxide site. Soluble porphryin concentrations are typically low in nature (McCarthy et al., 1997), and we don't expect them to account for a significant portion of our Mn(III)-L complexes, therefore HS^- is likely able to reduce the Mn(III)-L in the system.

The reduced samples represent a total dissolved Mn [Mn(II) + all Mn(III) forms], and the non-reduced sample represents the concentration of Mn(II) in the sample along with any Mn(III) bound to weak ligands. The Mn(III), which is operationally defined as bound to strong ligands, is determined by the difference of these two measurements. As shown in Madison et al. (2011), Mn(III) bound to desferrioxamine-B does not react readily with the porphyrin ligand, rather it goes into

the porphyrin slowly (see below); on adding a reducing agent to the Mn(III)-desferrioxamine-B, the resulting Mn(II) is quantitatively measured.

2.2.6 Reductive Dissolution of Colloidal MnO_2

A colloidal MnO_2 solution (1 mM, consisting of 50 nm nanoparticles) was prepared as described by Perez-Benito et al., (1989). The DFOB solution was made by dissolving solid DFOB into deionized water to a final concentration of 500 uM. The hydrogen sulfide solution was made by dissolving solid sodium sulfide nonanhydrate (Sigma Aldrich) into deoxygenated water, and this solution was made fresh daily to avoid oxidation overnight. Solutions of MnO_2 were made to 100 μM in deionized water. Tests were performed to examine the reductive dissolution of 100 μM MnO_2 and the resulting dissolved Mn speciation, in three cases: (i) with 100 μM H_2S, (ii) with 100 μM DFOB and (iii) with both 100 μM H_2S and 100 μM DFOB. The pH of these solutions was between 8 and 9.

The solutions were tested using the Hewlett Packard 8452B diode array spectrophotometer noted above. The absorbance peak for colloidal MnO_2 is measured at 362 nm, and at 310 nm for Mn(III)-DFOB. The decay of the MnO_2 peak over the course of the reaction was observed by scanning every 3 seconds over the course of 15 minutes reaction time. The growth of the Mn(III)-DFOB peak was similarly measured. Speciation of dissolved Mn was also performed using the porphyrin method also described in section 2.5.

2.2.7 Ligand Competition

Ligands that could bind Mn(III) were examined in laboratory experiments (Figure 2.1). A solution containing 250 μM Mn(III)-pyrophosphate was prepared by

dissolving Mn(III)-acetate (Alfa, Inc.) into deoxygenated water containing excess dissolved sodium pyrophosphate. The Mn(III)-pyrophosphate concentration was determined by UV/Vis spectroscopy at its absorption peak at 484 nm (Kostka et al., 1995). A solution of Mn(III)-desferrioxamine-B (DFOB) was prepared by dissolving $MnCl_2 \bullet 6H_2O$ into a solution with pH of 8 containing excess DFOB, and allowing it to oxidize by bubbling air overnight (Madison et al., 2011). Its final concentration, of 500 μM Mn(III)-DFOB was determined by UV/Vis spectrophotometry at its absorption peak at 310 nm. Other Mn(III)-L complexes were prepared by adding excess ligand to Mn(III)-pyrophosphate, and observing the complete disappearance of the Mn(III)-pyrophosphate (Mn(PP)) peak at 484 nm and the formation of new peaks, indicating conversion to the new Mn(III)-L complexes. The general reaction is given below, and ligand absorbance peaks are given in Table 2.1.

$$Mn(PP) + L \rightarrow MnL + PP$$

Several ligands were tested and they are: Tiron (4,5-dihydroxybenzene-1,3-disulfonate); 2,3-dihydroxybenzoic acid; (pyro)catechol (1,2-dihydroxybenzene); 2,3-dihydroxypyridine; Dopamine (3-hydroxytyramine or 3,4-dihydroxyphenethylamine); and Ferrozine (3-(2-Pyridyl)-5,6-diphenyl-1,2,4-triazine-p,p'-disulphonic acid monosodium salt hydrate). All ligands (Figure 2.1) were added in 10-fold excess to 12 uM Mn(III)-pyrophosphate.

The Mn(III)-L solutions were analyzed for classification of ligand strength using the method of the T(4-CP)P addition, in a final solution concentration of 1 uM Mn(III)-L. The kinetics observed for Mn(III)-DFOB were similar to the report by Madison et al. 2011; (see Figure 2.1 for Mn(III)-DFOB structure).

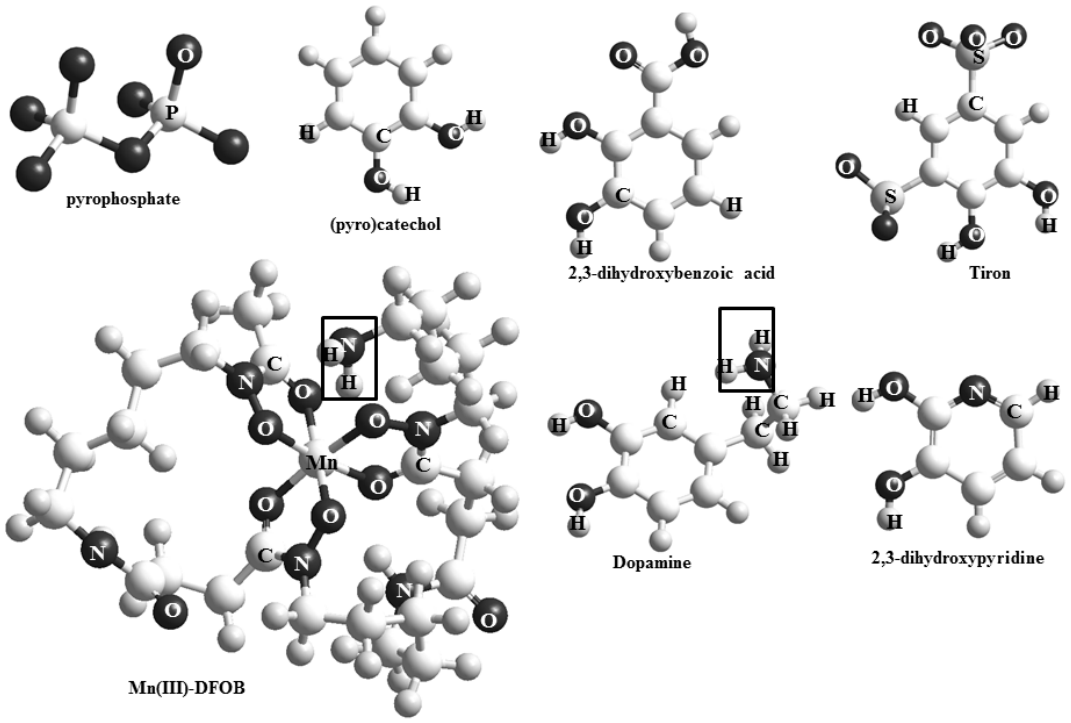

Figure 2.1 Structures of known ligands tested in this study. In addition to pyrophosphate and DFOB, which has three hydroxamate functional groups to bind Mn(III), there are five compounds with the ortho-dihydroxybenzene functional group to bind Mn(III). The rectangle shows the NH_2 group in DFOB and dopamine that reduces MnO_2.

Table 2.1 MnL complex absorbance peaks by UV/Vis spectrophotometry.

Ligand	Absorbance Peak(s) (nm)
Pyrophosphate	484
Desferrioxamine-B	310
Tiron (4,5-dihydroxybenzene-1,3-disulfonate)	292
2,3-dihydroxybenzoic acid	410, 622
Catechol (1,2-dihydroxybenzene)	356, 654
2,3-dihydroxypyridine	520
Dopamine (3-hydroxytyramine)	302

Ferrozine (3-(2-Pyridyl)-5,6-diphenyl-1,2,4-triazine-p,p'-disulphonic acid monosodium salt hydrate)	282, 316 (doublet)

2.3 Results and Discussion

In the summer months, decreased vertical mixing of the water column causes stratification, which creates oxic, suboxic and anoxic zones in the Chesapeake Bay. Figure 2.2 shows the water column profiles of dissolved O_2, salinity, temperature and H_2S from the first, second and fourth days of the sampling campaign. Over the course of sampling, the interface between the suboxic and oxic zones shifted from a partially mixed system to a more stratified system.

Depth profiles (Figure 2.2) showed that dissolved O_2 concentration decreased, from the surface with depth, to the suboxic zone, which was no more than 1-2 meters thick over the entire cruise, below which O_2 concentrations were near zero. Higher temperatures and lower salinity at the surface the surface resulted in a high level of stratification, which changed throughout the cruise as the sulfide moved up from a water column depth of 17 m to 12 m. On the first day, less stratification was observed and lower H_2S (4.51 ± 0.80 to 7.03 ± 1.10 μM) concentrations along with higher Mn(III)L concentrations were detected in the anoxic waters. On the last day of the sampling campaign, a higher stratification of the water column was observed, with a distinct O_2 penetration depth at approximately 10 m. In this latter profile, H_2S concentrations were more than four times higher (32.81 ± 0.39 to 39.70 ± 2.40 μM) than those on the first day of sampling, corresponding with an increase in stratification, as shown in the profiles of the other three parameters. The low oxygen here allowed for the accumulation of H_2S and a decrease in Mn(III)L concentration. In the presence of O_2, no H_2S was detected.

The concentrations of analytes measured in this study (dissolved Mn species, MnO_x, H_2S and dissolved Fe(II)) are summarized in Table 2.2, and Figure 2.2 shows their profiles from the first, second and fourth days of the sampling campaign.

Table 2.2 Results from August 2013 sampling. Blank spaces show where data were not available and 'ND' represents measurements below the detection limit. Time is EST, and tides are designated as 'HS'=High Slack and 'LS'=Low Slack. Percentage values represent the % Mn(III) of the Mn(Total). Errors represent the standard deviation where *n*= 2 or 3. Error value for MnO_x=0.01 µM, based on the limit of detection.

Date	CTD	Time	Depth (m)	Total Mn (µM)	Mn(III) (µM)	Mn(II) (µM)	MnOx (µM)	H_2S (µM)	Fe(II) (µM)
August 9	009-HS	18:55	22.8	12.23 ± 0.28	6.63 (54.2%)	5.60 ± 0.37	ND	7.03 ± 1.10	2.083 ± 0.007
			20.9	9.88 ± 0.25	3.16 (31.9%)	6.72 ± 0.17	ND	4.82 ± 0.80	
			18.6	15.02 ± 0.37	6.98 (46.5%)	8.04 ± 0.81	ND	4.51 ± 0.80	
			15.1	0.67 ± 0.08	ND	0.67 ± 0.08	4.89		
August 10	012-HS	7:17	22.1	6.11 ± 0.54	1.43 (23.4%)	4.68 ± 0.23	ND	12.35 ± 1.00	2.939 ± 0.065
			18.9	6.93 ± 0.21	1.33 (19.1%)	5.60 ± 0.23	ND	14.53 ± 1.60	3.000 ± 0.008
			17.1	8.02 ± 0.04	1.02 (12.7%)	7.00 ± 0.44	ND	4.28 ± 0.47	1.460 ± 0.094
	015-HS	20:11	22.6	6.53 ± 0.18	0.78 (11.9%)	5.75 ± 0.60	ND	14.05 ± 1.60	
			17.3	6.95 ± 0.21	0.26 (3.7%)	6.69 ± 0.21	ND	13.86 ± 1.10	
			14.5	2.06 ± 0.25	0.26 (12.4%)	1.80 ± 0.20	4.05		
			13.9	1.32 ± 0.46	0.73 (55.1%)	0.59 ± 0.11	4.01		
August 11	019-HS	7:27	22.4	7.25 ± 0.06	1.09 (15.0%)	6.16 ± 0.08	ND	12.75 ± 1.80	2.203 ± 0.031
			19.1	7.38 ± 0.08	0.73 (9.8%)	6.65 ± 0.28	ND	11.66 ± 1.90	2.557 ± 0.006
			15.8	2.30 ± 0.36	0.25 (10.7%)	2.05 ± 0.08	ND		0.022 ± 0.020
			14.2	1.61 ± 0.16	ND	1.61 ± 0.16	3.39		
	020-LS	13:54	21.3	7.97 ± 0.17	1.12 (14%)	6.85 ± 0.14	ND	38.37 ± 1.70	
			17.2	8.15 ± 0.12	0.78 (9.5%)	7.37 ± 0.06	ND	26.11 ± 2.10	
			11.4	2.52 ± 0.31	0.24 (9.5%)	2.28 ± 0.09	2.54		
			10.5	1.74 ± 0.26	ND	1.74 ± 0.26	3.01		
August 12	023-HS	7:16	21.8	7.22 ± 0.47	0.11 (1.5%)	7.11 ± 0.03	ND	24.15 ± 2.10	1.885 ± 0.031
			18.1	7.46 ± 0.06	0.71 (9.5%)	6.75 ± 0.07	ND	21.83 ± 1.90	2.167 ± 0.067
			13.3	6.84 ± 0.03	0.63 (9.2%)	6.21 ± 0.01	1.34		0.034 ± 0.089
			12.9	1.58 ± 0.25	0.43 (27.0%)	1.15 ± 0.04	6.58		
	026-LS	14:16	20.0	6.35 ± 0.35	0.62 (9.8%)	5.73 ± 0.40	ND	39.70 ± 2.40	
			17.0	6.18 ± 0.04	ND	6.18 ± 0.18	ND	37.79 ± 3.20	
			14.0	6.72 ± 0.05	ND	6.72 ± 0.21	ND	32.81 ± 0.39	
			10.3	2.80 ± 0.23	0.34 (12.1%)	2.46 ± 0.08	3.61		

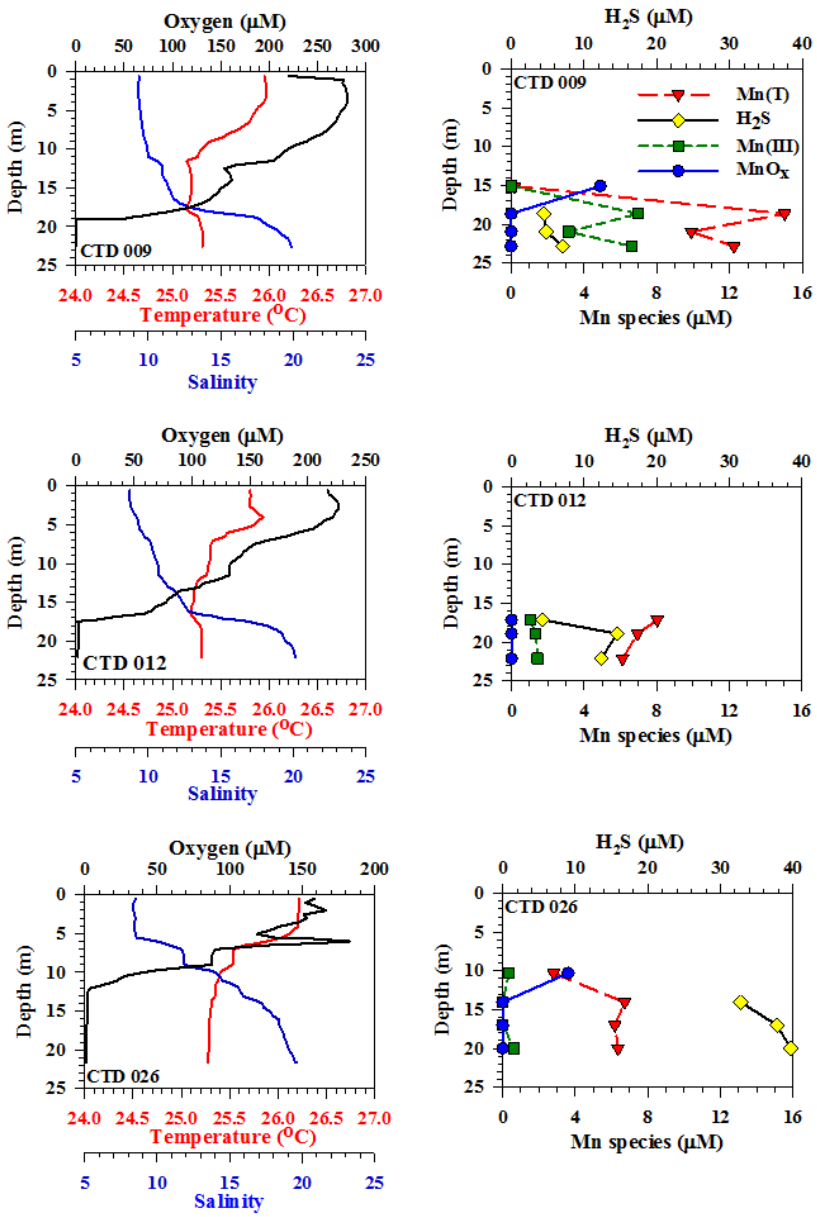

Figure 2.2 Depth profiles of Mn speciation and H_2S concentrations (right panels) in bottom waters and water column profiles of temperature, dissolved O_2 and salinity (left panels) from three casts (CTD009 = August 9, 18:55; CTD012 = August 10, 7:17; CTD29 = August 12, 14:16). The error bars are typically smaller than the symbols.

Measurements were made at three depths in the anoxic zone, and for most sampling events, at one depth in the oxic/suboxic interface. Dissolved Fe(II) in this study did not appear to be significantly correlated to Mn, and it ranged from non-detectable to 3.00 ± 0.008 μM throughout the sampling period. Total dissolved Mn [Mn_{total}] ranged from 0.67 ± 0.08 to 15.02 ± 0.37 μM at this site. Mn_{total} was below 3 μM near the suboxic zone, but increased over time. The lower Mn_{total} values corresponded with higher values of MnO_x, which ranged from 0.53 – 7.59 μM throughout the water column, with higher concentrations within and just above the suboxic zone. This inverse correlation with Mn_{total} suggests that the reduction of MnO_x particles acts as a source of dissolved Mn from oxic to anoxic waters. Herszage and dos Santos Afonso (2003) performed a kinetic study and observed the reductive dissolution of Mn(IV) oxides by H_2S, but they only measured total Mn by atomic absorption spectroscopy. The speciation results from our study indicate the potential presence of strong binding ligands, which could support some dissolution of Mn oxides as a source of Mn(III) to the suboxic water column.

The speciation of Mn changed over the course of this sampling campaign. On the first day of sampling, Mn(III) comprised 31.9 to 54.2 % of the total dissolved Mn in the suboxic zone, whereas on the last day of sampling it ranged from below the limit of detection to 9.5 %. This change in speciation can be explained by the reducing conditions of the system, as highlighted by the spectrophotometric results in Figure 2.3. This figure gives UV/Vis measurements made for two samples: one representative sample from the first day of sampling, and another from the last day of sampling. On the first day (Figure 2.3A), addition of the reducing agent hydroxylamine increased the

detected Mn by more than 2 μM (25 %). Subsequent addition of H_2S, an even stronger reducing agent, to that same sample yielded a total of more than 50% the first initial measurement. With the addition of excess reducing agent, Mn(III) complexes are reduced and the resulting Mn(II) is able to be bound to the added porphyrin (T(4-CP)P) and then detected. We found that an excess of H_2S acted as an even stronger reducing agent than hydroxylamine, which is significant because H_2S is present in the anoxic water column. On the last day of sampling (Figure 2.3B) addition of the reducing agent to the samples did not significantly increase the Mn_{total}. This sample already had a high sulfide concentration, so any Mn(III)-L complexes were already reduced in the water column. Thus, these data indicate that strong Mn(III)-L complexes are present in the suboxic and anoxic waters of the Chesapeake Bay.

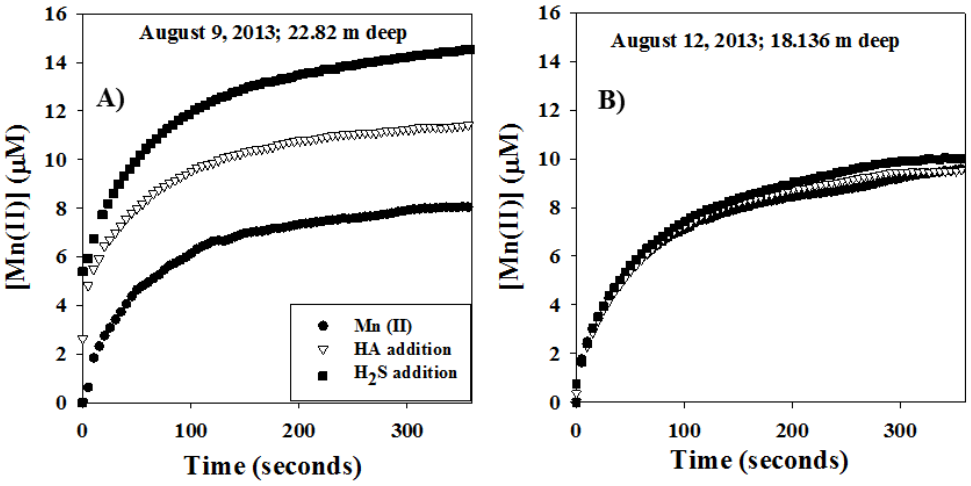

Figure 2.3 Change in kinetics plots for Mn species with and without the addition of reducing agents. Samples from (A) the beginning of the sampling campaign show an increase of Mn with addition of reducing agents and (B) the end of the sampling campaign show no increase in Mn with addition of reducing agents.

This relationship between Mn(III)-L complexes and H_2S, over the course of the sampling period, is highlighted in Figure 2.4, where the concentrations for the samples from our lowest two depths in the anoxic zone are shown. Where sulfide measurements were high, Mn(III) measurements were correspondingly lower, and vice versa. Where H_2S concentrations were low, Mn(III) was not completely reduced to Mn(II) by H_2S,

and was stabilized in solution by strong-binding ligands as Mn(III)-L. As the sampling campaign progressed and H_2S levels increased in the anoxic water column, Mn(III)-L complexes became reduced in the system, and Mn_{total} was only present as Mn(II). These data suggest a coupled cycling between Mn(III)-L complexes and H_2S. To determine if Mn(III)-L complexes were being released to the overlying waters from the sediments, we analyzed the overlying waters from a multi-core. Mn(III) was non-detectable as only a two-parameter fit (eq. 2.1) was needed with and without the addition of H_2S (H_2S in the overlying water was greater than 20 μM). This result suggests that sediment flux at this time was not a significant source of Mn(III) to the water column. These data suggest that, in the productive summer months, manganese oxides form through the microbial oxidation of Mn(II) by O_2 allowing MnO_x particle flux from the oxic/suboxic zone to the anoxic zone. Then these particles are partially reduced by low H_2S to form Mn(III), which is then stabilized by the presence of strong-binding organic ligands as Mn(III)-L. When oxygen penetrates to the sediment water interface, Mn(II) could be oxidized in the lower water column, particularly when O_2 concentrations are low but measurable. Then ambient organic ligands could stabilize Mn(III), which accumulates as Mn(III)-L in bottom waters. When intense stratification occurs, H_2S accumulates in the anoxic zone, completely reducing the Mn(III)-L complexes to dissolved Mn(II).

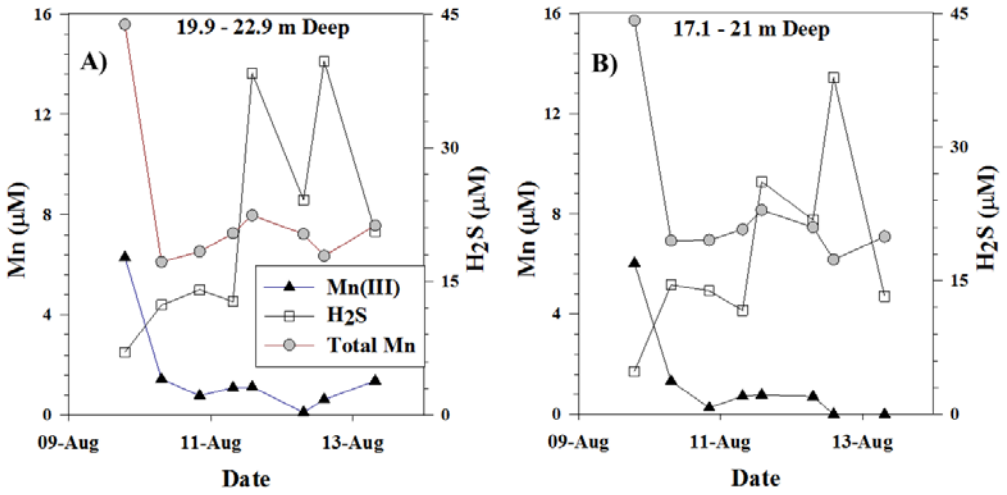

Figure 2.4 Change in Mn(III) and H_2S concentrations over time at the two bottom depths sampled (A=deepest, B=second deepest), throughout the sampling campaign.

Duckworth and Sposito (2005) found that the ligand DFOB promotes the dissolution of manganite (γ-MnOOH) through reductive and nonreductive reaction pathways at pH>6.5, followed by stabilization of the soluble complex Mn(III)-DFOB. In another experiment, Duckworth and Sposito (2007) found that synthetic and biogenic Mn(III/IV) oxides (including δ-MnO_2) underwent reductive dissolution promoted by DFOB, and that these rates were slightly higher for Mn(III) bearing oxides, and higher than that of Fe(hydr)oxides. Pena et al., (2007) also found that the rate of dissolution of hausmannite (Mn_3O_4) increased by several orders of magnitude in the presence of

DFOB, again forming a stable and soluble Mn(III)-DFOB complex. To test whether the dissolution of MnO_x particles was a likely source of Mn(III) in our system, an experiment was conducted in the laboratory where 100 μM colloidal MnO_2 suspensions were prepared to test MnO_2 reactivity with 100 μM H_2S and 100μM DFOB separately and in combination for a reaction time of 15 minutes. The results are displayed in Figure 2.5. All three solutions reduced MnO_2 to Mn(II) alone, or Mn(II) and Mn(III)DFOB. Figure 2.5A shows that Mn(III) was not detected in the presence of H_2S and MnO_2 alone. However, in the presence of DFOB alone (Figure 2.5C), more Mn(III)-DFOB was stabilized than when DFOB and H_2S were both present (Figure 2.5B). Figure 2.5C also indicates that DFOB reductively dissolves MnO_2, and the structure of DFOB indicates that the amine (NH_2) is the likely reducing ligand group. We also reacted MnO_2 with catechol and found that it was completely reduced to Mn(II), whereas dihydroxybenzoic acid did not dissolve MnO_2. Although Mn(III)-PP reacted with catechol forming Mn(III)-catechol, this complex was observed to be reduced to Mn(II) so the complex was not stable. Though more Mn(III)-DFOB was stabilized in the solution containing MnO_2 and DFOB alone, it is significant that Mn(III)-DFOB was still stable in the presence of 100 μM H_2S (1:1:1 ratio of all three reactants in Figure 2.5B). These data confirm that ligands are likely stabilizing Mn(III) as an intermediate of MnO_2 reduction in the Chesapeake system, despite H_2S also being present. Early in our Chesapeake Bay cruise the ratio of H_2S:Mn(III)-L complexes was near 1 in the anoxic zone; thus, we posit that these chemical species coexist due to kinetic considerations.

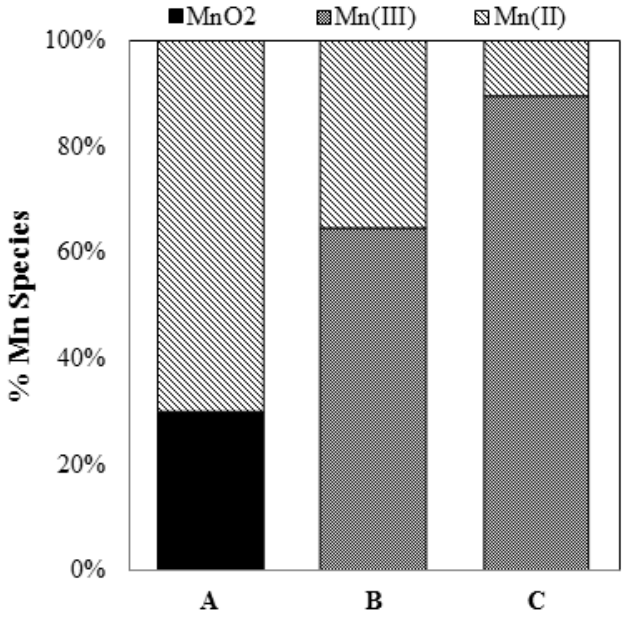

Figure 2.5 Relative percentages of Mn(II), Mn(III)-DFOB and MnO_2 are shown after three separate additions to 100 µM MnO_2: (A) 100 µM H_2S, (B) 100 µM H_2S and 100 µM DFOB and (C) 100 µM DFOB.

The dissolution of MnO_2 (Trouwborst et al., 2006) is a likely source of Mn(III) to the anoxic water column. Also, the water column here is a decomposition zone in the summer. Therefore, the flux of particulate organic matter to the suboxic and anoxic zones is high, and the lysing of phototrophic cells could act as a source of Mn(III), since Mn(III) is an important component of photosystem II.

To determine whether the natural ligand(s) of the Chesapeake Bay falls into a strong, or weak binding ligand class, its kinetics with respect to the addition of T(4-CP)P was assessed. Our adopted value for k_f is 10^9 $M^{-1}s^{-1}$ based on the water exchange rate for Mn(III) and other Jahn-Teller distorted ions. Using the steady state approximation, Luther et al (2015) showed that k_2 in eq. 3 is k_d; thus, K_{cond} can be

evaluated with these kinetic data and eq. 1a for weaker binding ligands. First, when a two-parameter fit followed the kinetic data (eq. 2.2), and no reduction of a Mn(III)-L was observed upon addition of excess H_2S, it was deemed that Mn(III) bound to ligands was not present in detectable concentrations (less than 50 nM). Second, when a two-parameter fit followed the kinetic data and there was an increase in total Mn concentration upon addition of H_2S, reduction of a Mn(III)-L was observed and a strong binding ligand was deemed present. Third, when the four-parameter fit followed the kinetic data (eq. 2.3), a weak binding Mn(III) ligand was deemed present; however, in this study we did not find evidence for weak binding ligands as they likely could not compete with the stronger binding ligands. In the suboxic St. Lawrence sediment pore-waters, a weak ligand class was determined (Madison et al., 2013), and Luther et al (2015) determined that $K_{Mn'L}$ for those complexes ranged from 1.39 to 4.35 x 10^{11} M^{-1}. The data from this study indicate that the complexes in the anoxic Chesapeake Bay waters were much stronger, even stronger than laboratory complexes with DFOB ($K_{Mn'L}$ = 3.53 x 10^{12} M^{-1}) and the other known ligands examined in this study. Table 2.3 gives the kinetic data for the reaction of three Mn(III)-catecholate complexes treated with the porphyrin method, in deionized water. The Mn(III) complexes of Tiron, Catechol and dihydroxybenzene have very similar reaction kinetics, and are less reactive than Mn(III)DFOB by a factor of 2.3 indicating that they have a value of 8.07 x 10^{12} M^{-1} for $K_{Mn'L}$ in seawater. The ligands 2,3-dihydroxypyridine, dopamine and Ferrozine bound to Mn(III) all had curves overlapping these catechol compounds. The Mn(III)-2,3-dyhydroxybenzoic acid and Mn(III)-Tiron were stable in the lab for six weeks, but the other Mn(III)-L complexes degraded more rapidly. For example, the Mn(III)-catechol undergoes internal redox reactions to form Mn(II) within 30 minutes, whereas the

Mn(III)-ferrozine and Mn(III)-dihydroxybenzoic acid were stable for a day. The complexes observed in the laboratory eventually were able to be substituted using the porphyrin method here, but the Chesapeake Bay samples required reduction with H_2S before they were detectable. These data indicate that the natural ligands in the Chesapeake Bay have higher stability constants (>8.07 x 10^{12} M^{-1}) than the ligands we examined in the laboratory, and are on very similar to the highest constants found for Fe(III) binding ligands (Gledhill and Buck, 2012). Estuarine DOC is often comprised mostly of humic matter, and therefore it is possible that functional groups from humic matter are responsible for stabilizing Mn(III) in the Chesapeake Bay.

Table 2.3 The resulting kinetic constants are from the first order regression analysis of the formation curve as in eqs 2 and 3.. The kinetic formation constant from the ligand exchange reaction, k_2, from eq. 5 represents k_d from eq. 1 as shown in Luther et al (2015). The reactions were performed in deionized water.

ID	$k_2 = k_d$ (s^{-1})	R^2
Tiron	1.4 x 10^{-3}	0.999
Dihydroxybenzoic Acid	1.4 x 10^{-3}	0.999
Catechol	1.3 x 10^{-3}	0.997
Desferrioxamine-B	3.2 x 10^{-3}	0.999

2.4 Conclusion

In this study, measurements for manganese speciation were made over depth at one location over four days in the Chesapeake Bay, which was undergoing an increase in stratification. At the beginning of the sampling campaign, a weakly stratified zone with low H_2S in the anoxic zone had high levels of Mn(III)-L complexes (54.2 ± 2.71 %

of the total dissolved Mn). Four days later, an intensely stratified system was observed with higher H_2S levels in the anoxic bottom waters and lower to non-detectable levels of Mn(III)-L complexes were observed. These results indicate that Mn(III)-L complexes were reduced by the higher levels of H_2S. In this study, we posit that the partial reductive dissolution of MnO_2 acts as a source of Mn(III) to the anoxic zones. The reduction could occur from the ambient ligands, the H_2S, or a combination of the two as demonstrated in the DFOB and H_2S experiments in Figure 2.5. The Mn(III) detected in the Chesapeake Bay was stabilized by strong binding natural ligands. This is in contrast with previous work by Madison et al. (2013) in suboxic and non-sulfidic pore waters of the St. Lawrence Estuary, where only a weak ligand class was detected. The difference between the strong and weak class was determined based on the kinetics of Mn(III)-porphyrin formation. Mn(III) in the weak complexes is slowly transferred to the porphyrin to form Mn(III)-porphyrin chelates, whereas the Mn(III) complexes with strong ligands is not transferred. The results from this study highlight how Mn(III)-L complexes play an important role in the cycling of Mn in the water column. Here these complexes are important in oxidizing sulfide.

2.5 Acknowledgements

This work was supported primarily by research grants from the chemical oceanography program of the National Science Foundation (OCE-1155385 to GWL and OCE-1154357 to BMT) and with partial support from the U.S. National Oceanic and Atmospheric Administration Sea Grant program (NA14OAR4170087). Veronique Oldham thanks University of Delaware for receipt of a Marian R. Okie Fellowship. Thanks to Alyssa Findlay and Dan MacDonald for the Fe and sulfide analyses. Thanks

also to Gabriel Browning, for his technical assistance with UV/Vis analyses, and the crew and staff of the R/V *Sharp*, who made sampling for this research possible.

REFERENCES

Boynton, W.R., Kemp, W. M., and Keefe, C.W. (1982). A comparative analysis of nutrients and other factors influencing estuarine phytoplankton production. In: Kennedy, V.S. (ed.) Estuarine comparisons. Academic Press, New York, p.69-90.

Bricker, O. (1965). Some stability relations in the system Mn-O_2-H_2O at 25 degrees and one atmosphere total pressure. *Am. Mineralog.* 50, 1296-1354.

Brendel, P. J. and Luther, III, G.W. (1995). Development of a gold amalgam voltammetric microelectrode for the determination of dissolved Fe, Mn, O_2 and S(-II) in porewaters of marine and freshwater sediments. *Environ. Sci. Technol.* 29, 751-761.

Dismukes, G. C. (1986). The Metal Centers of the Photosynthetic Oxygen-Evolving Complex. *Photochem. Photobiol.* 43, 99–115.

Duckworth O. W. and Sposito G. (2005). Siderophore-manganese(III) interactions I. Manganite dissolution promoted by desferrioxamine-B. *Environ. Sci. Technol*. 39, 6045-6051

Duckworth, O.W. and G. Sposito (2007). Siderophore-promoted dissolution of synthetic and biogenic layer-type Mn oxides. *Chem. Geolog.* 242, 497-508.

Duckworth, O. W., Bargar, J. R., and Sposito, G. (2009). Coupled biogeochemical cycling of iron and manganese as mediated by microbial siderophores. *Biometals*. 22, 605–13.

Gledhill, M., and Buck, K.N. (2012). The organic complexation of iron in the marine environment: a review. *Front. Microbiol.* 3, 1-17.

Herszage, J., and dos Santos Afonso, M. (2003). Mechanism of Hydrogen Sulfide Oxidation by Manganese (IV) Oxide in Aqueous Solutions. *Langmuir*. 19, 9684–9692.

Klewicki, J. K. and Morgan, J.J. (1998). Kinetic behavior of Mn(III) complexes of pyrophosphate, EDTA and citrate. *Environ. Sci. Technol.* 32, 2916-2922.

Konovalov, S. K., Luther, III, G.W., Friederich, G.E., Nuzzio, D. B., Tebo, B.M., Murray, J.W., Oguz,, T., Glazer, B., Trouwborst, R.E., Clement, B., Murray, K.J., and Romanov, A.S. (2003). Lateral injection of oxygen with the Bosporus plume: fingers of oxidizing potential in the Black Sea. *Limnol. Oceanogr.* 48, 2369-2376.

Kraemer, S.M., (2004). Iron oxide dissolution and solubility in the presence of siderophores. *Aqu. Sci.* 66, 3-18.

Lin, H., Szeinbaum, N. H., DiChristina, T. J., & Taillefert, M. (2012). Microbial Mn(IV) reduction requires an initial one-electron reductive solubilization step. *Geochim. Cosmochim. Acta.* 99, 179–192.

Luther, III, G. W., Nuzzio D. B., and Wu J. (1994). Speciation of manganese in Chesapeake Bay waters by voltammetric methods. *Anal. Chim. Acta.* 284, 473-480.

Luther III, G. W., Sundby, B., Lewis, B.L., Brendel, P.J., and Silverberg, N. (1997). Interactions of manganese with the nitrogen cycle: Alternative pathways to dinitrogen. *Geochim. Cosmochim. Acta.* 61, 4043-4052.

Luther, III, G. W. (2005). Manganese(II) oxidation and Mn(IV) reduction in the environment—two one-electron transfer steps versus a single two-electron step. *Geomicrobiol. J.* 22, 195-203.

Luther III G. W., Glazer B. T., Ma S., Trouwborst R. E., Moore T. S., Metzger E., Kraiya C., Waite T. J., Druschel G., Sundby B., Taillefert M., Nuzzio D. B., Shank T. M., Lewis B. L. and Brendel P. J. (2008) Use of voltammetric solid-state (micro)electrodes for studying biogeochemical processes: Laboratory measurements to real time measurements with an in situ electrochemical analyzer (ISEA). *Mar. Chem.* 108, 221-235.

Luther, III, G. W. (2010) The role of one and two electron transfer reactions in forming thermodynamically unstable intermediates as barriers in multi-electron redox reactions. *Aquat. Geochem.* 16, 395-420.

Luther, G.W. III, A.S. Madison, A. Mucci, B. Sundby and V. E. Oldham. 2015. A kinetic approach to assess the strengths of ligands bound to soluble Mn(III). *Mar. Chem.* 173, 93-99.

Luther, III, G. W. (2010). The role of one- and two-electron transfer reactions in forming thermodynamically unstable intermediates as barriers in multi-electron redox reactions. *Aqu. Geochem.* 16, 395–420

Madison, A.S., Tebo, B.M., Luther, G.W. (2011) Simultaneous determination of soluble manganese(III), manganese(II) and total manganese in natural (pore)waters. *Talanta*. 84, 374-381.

Madison, A. S., Tebo, B.M., Mucci, A., Sundby, B., and Luther, III, G.W. (2013). Abundant porewater Mn(III) is a major component of the sedimentary redox system. *Science.* 341, 875-878.

McCarthy, M., Pratum, T., Hedges, J., and Benner, R. (1997). Chemical composition of dissolved organic nitrogen in the ocean. *Nature.* 390, 150-154.

Nico, P. S. and Zasoski, R.J. (2001). Mn(III) center availability as a rate controlling factor in the oxidation of phenol and sulfide on δ-MnO_2. *Environ. Sci. Technol.* 35, 3338.

Pena, J., Duckworth, O.W., Bargar, J., and Sposito, G. (2007). Dissolution of hausmannite (Mn_3O_4) in the presence of the trihydroxamate siderophore desferrioxamine B. *Geochim. Cosmochim. Acta.* 71, 5661-5671.

Perez-Benito J. F., Brillas E. and Pouplana R. (1989) Identification of a soluble form of colloidal manganese (IV). *Inorg. Chem.* 28, 390–392.

Rozan, T. F., Theberge, S.M., and Luther, III, G.W. (2000). Quantifying elemental sulfur (S^0), bisulfide (HS^-) and polysulfides (S_x^{2-}) using a voltammetric method. *Anal. Chim. Acta.* 415, 175-184.

Stookey L.L. (1970). Ferrozine- A New Spectrophotometric Reagent for Iron. *Anal. Chem.* 42, 779-781.

Stumm, W. and Morgan, J.J., 1996. Aquatic Chemistry. Wiley-Interscience, New York (1996): 1022 pp.

Tebo, B. M. (1991). Manganese(II) oxidation in the suboxic zone of the Black Sea. *Deep-Sea Res.* 38, S883-S905.

Trouwborst, R. E., Clement, B.G., Tebo, B.M., Glazer, B.T., and Luther, III, G.W. (2006). Soluble Mn(III) in suboxic zones. *Science*. 313, 1955-1957.

Webb, S. M., Dick, G. J., Bargar, J. R., and Tebo, B. M. (2005). Evidence for the presence of Mn(III) intermediates in the bacterial oxidation of Mn(II). *Proceed. Nat. Acad. Sci. Am.* 102, 5558–5563.

Yakushev,E., Pakhomova, S., Sørenson, K., and Skei, J. (2009). Importance of the different manganese species in the formation of water column redox zones: Observations and modeling. *Mar. Chem.* 117, 59-70.

Yakushev, E.V., F. Pollehne, G. Jost, I. Kuznetsov, B. Schneider and L. Umlauf. (2007). Analysis of the water column oxic/anoxic interface in the Black and Baltic seas with a numerical model. *Mar. Chem*. 107, 388-410.

Chapter 3

OXIDATIVE AND REDUCTIVE PROCESSES CONTRIBUTING TO MANGANESE CYCLING AT OXIC-ANOXIC INTERFACES[2]

Abstract

Manganese (Mn) is important in seawater as a micronutrient, scavenger and as a reactant in the redox cycles of many other biologically important elements. In seawater, Mn cycles between oxidized insoluble Mn(III/IV) oxides (MnO_x) and soluble Mn (II/III) species (dMn_T), which include Mn(III)-L complexes and reduced Mn(II). The Mn(III)-L complexes have been shown to be stable in oxic, suboxic and anoxic systems, but the formation pathways for these complexes have not been well described at one location over a short timescale. In order to better understand these pathways, dissolved and particulate Mn speciation was determined in the water column of the seasonally stratified Chesapeake Bay basin over a 2 day period, using pump profiling for better spatial resolution (10 cm) of redox active species and a modified, low-level spectrophotometric method for soluble Mn speciation (detection limit = 3 nM). The concentrations of Mn species, H_2S and O_2 with depth were used to determine potential pathways of Mn(III)-L formation at the oxic-anoxic interface. Our data show that Mn(II) fluxes out of the anoxic sediments (bottom water total Mn: 2.23 – 3.80 μM; *Mn(II) = 61 – 84 % of total Mn*) and is oxidized to MnO_x at the top of suboxic zone of the water column at non-detectable dO_2 levels (≤ 3 μM; suboxic water total Mn: 1.51 –

---

[2] *Chapter 3 submitted to Marine Chemistry: Special Issue Honoring Frank Millero.*

3.78 µM; *9.6 – 97.7 % MnO_x*), probably through microbial activity. These biogenic Mn oxides are reduced at the suboxic-anoxic interface via a combination of strong ambient Mn(III)-binding ligands, H_2S and/or microbial activity, resulting in the disappearance of MnO_x and formation of Mn(III)-L complexes and Mn(II). The Mn(III)-L complexes are kinetically stable against complete reduction by H_2S in the presence of 10-fold excess H_2S to dMn_T. The oxic water column has lower concentrations of dMn_T (0.05 – 0.18 µM), with Mn(III)-L complexes present in all oxic samples (33 – 80 % of dMn_T). The complexes in the oxic water column likely arise from processes distinct from the suboxic and anoxic zones below. Our results highlight that redox cycling of Mn(III) is occurring at least daily at this site and is likely dominated by microbial Mn(II) oxidation at the top of the suboxic zone and MnO_x reduction pathways at the base of the suboxic zone.

3.1 Introduction:

Manganese is an essential micronutrient that exists in oxygenated systems as thermodynamically stable insoluble Mn(III/IV) oxides (defined as MnO_x), which are not directly available to organisms for uptake. Because Mn(IV) is an inert cation, reductive dissolution is required to solubilize it; however, Mn(III) is a labile cation and can be solubilized by both reductive and non-reductive processes (Duckworth and Sposito, 2007; Luther et al, 2015). Bioavailable soluble Mn exists as Mn(II), which is thermodynamically unstable in oxic waters, but due to slow abiotic oxidation of Mn(II), is considered to be present in most surface seawater (Landing and Bruland, 1980). In the last decade, soluble Mn has been found to also include Mn(III)-L complexes. These were first measured in suboxic (Trouwborst et al, 2006; Yakushev et al, 2007, 2009; Dellwig et al, 2012; Madison et al, 2013) and anoxic seawater systems (Oldham et al,

2015). However, more recently, Oldham et al, (in press) showed that Mn(III)-L complexes can also be stabilized in oxygenated surface waters, indicating that these complexes are likely ubiquitous in seawater. Due to the limited number of studies on Mn(III)-L complexes in the environment, their pathways of formation are not well studied but are thought to be diverse. Seven potential pathways of Mn(III)-L formation are summarized in Table 3.1, and were adapted from Madison et al (2013) and Oldham et al (2017): (eq. 3.1) bacterial oxidation and subsequent ligand stabilization (Parker et al, 2004; 2007), (eq. 3.2) ligand-promoted oxidation of Mn(II) (Duckworth and Sposito, 2005) (eq. 3.3) superoxide-promoted oxidation of Mn(II) and ligand stabilization (Learman et al, 2013), (eq. 3.4) bacterial reduction of Mn(IV) solid phases and ligand stabilization (Lin et al, 2012), (eq. 3.5) non-reductive organic ligand-promoted dissolution of Mn(III) in MnO_x (Duckworth and Sposito 2005; 2007) and (eq. 3.6) chemical reduction of Mn(IV) in MnO_x by reductants such as H_2S or Fe(II) followed by ligand stabilization (Madison et al, 2013; Oldham et al, 2015) and (eq. 3.7) chemical reduction of Mn(IV) in MnO_x by ligands (Duckworth and Sposito, 2007; Parker et al, 2007; Oldham et al, 2015). Both oxidative and reductive reactions are likely important in the formation of Mn(III)-L complexes in seawater, depending on the conditions of the marine environment. Thus, in a given system, the dominant pathway by which Mn(III)-L complexes are formed depends on the concentration of dissolved O_2 (dO_2), the concentration of reductant, the bacterial community, as well as the abundance and nature of organic ligands.

Table 3.1 Summary of potential Mn(III)-L formation pathways in the Chesapeake Bay. Reactions are unbalanced. See text in the introduction for appropriate references for each equation.

Equation	Reaction mechanism (unbalanced)	Process
3.1	$Mn(II) + O_2 + L \xrightarrow{bacteria} Mn(III) - L$	Bacterial oxidation
3.2	$Mn(II) + L_{ox} \rightarrow Mn(III) - L$	Ligand-promoted oxidation
3.3	$Mn(II) + O_2^- + 2H^+ + L \rightarrow Mn(III) - L + H_2O_2$	Superoxide-promoted oxidation
3.4	$MnO_2 + L \xrightarrow{bacteria} Mn(III) - L$	Bacterial reduction
3.5	$Mn(III)O_x + \mathrm{L} \rightarrow Mn(III) - L$	Ligand-promoted non-reductive dissolution
3.6	$Mn(IV)O_x + H_2\mathrm{S} + \mathrm{L} \rightarrow Mn(III) - L$	Chemical reduction
3.7	$Mn(IV)O_x + \mathrm{L} \rightarrow Mn(III) - L$	Ligand-promoted reductive dissolution

The Chesapeake Bay is an ideal model system for examining the formation of Mn(III)-L complexes because dissolved Mn concentrations can exceed 18 µM (Trouwborst et al, 2006); the bay is highly productive in the summer months; the bay exhibits seasonal stratification due to density differences in the water column, resulting in bottom water anoxia (Boynton et al, 2006); and Mn(III)-L complexes have been shown to make up to 54 % of the total dissolved Mn (dMn_T) in the bay's anoxic bottom waters (Oldham et al, 2015). Therefore, many Mn(III)-L formation pathways are possible in this system as it is bacterially active, contains ligands capable of binding Mn(III) and other metals, and has the conditions for chemical reduction of Mn(IV) in MnO_x by H_2S in the summer months. The summer stratification of the Chesapeake is

due to decreased vertical mixing controlled by water masses of different density: warmer, fresher surface waters sit atop colder more saline waters, with a thin suboxic zone between (no more than 2-3 m thick, in this study). The resulting three layers have different chemistries due to the accumulation of different redox active species. The surface waters are oxic and contain more oxidized chemical species. There is a decreasing gradient in oxygen concentration to the mid-waters, with an interface marked by the disappearance of measureable oxygen. Beneath this interface is the suboxic mid-zone, containing neither oxygen nor hydrogen sulfide, and which is a dynamic part of the water column as a zone of mixing. The base of the suboxic zone is delineated by the appearance of H_2S, which accumulates in the bottom waters and in the absence of detectable O_2 as a result of sulfate reduction in the sediments releasing H_2S. These anoxic bottom waters are highly reducing, and chemical reduction by H_2S can result in the accumulation of other reduced species [i.e. Fe(II) or Mn(II)].

Previous work conducted in 2013 (Oldham et al, 2015) found Mn(III)-L complexes in the bottom waters of the Chesapeake Bay that were kinetically stable against reduction by H_2S, a strong reducing agent, as the two species were found to coexist at near equimolar concentrations (4.8 µM H_2S: 7.0 µM Mn(III)-L). The concentration of MnO_x was non-detectable (< 0.21 µM) in these anoxic bottom waters, which was interpreted to mean that the one electron reductive dissolution of Mn(IV) in MnO_x was responsible for the formation and subsequent stabilization of Mn(III)-L in this system (Oldham et al, 2015).

Lin et al (2012) indicate that because the partitioning between dissolved Mn(II) and MnO_2 occurs by two separate one-electron transfers, Mn(III)-L complexes should be stabilized as an intermediate during the reduction of solid phases containing Mn(IV). Mn(III) has also been shown to be an intermediate in the bacterial oxidation of Mn(II) to Mn(IV) (Webb et al, 2005; Parker et al, 2007). Mn redox cycling is expected to be most intense in systems where high concentrations of Mn(II) encounter O_2, such as at oxic-anoxic interfaces (Tebo et al, 2004, 2005). Thus the Chesapeake Bay, with the high concentration of dissolved Mn in the summer months (Trouwborst et al, 2006) and conditions in the water column that favor both reductive and oxidative pathways for Mn at different depths, presents an ideal system for studying the redox cycling of Mn between its solid and dissolved phases.

The aim of this study was to examine Mn cycling in different zones of the water column of the Chesapeake Bay, and to use chemical profiles to assess the relative importance of oxidative and reductive processes at redox gradients. To accomplish this, the water column above a 25 m deep depression in the Chesapeake Bay was sampled in August 2014. Pump cast profiling was used in this study to provide better spatial resolution (10 cm) and real-time voltammetric profiles, which allowed for sample selection based on redox gradients. Three pump profile casts were sampled and measured on board ship for Mn speciation using UV-Vis spectroscopy, and for hydrogen sulfide (defined as the sum of H_2S, HS^-, S_x^{2-}, and S_8) and dO_2 using voltammetry. Pump cast profiling provides better resolution than CTD sampling, and allows for samples to be taken based on the presence or non-detection of dO_2 or H_2S. Therefore, we were able to take samples above, in, and below the suboxic zone of the

Chesapeake Bay, where we anticipated intense biogeochemical cycling. The findings from this study provide environmental evidence for Mn(II) oxidation at the top of the suboxic zone, at extremely low concentrations (below the voltammetric detection limits) of oxygen, and for reductive dissolution of Mn(IV) solid phases by microbes and/or ligands as a source for Mn(III)-L complexes at the suboxic-anoxic interface of the Chesapeake Bay. This work also highlights the importance of Mn(III) as an electron acceptor and donor in low oxygen systems.

3.2 Methods

3.2.1 Sampling

During a sampling campaign from August 20th to 22nd, 2014, a 25 m depression in the Chesapeake Bay (Station 848, 38°58.54′ N; 076°22.22′ W), three pump profile casts were sampled for Mn speciation. A pump profiling system was used to pump water onto the deck of the ship, where it could pass through various flow cells for salinity, temperature and voltammetry measurements, and for water collection of discrete samples for Mn (MacDonald et al, 2014). The pump sampling provides 10 cm vertical resolution in the absence of wave action, as opposed to sampling from CTD rosette bottles from the ship with a 1 meter depth resolution. The pump profiler consisted of high pressure clear PVC tubing (30 m of 2.54 cm ID diameter) attached to a West Marine water pump (12VDC; flow rate of 4160 liters/hour) that was secured on to a stainless steel cage. Total time for water to pass through all the tubing is about 1 minute. On deck, the outlet of the tubing was split so water could be collected for discrete samples and to pass through the flow cells.

Samples were collected during slack portions of the high and low tides to ensure minimal tidal influence. Samples were taken from surface waters at several depths in and near the suboxic zone, and into the anoxic zone, as determined by the oxygen and hydrogen sulfide electrochemical profiles. Samples were collected directly from the pump cast apparatus into new, 50 mL falcon tubes (Fisher Scientific). Sampling contamination was minimized through the use of gloves and acid-washed tubing during sample collection. The exposure of samples to oxygen was minimized by removing air bubbles in the tubing and head-space of the tubes by overflowing the tubes three times, then capping the tubes. Samples were filtered within 15 minutes of collection through a 0.2 μm Millipore® syringe filter in a glove bag with an argon atmosphere to prevent oxygenation of the sample prior to analysis.

3.2.2 Voltammetric Measurements of O_2 and H_2S

Using the pump profiling system, sulfide and oxygen were determined in quintuplicate at each depth using a DLK-60 electrochemical analyzer (Analytical Instrument Systems Inc.). The flow cell was used in conjunction with a 100 μm Au/Hg amalgam PEEK microelectrode prepared according to Luther et al (2008). Cyclic voltammetry was performed from -0.1 V to -1.8 V, and back to -1.8 V at a scan rate of 2 V s^{-1} after conditioning at -0.9 V for 5 s then at -0.1 V for 2 s. These electrodes are capable of measuring an array of redox active species including oxygen, sulfide, thiosulfate, elemental sulfur, iron, and manganese (Luther et al, 2008). The detection limit of this method is 0.2 μM for sulfide and polysulfides, and 3 μM for oxygen.

3.2.3 Soluble Mn Speciation

The samples for dissolved Mn(II) were analyzed ship-board, in triplicate, within 1 hour of collection. Total dissolved Mn was analyzed in triplicate, either within 1 hour of collection, or the filtered sample was immediately frozen and later thawed and analyzed in the trace metal biogeochemical laboratory at the University of Delaware. Filtering and freezing has been shown to be a reliable storage method for soluble Mn speciation (Oldham et al, in press). In previous work, samples were analyzed using the established method of a spectrophotometric ligand ([α, β, γ, δ-tetrakis(4-carboxyphenyl)porphine] or T(4-CP)P (E= 95,400 M^{-1} cm^{-1}) previously developed by Ishii et al, (1982) and modified by Madison et al (2011) to speciate dissolved Mn(II) and weak Mn(III)-L. In this spectrophotometric method the sample solution in a 1 cm pathlength cell is brought to a pH of 7.5 – 8.0, conditions where Mn(II) outcompetes added Cd(II) to form a complex with T(4-CP)P when catalyzed by imidazole. The Mn(II) is rapidly oxidized to Mn(III) by dissolved oxygen, and the Mn(III)-T(4-CP)P exhibits an absorption peak at 468 nm and is measured using UV/Vis spectroscopy. Weak Mn(III)-L complexes undergo ligand substitution with the added porphyrin ligand, and reaction kinetics can be used to speciate Mn(II) from weak Mn(III)-L weak complexes ($\log K_{cond}$<13.2, Luther et al, 2015). The addition of a strong reducing agent, such as hydroxylamine or hydrogen sulfide, prior to analysis reduces any strong binding Mn(III)-L complexes in solution (i.e. complexes that are not outcompeted by the porphyrin ligand) allowing for a total dissolved Mn concentration; strong Mn(III)-L complexes can be determined from difference between the total dissolved Mn in the presence and absence of the reducing agent (Oldham et al, 2015).

In our previous 2013 cruise (Oldham et al, 2015), we found no evidence for Mn(III)-L weak complexes. Thus, the method was modified, as described in Oldham et

al, (in press), for a lower detection limit to measure Mn speciation for the entire water column since it was anticipated that dissolved Mn values would be near or below the detection limit from the methodology used in 2013 (50 nM; Oldham et al, 2015).

We modified the method of Madison et al (2011) for water column samples to achieve a detection limit of 0.3 nM (3× the standard deviation of a blank, 3 nM sample detection limit with dilution) by using a 100-cm pathlength liquid waveguide capillary cell and the addition of a heating step as well as a strong reducing agent for Mn speciation. All chemicals were A.C.S. reagent grade, and all solutions were prepared with deionized water (18.2 mΩ). As the absorbance is proportional to the cell pathlength, for low levels of Mn, the reagents described by Madison et al (2011) were diluted 100-fold to fit into the analytical detection window. The [T(4-CP)P] stock solution was 2.00×10^{-4} M (final sample concentration of 2.33×10^{-7} M), the borate buffer was made up to pH 8.0-8.2 using trace metal clean NaOH (final sample buffer concentration 4.16×10^{-4} M), and the $CdCl_2$ stock solution was prepared to 1.20×10^{-4} M (final sample concentration 2.40×10^{-7} M). All samples were analyzed in triplicate following 12 to 30-fold dilution into the reagents to yield a total Mn concentration in the range of 10-100 nM.

The rate of reaction is proportional to the concentration of reactants, and at the low levels of the modified method, the reaction is slow. Hence, a heating step, prior to analysis, is employed to accelerate the reaction kinetics. Because the Cd(II) in the porphyrin reacts with chloride in seawater, seawater samples are diluted to ensure reaction of the porphyrin with Mn(II); thus, the practical detection limit of the method is 3.0 nM. Recovery tests with $MnCl_2$ standards were performed, and the most successful recovery in a reasonable time period was achieved by heating at 90 °C for 1 hour (98-

106 % recovery; Oldham et al, 2017). For Mn speciation, strong Mn(III)-L complexes are reduced by an excess of a strong reducing agent, hydroxylamine (at least 100-fold expected dMnT concentration). Samples are analyzed first without hydroxylamine for dissolved Mn(II) and then with the addition of hydroxylamine for dMn_T (Mn(II) + Mn(III)-L). This method does not allow for the independent kinetic assessment of weak Mn(III)-L complexes, and can only determine the concentration of Mn(II) and strong Mn(III)-L complexes. Hence, any weak Mn(III)-L complexes would be reacted during this heating step. Oldham et al (2015) found strong Mn(III)-L complexes were present in the anoxic bottom waters of the Chesapeake Bay, however, due to the different methodology from Madison et al 2011, the data from this study doesn't allow for extrapolating on the presence or absence of weak Mn(III)-L complexes.

The liquid waveguide capillary cell (World Precision Instruments) was coupled to a UV-Vis spectrophotometer (Ocean Optics). In this spectrophotometric set up, a mini deuterium halogen light source (DT-Mini-2-GS) was coupled to a USB2000+ fiber optic spectrometer controlled with SpectraSuite software. The Mn(III)-T(4-CP)P complex was measured at its absorbance maximum (468 nm) against a reagent and sample blank. For small peaks, peak height was determined using an algorithm adapted to resolve small peaks with the application of linear fit tangent baseline subtraction (ECDSOFT, which can be found at: https://mojoblak.irb.hr/index.php/s/dxB24S8m5H6fsZW?path=%2FProMCC).

3.2.4 Particulate MnO_x Measurements

Known volumes of sample (20 mL) were filtered through 20 mm diameter 0.20 µm Whatman Nucleopore track-etched polycarbonate filters. Using the method of Altmann (1972), filters were amended with 2 mL of 0.0032 % leucoberbelin blue dye

(LBB, 65 % diluted, Sigma-Aldrich) in 1% acetic acid. The dye color, formed on oxidation by particulate manganese or MnO_x, was measured in a 1 cm cuvette at 624 nm using the Ocean Optics spectrophotometric set-up described above except the 1 cm cuvette holder. The LBB (410.5 g mol-1) stock solution is prepared by dissolution in Milli-Q water to a strength of 3.2 % w/w and adding 40 µL of 10 M sodium hydroxide (NaOH) per 10 mL of solution. Working solutions are made by diluting the stock into 1% acetic acid (made up in Milli-Q water), to 0.0032 % w/w. A calibration curve was generated using potassium permanganate (KMnO4). We expect that to produce an equivalent absorbance, 2.5 times more Mn(IV) is required than Mn(VII), since Mn(VII) oxidizes 5 LBB molecules, compared to 2 LBB molecules for Mn(IV). In a 100-cm pathlength cell, the limit of detection is 2.7 nM.

3.3 Results

The profiles of Mn speciation, dissolved O_2, H_2S, and salinity for the water column of the Chesapeake Bay are given in Figure 3.1 for the first two pump-casts; the third pump-cast, which focuses more on the suboxic zone, is given in Figure 3.2. Because the temperature gradient was minimal, it was not plotted, but data are given in Table 2. The water column in all three casts can be broken into three zones (Table 2): the *oxic surface waters* (~0 – 10 m; dO_2 = 273.58 µM – non-detectable; H_2S = non-detectable), the *suboxic mid waters* (~10 – 13 m; dO_2 and H_2S = non-detectable) and the *anoxic bottom waters* (~13 – 25 m; dO_2 = non-detectable; H_2S = non-detectable – 23.54 µM). These three zones are also delineated by a change in salinity: low salinity (9.5 – 13.4) in the oxic zone, mid-salinity (13.4 – 16.0) in the suboxic zone, and high salinity (16.0 – 18.2) in the anoxic zone. Thus, bottom waters represent more saline, oceanic water flowing into the Bay and surface waters represent fresher surface waters flowing

out of the Bay. This stratification of the Bay is more pronounced in the summer months, predominantly due to water masses of different salinity, but also because of slightly higher temperatures in surface waters (Table 3.2). Although all three casts show the same three zones of vertical stratification, the depth of each interface shifted between pump-casts. For example, from the first to second pump-cast, the suboxic-anoxic interface shifts: In the first pump-cast, the first detectable H_2S (4.01 µM) occurs at 13.4 m depth, compared to the second pump-cast, where H_2S is detectable at 12.1 m and the concentration is four times higher than in the first pump-cast (16.72 µM). Correspondingly, the speciation of Mn is variable between each pump-cast.

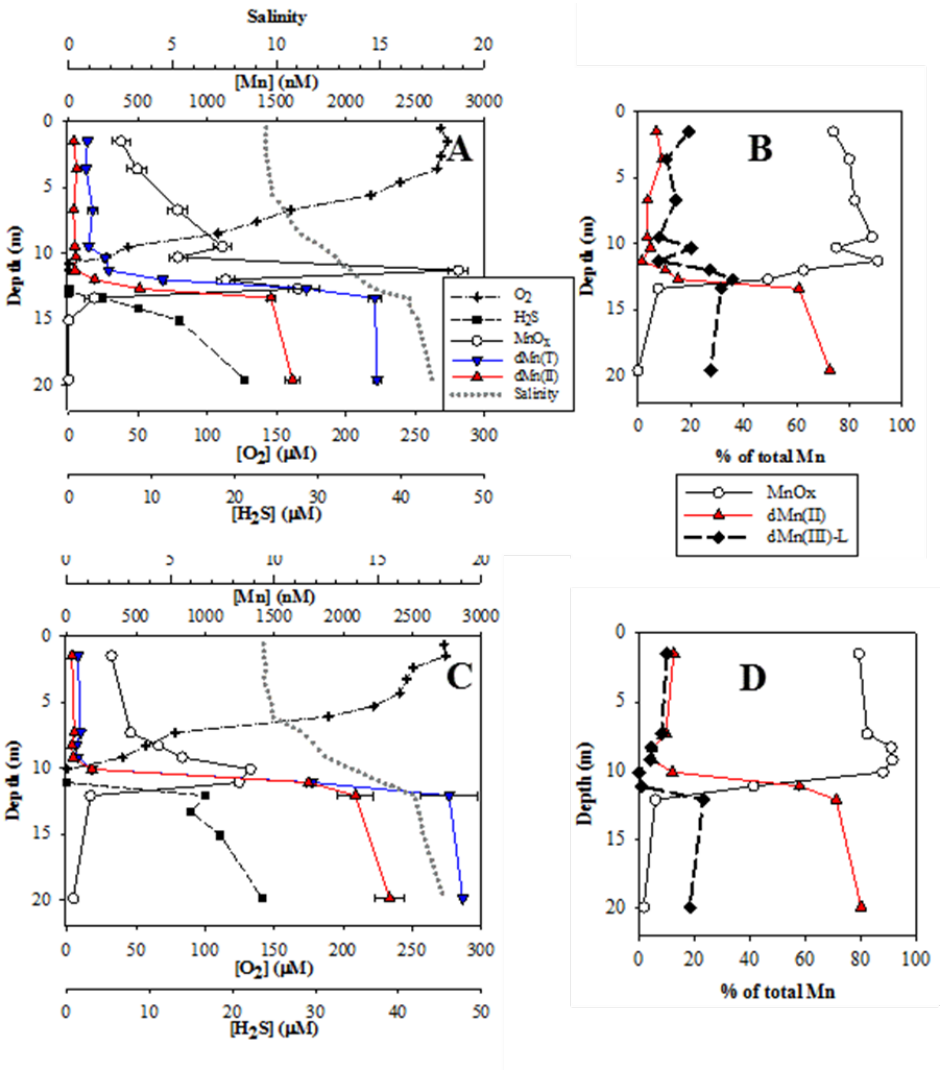

Figure 3.1 Water column Mn speciation data from August 21st (A and B) and 22nd (C and D) at slack tide. In Panels A and C, Mn speciation, dissolved O_2 and H_2S concentrations are shown. Standard deviations are given for Mn speciation measurements, and where not visible, are smaller than the symbols. Panels B and D show % Mn species of total Mn ([Mn species]/[MnT]*100).

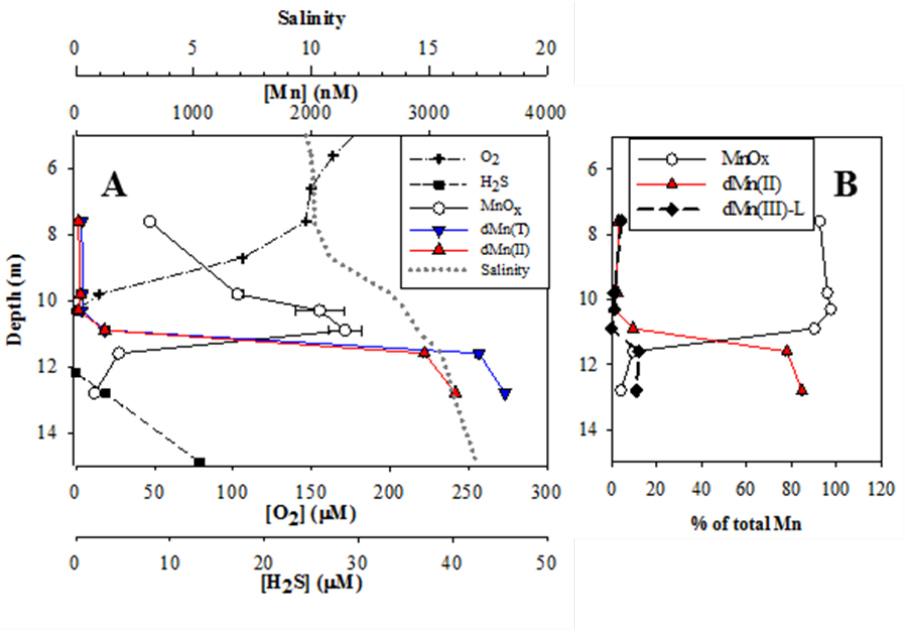

Figure 3.2 Panel A shows the suboxic zone Mn speciation data from August the afternoon of 22nd at slack tide. Mn speciation, dissolved O_2 and H_2S concentrations are shown. Standard deviations are given for Mn speciation measurements, and where not visible, are smaller than the symbols. Panel B shows the % of total Mn for each species of Mn

Total Mn (= MnO_x + dMn_T) concentrations were between 0.51 – 3.80 µM throughout the sampling campaign. These concentrations were lower than previous years at the same site (up to 18 µM dMn_T in 2005, Trouwborst et al, 2006; 0.5 – 15.0 µM dMn_T in 2013, Oldham et al, 2015), which highlights the inter-annual variability of biogeochemical cycling at this site (Lewis et al, 2007). The total Mn was below 1.50 µM in the oxic zone, increased within the suboxic zone (1.51 – 3.78 µM), and remained

high in the anoxic zone (2.23 – 3.80 µM), for all three pump-profiles (Table 3.2). However, the speciation of Mn changed significantly in each of the three zones.

Table 3.2 Results from the three pumpcasts sampled in August 2014. Blank spaces show where data were not analyzed and ND represents where measurements fell below the sample detection limit. Time is taken as local, EST. Percentage of each Mn species represents the % of total Mn (MnT in table). Errors reported the standard deviation where n= 3, where these = 0.00, they are smaller than 5 nM.

Date	Depth (m)	Salinity	Temp. (°C)	dO_2 (µM)	H_2S (µM)	Mn_T (µM)	MnO_x (µM)	% MnO_x	dMn_T (µM)	dMn(II) (µM)	% Mn(II)	dMn(III) (µM)	% Mn(III
21-Aug	1.5	9.5	27.8	273.6 ± 15.8	ND	**0.51**	0.38 ± 0.07	*73.9*	**0.13 ± 0.01**	0.04 ± 0.00	*7.0*	0.10	*19.2*
12:50	3.6	9.6	27.4	265.8 ± 7.7	ND	**0.62**	0.49 ± 0.07	*80.0*	**0.12 ± 0.01**	0.06 ± 0.00	*9.2*	0.07	*10.9*
	6.7	10.4	27.3	160.4 ± 6.8	ND	**0.96**	0.78 ± 0.07	*82.0*	**0.17 ± 0.04**	0.03 ± 0.00	*3.6*	0.14	*14.4*
Tide	9.5	12.2	27.1	42.9 ± 4.3	ND	**1.25**	1.11 ± 0.07	*88.6*	**0.14 ± 0.00**	0.04 ± 0.00	*3.5*	0.10	*7.9*
going	10.3	12.9	27.1	27.4 ± 2.5	ND	**1.05**	0.79 ± 0.07	*75.0*	**0.26 ± 0.02**	0.05 ± 0.00	*4.8*	0.21	*20.2*
out	11.3	13.6	27.1	ND	ND	**3.10**	2.81 ± 0.07	*90.7*	**0.29 ± 0.01**	0.04 ± 0.00	*1.4*	0.24	*7.9*
	12.0	14.0	27.3	ND	ND	**1.81**	1.13 ± 0.07	*62.6*	**0.68 ± 0.03**	0.19 ± 0.00	*10.3*	0.49	*27.1*
	12.7	14.7	27.1	ND	ND	**3.37**	1.65 ± 0.07	*49.1*	**1.71 ± 0.09**	0.51 ± 0.01	*15.2*	1.20	*35.8*
	13.4	16.4	27.1	ND	4.01 ± 0.69	**2.39**	0.18 ± 0.07	*7.7*	**2.21 ± 0.04**	1.46 ± 0.03	*61.0*	0.75	*31.3*
	14.2	16.4	26.9	ND	8.33 ± 1.64								
	15.1	16.8	27.1	ND	13.30 ± 0.82								
	19.6	17.5	27.1	ND	21.16 ± 1.23	**2.23**	ND	*0.0*	**2.23 0.03**	1.61 ± 0.05	*72.6*	0.61	*27.4*
	1.5	9.5	25.1	273.9 ± 11.0	ND	**0.40**	0.32 ± 0.00	*79.4*	**0.10 ± 0.00**	0.05 ± 0.00	*12.4*	0.04	*9.9*
22-Aug	7.3	11.4	25.4	78.2 ± 4.0	ND	**0.56**	0.46 ± 0.00	*82.4*	**0.10 ± 0.00**	0.05 ± 0.00	*9.6*	0.04	*8.0*
6:45	8.3	12.0	25.4	56.8 ± 2.9	ND	**0.73**	0.66 ± 0.00	*91.1*	**0.06 ± 0.00**	0.03 ± 0.00	*4.7*	0.03	*4.2*
	9.2	12.5	25.4	40.0 ± 3.9	ND	**0.91**	0.83 ± 0.00	*91.4*	**0.08 ± 0.00**	0.04 ± 0.00	*4.7*	0.03	*3.8*
Tide	10.1	13.8	25.3	ND	ND	**1.51**	1.33 ± 0.00	*88.1*	**0.18 ± 0.01**	0.18 ± 0.01	*11.9*	0.00	*0.0*
going	11.1	15.2	25.3	ND	ND	**3.02**	1.25 ± 0.00	*41.2*	**1.78 ± 0.03**	1.75 ± 0.02	*57.9*	0.03	*0.9*
in	12.1	16.8	25.4	ND	16.72 ± 1.16	**2.94**	0.17 ± 0.00	*5.8*	**2.77 ± 0.20**	2.09 ± 0.13	*71.1*	0.68	*23.1*
	13.3	17.0	25.3	ND	14.90 ± 0.74								
	15.1	17.2	25.1	ND	18.49 ± 0.59								
	19.9	18.2	25.0	ND	23.54 ± 0.57	**2.91**	0.05 ± 0.01	*1.6*	**2.87 ± 0.00**	2.34 ± 0.11	*80.2*	0.53	*18.2*
22-Aug	7.6	10.1	25.8	146.4 ± 57.3	ND	**0.67**	0.63 ± 0.02	*92.8*	**0.05 ± 0.00**	0.02 ± 0.00	*2.9*	0.03	*4.3*
17:50	9.8	13.4	25.8	14.5 ± 7.6	ND	**1.43**	1.37 ± 0.05	*96.1*	**0.06 ± 0.00**	0.04 ± 0.00	*2.6*	0.02	*1.3*
	10.3	14.0	25.8	ND	ND	**2.12**	2.07 ± 0.21	*97.7*	**0.05 ± 0.00**	0.02 ± 0.00	*0.9*	0.03	*1.3*
Tide	10.9	14.5	25.7	ND	ND	**2.53**	2.28 ± 0.14	*90.4*	**0.24 ± 0.00**	0.24 ± 0.00	*9.6*	0.00	*0.0*
going	11.6	15.5	25.7	ND	ND	**3.78**	0.36 ± 0.02	*9.6*	**3.42 ± 0.02**	2.96 ± 0.01	*78.2*	0.46	*12.2*
out	12.8	16.0	25.6	ND	3.09 ± 0.55	**3.80**	0.16 ± 0.02	*4.1*	**3.64 ± 0.02**	3.22 ± 0.02	*84.8*	0.42	*11.1*
	14.9	17.0	25.6	ND	13.10 ± 0.73								

In the oxic zone, MnO_x dominated total Mn speciation (73.9 – 96.1 % of total Mn) in all three casts, whereas soluble Mn speciation changed in each cast (Table 3.2). In the first cast, Mn(III) dominated dMn_T speciation (0.067 – 0.212 µM; 54.3 – 80.8 % of dMn_T), whereas in the second cast, Mn(III) was lower (0.031 – 0.045 µM; 44.5 – 47.5 % of dMn_T). In all three casts, the highest total Mn in the oxic zone occurred just above the oxic suboxic interface.

The suboxic zone had markedly higher total Mn than the overlying oxic zone, a trend best seen in the first cast, where total Mn nearly triples (1.05 – 3.10 µM) in the 1 meter interface where dO_2 becomes non-detectable. The speciation of Mn in the suboxic zone is variable between casts, but MnO_x is consistently highest for each cast in this zone. The MnO_x maximum for each cast appears at the top of the suboxic zone in the absence of detectable dO_2, with a range of 1.33 – 2.81 µM MnO_x (88.1 – 97.7 % of total Mn). Soluble Mn speciation is again variable in this zone, with % Mn(III)-L of the total Mn ranging 7.9 – 35.8 % in the first cast, versus 0 – 0.9 % in the second cast, and 0 – 12.2 % in the third cast. Concentrations of dMn_T were low at the top of the suboxic zone (0.05 – 0.29 µM) but increased drastically at the base of the suboxic zone (1.71 – 3.42 µM), just above the suboxic-anoxic interface.

The speciation of Mn in the anoxic zone was dominated by dMn_T, with MnO_x below 0.20 µM in all samples, and making up only 0 – 7.7 % of total Mn. Soluble speciation was dominated by Mn(II), with Mn(III)-L complexes ranging from 11.6 – 34.0 % of dMn_T. These complexes were stable in the presence of 5-fold to 45-fold excess H_2S ([H_2S] = 3.09 – 23.54 µM; [Mn(III)-L] = 0.42 – 0.75 µM).

3.4 Discussion:

The speciation of Mn was variable throughout this sampling campaign, but distinct trends allow for insights into the cycling of Mn: Mn(III)-L complexes present in in all zones (oxic, suboxic and anoxic) of the water column; MnO_x accumulating at the top of the suboxic zone; and reduction of MnO_x at the suboxic-anoxic interface. The profiles in Figure 3.1 indicate that MnO_x is primarily produced within the suboxic zone, but rapidly disappears at the base of the suboxic zone, just above the appearance of H_2S.

This is more clearly seen in Figure 3.2, which shows the results from the third pump profile cast where sampling was focused in the suboxic zone. In this profile, MnO_x is highest at the top two depths sampled in the suboxic zone, and replaced by soluble Mn species at the base of the suboxic zone, just above the appearance of H_2S. Thus, it is possible that partial reductive dissolution of Mn(IV) solid phases, by ambient ligands or MnO_x reducers, occurs above the appearance of H_2S, and that MnO_x is further reduced by H_2S below. Another possibility is small amounts of sulfide mixing upwards from the anoxic to suboxic zone, reacting with the MnO_x, leading to the absence of both H_2S and MnO_x. The discrepancies between each pump profile are likely influenced by tidal cycling and the resulting shifts of the chemical gradients. However, despite physical mixing processes, there are distinct trends in all three profiles which provide insight into the chemical and biological pathways occurring within the water column.

Figure 3.3 summarizes the likely biotic and abiotic pathways for Mn cycling in the suboxic and anoxic waters of this system. High dMn_T in bottom waters (2.39 – 3.80 µM), predominantly as Mn(II) (61.0 – 84.8 % of total Mn), indicates that Mn(II) is most probably fluxing out of the sediments (Eaton, 1979). Once this Mn(II) enters the suboxic zone, it is likely oxidized by Mn-oxidizing bacteria (Table 3.1, eq.3.1) to solid MnO_x phases containing Mn(IV) and/or Mn(III) at the base of the O_2 gradient (Tebo et al, 2004). The highest concentration of MnO_x occurs at the top of the suboxic zone, *at concentrations of* $dO_2 < 3\ \mu M$ (our method detection limit). Clement et al (2009) reported rapid Mn(II) oxidation to MnO_x phases in the suboxic zone of the Black sea, stimulated by dO_2 below 3-5 µM, consistent with the short Mn(II) residence times in their samples (residence time ≤ 10 days). Thus, our findings agree well with previous

results and suggest that the production of MnO_x can occur at very low dO_2 concentrations. This MnO_x maximum in the absence of high O_2 has several implications for the importance of Mn cycling in suboxic regions, and may represent diverse metabolic pathways in one system. For example, MnO_x may play an important role as electron acceptors in the anaerobic oxidation of organic matter (Clement et al, 2009). Additionally, the oxidation of Mn(II) via reactive oxygen species (ROS) has been demonstrated in seawater (Table 3.1, eq. 3.3), even at nanomolar concentrations of ROS (Hansard et al, 2011; Wuttig et al, 2013). Extracellular bacterially generated superoxide has been shown to oxidize Mn(II) in both light and dark conditions (Learman et al, 2011). Thus, in the suboxic zone in our system, this indirect bacterially-mediated mechanism may be possible at low oxygen concentrations.

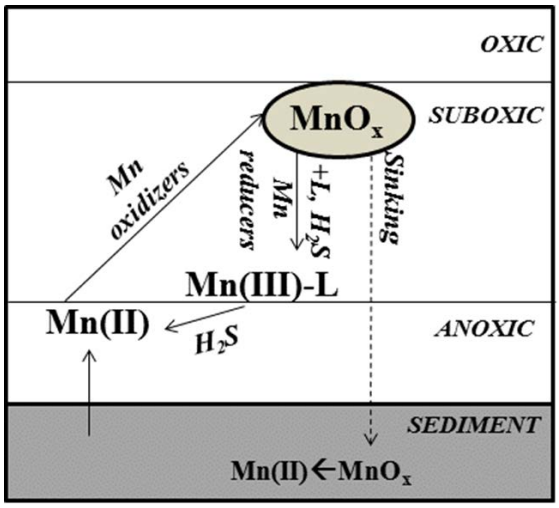

Figure 3.3 Schematic of Mn cycling in and below the suboxic zone in the water column of the Chesapeake Bay

We propose that these newly formed Mn oxides are removed from the water column via three mechanisms (Figure 3.3): (A) Mn oxide particles sink to the anoxic zone where they are chemically reduced (Table 1, eqs.6 and 7; Oldham et al, 2015); (B) Mn(III) in MnO_x oxide particles are non-reductively dissolved at the base of the suboxic zone via ambient ligands (Table 3.1, eq. 3.5; Duckworth and Sposito, 2007; Oldham et al, 2015; see next paragraph); or (C) MnO_x reducing microorganisms are active at the base of the suboxic zone (Table 3.1, eq. 3.4; Lin et al, 2012). The products of these reactions are Mn(III)-L complexes and Mn(II). The concentration of MnO_x was low in the presence of H_2S, indicating that the reductive dissolution of Mn oxides by H_2S is likely in the anoxic zone. Additionally, the percentage of Mn(III) in anoxic bottom waters was lower than in oxic surface waters, indicating that H_2S reduces strong Mn(III)-L complexes, but not as rapidly as H_2S reduces MnO_x.

These field results agree well with laboratory results from 2013 reported by Oldham et al, (2015) where MnO_2 was reduced to Mn(II) in the presence of 1:1 ratio of H_2S, but was partially stabilized as Mn(III)-DFOB (an equal molarity of DFOB and MnO_2). In the 2013 study (Oldham et al, 2015), when ambient concentrations of H_2S in the Chesapeake Bay were 100 times greater than concentrations of dissolved Mn, dMn_T was completely reduced to Mn(II), even in the presence of strong Mn(III)-binding ligands. In this study, bottom water H_2S concentrations reach a near 10-fold excess of dMn_T, but Mn(III)-L complexes are still partially stabilized (~30 % of dMn_T). This likely means that strong ligands ($\log K_{cond} > 13.2$) that can kinetically stabilize Mn(III) against H_2S reduction, are present, and/or that the rate of Mn(III) formed from Mn(III,IV) oxide dissolution exceeds the rate of Mn(III) reduction. That the dissolution

of Mn oxides occurs above the appearance of H_2S in all profiles suggests the latter possibility is unlikely. Rather it indicates that tidal mixing allows for sulfide mixing and reacting rapidly in the suboxic zone; or that the strong ligands are participating in the reductive dissolution of Mn oxides, and partially stabilizing the Mn as Mn(III)-L complexes; and/or that the microbial reduction of MnO_x is occurring. Tebo et al (1991) documented evidence for the presence of both microbial Mn(II) oxidation and MnO_x reduction just above the appearance of sulfide in the suboxic zone of the Black Sea. They indicated that Mn(II) oxidation and Mn(IV) reduction can occur simultaneously at low oxygen levels when H_2S is not detectable, and they highlight that 60 % of their MnO_x reductive capacity was still present in filtered samples. Tebo et al (1991) attributed this discrepancy to non-microbial reduction mechanisms for Mn(IV); thus we predict that reduction of Mn(IV) by ligands in their system is likely, as we see in this study for the Chesapeake Bay.

The chemical reduction of MnO_2 (Table 3.1, eq. 3.6) can occur via reduction by Fe(II) in seconds (Siebecker et al, 2015) and H_2S in minutes (Burdige and Nealson, 1986; Yao and Millero, 1993), with Mn(II) as the known product. In the presence of the siderophore desferrioxamine-B (DFOB), Mn(III) was shown to be stabilized in freshwater as the Mn(III)-DFOB complex during the reduction of MnO_2 in the presence of H_2S (Oldham et al, 2015) and Fe(II) (Madison et al, 2013; Siebecker et al, 2015). MnO_x can also be dissolved by DFOB and other organic compounds including natural organic matter (Table 3.1, eqs. 3.5 and 3.7) (Duckworth and Sposito, 2007). Whether the reduction of Mn(IV) in MnO_x in the Chesapeake Bay occurs as a result of the reductant H_2S (Table 1, eq.6, Oldham et al., 2015) or via the ambient ligand (Table 3.1,

eq. 3.7, Duckworth and Sposito 2005; 2007; Parker et al, 2007; Oldham et al, 2015) may be difficult to discern. Likely, a combination of these pathways is responsible because during the reductive dissolution of MnO_x, surface protonation occurs which facilitates electron transfer, further favoring reductive dissolution.

The microbial reduction of metal oxides and (oxy)hydroxides (Table 3.1, eq. 3.4) often occurs in stratified environments with high organic matter input, like the Chesapeake Bay. In such environments, after O_2 depletion, anaerobic degradation of organic matter dominates (Nealson et al, 1991). Mn(IV) can be an important anaerobic oxidant, and the reduction of MnO_x has been coupled with the degradation of organic matter (Canfield et al, 1993a, b) with some microbes capable of using either Mn(III) or Mn(IV) oxides as terminal electron acceptors (Kostka et al, 1995; Lin et al, 2012). It has also been shown that microbial Mn(IV) reduction requires solubilization of Mn(IV) to Mn(III), which increases Mn bioavailability (Lin et al, 2012), and may thus favor the production of Mn(III)-L complexes when ambient ligands are abundant. Indirect microbial reduction of MnO_x has been reported for some organisms, including sulfate reducers of the *Desulfovibrio* group. This group produces sulfide in their metabolism, which chemically reduces Mn(IV) to Mn(II) (Burdige and Nealson, 1986), a pathway of particular interest for systems like the Chesapeake Bay.

Mn(III)-L complexes were detected in all parts of the water column, including oxygenated samples, indicating that they are stable in oxic waters, as previously reported (Oldham et al, 2017). There is no discernable trend in the soluble Mn speciation in oxic waters, however, total Mn is higher at the base of the oxic zone in all

samples (0.91 – 1.43 µM) compared to the rest of the oxic zone (0.51 – 1.25 µM). Our measurements of Mn(III)-L complexes, ranging from 0.018 – 0.212 µM are consistent with measurements in other coastal waters (Oldham et al, 2017). Some Mn may be fluxing from the suboxic zone to the oxic zone, as Mn(III)-L or Mn(II), via tidal mixing. Because MnO_x is higher in the suboxic zone, it is likely that larger MnO_x particles are sinking to the suboxic zone from the oxic zone, rather than the reverse. It does not appear that dissolved Mn species are fluxing across the oxic-suboxic interface, as there is no enrichment of either Mn(II) or Mn(III)-L complexes at this interface. Thus, the mechanisms driving Mn cycling in the oxic water column are distinct from those controlling Mn cycling in the suboxic and anoxic zones of the water column.

These fresher and oxygenated surface waters represent a water mass where Mn(III)-L complexes may originate via different pathways than those driving the formation of Mn(III)-L in the anoxic and suboxic zones. It is possible that Mn(III)-L is being stabilized via ligand exudates from microorganisms in this zone (Tebo et al, 2004), as these oxic waters experience intense primary productivity in the summer months. The stabilization of Mn(III)-L by terrestrial ligands may also be a source of Mn(III)-L to this site. It has been shown that terrestrial ligands from freshwater sources bind Mn(III) strongly (Oldham et al, 2017); given the high terrestrial load of organic matter to the Chesapeake Bay, it is not surprising that dMn would be stabilized as organic complexes.

Finally, we note that at each depth, there is variability in the concentrations of Mn(II) oxidation or MnO_x reduction products and reactants, indicating that there may

be different Mn redox reactions occurring at different pump-casts, as well as mixing during tidal cycling. For example, in the first pumpcast, Mn oxidation products dominate at the base of the suboxic zone, whereas at the same tidal cycle, a day later, Mn reduction products dominate. That is, in the first pump-cast at the *base of the suboxic zone* (Figure 3.1A, 12.7 m), the concentration of MnO_x (1.65 µM, 49.1 % of total Mn) is triple that of Mn(II) (0.51 µM, 15.2 % of total Mn), and the concentration of Mn(III)-L (1.20 µM, 25.8 % of total Mn) is double that of Mn(II). Comparatively, at the same interface, in the third cast (Figure 3.2A, 11.6 m), one day later during the same tidal phase, there is nearly a 10-fold excess of Mn(II) to MnO_x ([Mn(II)] = 2.96 µM, 78.2 % of total Mn; [MnO_x] = 0.36 µM, 9.6 % of total Mn) with 0.46 µM Mn(III)-L (12.2 % of total Mn). Given that H_2S and dO_2 are not detectable in these samples, ligand reduction and/or high microbial activity is likely. Tidal mixing, a lateral process, is also likely important at this site. As fluids of different density flow across each other, shear and advective mixing likely occur, and the suboxic zone shifts in depth. Our study site is in a 25 m depression, and thus we expect not only vertical fluxes from the sediments, but also lateral fluxes along the sides of the depression. Associated with this shift in depth, there may be upwelling of H_2S across the suboxic/anoxic interface, resulting in the reductive dissolution of MnO_x at the base of the suboxic zone. Thus, redox cycling occurs on the order of hours for Mn, and indicates that other variables including tide, winds, and terrestrial inputs of organic matter, likely impact the speciation of Mn at sites like the Chesapeake Bay.

3.5 Conclusions:

Results from this study suggest that Mn(II) fluxes out of the sediments into the anoxic bottom waters of the Chesapeake Bay, and that this Mn(II) is microbially

oxidized to MnO_x at the top of the suboxic zone, at oxygen concentrations below 3 μM. At the base of the suboxic zone, the appearance of strong Mn(III)-L complexes (log K > 13.2) coincided with the disappearance of MnO_x, just above the appearance of H_2S, indicating that Mn oxides are acting as a source of dissolved Mn(III)-L to the anoxic bottom waters of the Chesapeake Bay by non-reductive and reductive dissolution by strong ambient ligands, or reductive dissolution by H_2S below our 0.2 μM detection limit, or by microbes, or a combination thereof. The Mn(III)-L in the oxic zone does not likely originate from MnO_x fluxing from the suboxic zone to the oxic zone, but rather from biological activity or via terrestrial inputs. The three pump cast profiles also exhibit variability over the course of 6 – 12 hours between sampling events. The suboxic zone exhibited the most change, with the concentrations of all three Mn species shifting in each cast. Redox conditions in systems like the Chesapeake Bay that are influenced by tides, winds and terrestrial inputs are thus driven by a combination of biological, chemical and physical processes. Mn cycling appears to be most intense at the suboxic-anoxic interface of this site, given the high total Mn and the presence of all three Mn species (Mn(II), Mn(III)-L and MnO_x). Under these conditions the Mn cycle may be a key driver in the biogeochemical cycling of other elements. Reduced Mn(II) contributes to O_2 consumption; ligands stabilize soluble Mn as Mn(III)-L, which may then act as an electron acceptor with Fe(II) and H_2S or as an electron donor with O_2; and MnO_x may act as an oxidant for reduced sulfur and serve as an electron acceptor in the remineralization of organic matter. Neither O_2 nor H_2S are present; therefore, microorganisms that use electron acceptors other than O_2 or sulfate and/or reduced inorganic or organic electron donors can occur in the suboxic zone. This presents the

possibility that both Mn reducers (able to use Mn(IV) and Mn(III)) and Mn oxidizers (able to use Mn(II) and Mn(III)) may coexist at the same depth in the suboxic zone.

3.6 Acknowledgements:

This work was funded by grants from the Chemical Oceanography program of the National Science Foundation (OCE-1558738 and OCE-1155385 to GWL; OCE-1558692 and OCE-1154307 to BMT). Véronique Oldham thanks the University of Delaware for receipt of a University of Delaware Graduate Fellowship and Dissertation Fellowship. Thanks also to the crew of the R/V *Sharp* who made sampling for this research possible, as well as to Daniel MacDonald who assisted with the pump-cast sampling and voltammetric measurements, and Laramie Jensen who assisted with sample filtration and soluble Mn analyses. GWL thanks Frank and Judy Millero for their friendship and especially all the stimulating discussions about science and life over the years

REFERENCES

Altmann H.J. (1972). Determination of dissolved oxygen in water with Leukoberbelin-Blue I. A quick Winkler method. *Anal. Chem.* 262, 97-99.

Boynton, W.R., Kemp, W. M., and Keefe, C.W. (1982). A comparative analysis of nutrients and other factors influencing estuarine phytoplankton production. In: Kennedy, V.S. (ed.) Estuarine comparisons. Academic Press, New York, p.69-90.

Burdige, D. J., and Nealson, K. H. (1986). Chemical and microbiological studies of sulfide-mediated manganese reduction. *Geomicrobio.* J. 4, 361-387.

Canfield, D. E., Jørgensen, B. B., Fossing, H., Glud, R., Gundersen, J.,Ramsing, N. B. Thamdrup, B., Hassen, J. W., Neilsen, L. P., and Hall, P.O.J. (1993a). Pathways of carbon oxidation in three Continental margin sediments. *Mar. Geol.* 113, 27–40.

Canfield, D. E., Thamdrup, B., and Hassen, J. W. (1993b). The anaerobic degradation of organic matter in Danish coastal sediments: iron reduction, manganese reduction and sulfate reduction. *Geochim. Cosmochim. Acta.* 57, 3867-3883.

Clement, B.G., Luther, G.W., and Tebo, B.M. (2009). Rapid, oxygen-dependent microbial Mn(II) oxidation kinetics at sub-micromolar oxygen concentrations in the Black Sea suboxic zone. *Geochim. Cosmochim. Acta.* 73, 1878-1889.

Dellwig, O., Schnetger, B., Brumsack, H. J., Grossart, H. P., and Umlauf, L. (2012). Dissolved reactive manganese at pelagic redoxclines (part II): Hydrodynamic conditions for accumulation. J. Mar. Syst. 90, 31–41.

Duckworth, O.W., and Sposito, G. (2007). Siderophore-promoted dissolution of synthetic and biogenic layer-type Mn oxides. *Chem. Geol.* 242, 497-508.

Duckworth O.W., and Sposito G. (2005). Siderophore-manganese(III) interactions I. Manganite dissolution promoted by desferrioxamine-B. *Environ. Sci. Technol*. 39, 6045-6051.

Eaton, A. (1979). The impact of anoxia on Mn fluxes in the Chesapeake Bay. *Geochim. Cosmochim. Acta.* 43, 429–432.

Hansard, S. P., Easter, H. D., and Voelker, B. M. (2011). Rapid reaction of nanomolar Mn(II) with superoxide radical in seawater and simulated freshwater. *Environ. Sci. Technol.* 45, 2811−2817.

Ishii, H., Koh, H., and Satoh, K. (1982). Spectrophotometric determination of manganese

utilizing metal-ion substitution in the cadmium-alpha, beta-gamma,deltatetrakis(4-carboxyphenyl)porphine complex. *Anal. Chim. Acta.* 136, 347-352.

Kostka J.E., Luther, G.W., and Nealson, K.H. (1995). Chemical and biological reduction of Mn(III)-pyrophosphate complexes: Potential importance of dissolved Mn(III) as an environmental oxidant. *Geochim. Cosmochim. Acta.* 59, 885-894.

Landing, W.M., and Bruland, K.W. (1980). Manganese in the North Pacific. *Earth. Planet. Sci. Lett.* 49, 45-56.

Learman D.R., Voelker B.M., Vazquez-Rodrigues A.I., and Hansel C.M. (2011). Formation of manganese oxides by bacterially generated superoxide. *Nat. Geosci*. 4, 95 – 98.

Lewis, B. L., Glazer, B. T., Montbriand, P. J., Luther, G. W., Nuzzio, D. B., Deering, T., Ma, S., and Theberge, S. (2007). Short-term and interannual variability of redox-sensitive chemical parameters in hypoxic/anoxic bottom waters of the Chesapeake Bay. *Mar. Chem.* 105, 296-308.

Lin, H., Szeinbaum, N. H., Dichristina, T. J., and Taillefert, M. (2012). Microbial Mn(IV) reduction requires an initial one-electron reductive solubilization step. *Geochim. Cosmochim. Acta*. 99, 179–192.

Lovley, D.R. (1991). Dissimilatory Fe(III) and Mn(IV) reduction. *Microbial Rev.* 55, 259-287.

Luther, G. W., Glazer B. T., Ma S., Trouwborst R. E., Moore T. S., Metzger E., Kraiya C., Waite T. J., Druschel G., Sundby B., Taillefert M., Nuzzio D. B., Shank T. M., Lewis B. L., and Brendel P. J. 2008. Use of voltammetric solid-state (micro)electrodes for studying biogeochemical processes: Laboratory measurements to real time measurements with an in situ electrochemical analyzer (ISEA). *Mar. Chem*. 108, 221-235.

Luther, G.W., Madison, A.S., Mucci, A., Sundby, B., Oldham, V. E. (2015). A kinetic approach to assess the strengths of ligands bound to soluble Mn(III). *Mar. Chem.* 173, 93-99.

MacDonald D.J., Findlay A.J., Mcallister S.M., Barnett J.M., Hredzak-Showalter P., Krepski S.T., Cone S.G., Scott J., Bennett S.K., Chan C.S., Emerson D., and Luther G.W. (2014). Using in situ voltammetry as a tool to identify and characterize habitats of iron-oxidizing bacteria: from fresh water wetlands to hydrothermal vent sites. *Environ. Sci.: Proc. Impacts.* 16, 2117–2126.

Madison, A.S., Tebo, B.M., and Luther, G.W. (2011). Simultaneous determination of soluble manganese (III), manganese (II) and total manganese in natural (pore)waters. *Talanta.* 84, 374-381.

Madison, A. S, Tebo, B. M., Mucci, A., Sundby. B., and Luther, G.W. (2013). Abundant Mn(III) in porewaters is a major component of the sedimentary redox system. *Science.* 341, 875-878.

Nealson, K. H., Myers, C.R., and Wimpe, B.B. (1991). Isolation and identification of manganese-reducing bacteria and estimates of microbial Mn(IV)-reducing potential in the Black Sea. *Deep-Sea Res.* 38, S907-920.

Oldham, V.E., Owings, S. M., Jones, M., Tebo, B.M., and Luther, G.W. (2015). Evidence for the presence of strong Mn(III)-binding ligands in the water column of the Chesapeake Bay. *Mar. Chem.* 171, 58-66.

Oldham, V.E., Mucci, A., Tebo, B.M., Luther, G.W. (2017). Soluble Mn(III)-L complexes are abundant in oxygenated waters and stabilized by humic ligands. *Geochim. Cosmochim. Acta.* 199, 238-246.

Parker, D.L., G. Sposito, and Tebo, B.M. (2004). Manganese(III) binding to a pyoverdine siderophore produced by a manganese(II)-oxidizing bacterium. *Geochim. Cosmochim. Acta.* 68, 4809-4820

Parker D.L., Takami M., Mylene L., Mozafarzadeh R.V., McCarthy J.K., and Tebo B.M. (2007). Inter-Relationships of MnO2 Precipitation, siderophore–Mn(III) Complex Formation, Siderophore Degradation, and Iron Limitation in Mn(II)-Oxidizing Bacterial Cultures. *Geochim. Cosmochim. Acta*. 71, 5672-83.

Siebecker, M. G., Madison, A. S., and Luther, G. W. (2015). Reduction Kinetics of Polymeric (Soluble) Manganese (IV) Oxide (MnO_2) by Ferrous Iron (Fe^{2+}). *Aqu. Geochem.* 21, 143–158.

Stone, A.T., and Morgan, J.J. (1984). Reduction and Dissolution of manganese(III) and manganese(IV) Oxides by Organics 2: Survey of the Reactivity of Organics. *Environ. Sci. Technol.* 18, 617–24.

Tebo, B.M., Rosson, R.A., and Nealson, K.H. (1991). Potential for manganese(II) oxidation and manganese(IV) reduction to co-occur in the suboxic zone of the Black Sea. In: Black Sea Oceanography, E.Izdar and J.Murray (eds). Kluwer Academic Publishers. p.173-185.

Tebo B.M., Ghiorse W.C., vanWaasbergen L.G., Siering P.I., and Caspi R. (1997). Review in Mineralogy. *Mineralog. Soc. Am.* 35, 225-266.

Tebo, B.M., Bargar J.R., Clement, B.G., Dick, G.J., Murray, K.J., Parker, D., Verity, R., and Webb, S.M. (2004). Biogenic manganese oxides: properties and mechanisms of formation. *Ann. Rev. Earth Planet. Sci*. 32, 287-328.

Tebo, B.M., H.A. Johnson, J.K. McCarthy, and Templeton, A.S. (2005). Geomicrobiology of manganese(II) oxidation. *Trends in Microbiol.* 13, 421-428.

Trouwborst, R. E., Clement, B. G., Tebo, B. M., Glazer, B. T., and Luther, G. W.. (2006). Soluble Mn(III) in suboxic zones. *Science.* 313, 1955-1957.

Wuttig, K., Heller, M.I., Croot, P. (2013). Reactivity of inorganic Mn and Mn Desferrioxamine B with O_2, O_2^-, and H_2O_2 in seawater. *Environ. Sci. Technol.* 47, 10257-10265.

Yakushev, E., Pakhomova, S., Sørenson, K., and Skei, J. (2009). Importance of the different manganese species in the formation of water column redox zones: Observations and modeling, *Mar. Chem*. 117, 59-70.

Yakushev, E.V., F. Pollehne, G. Jost, I. Kuznetsov, B. Schneider and L. Umlauf. (2007). Analysis of the water column oxic/anoxic interface in the Black and Baltic seas with a numerical model. *Mar. Chem.* 107, 388-410.

Yao, W. and Millero, F.J. (1993). The rate of sulfide oxidation by MnO_2 in seawater. *Geochim. Cosmochim. Acta.* 57, 3359-3365.

Chapter 4

SOLUBLE MANGANESE(III)-L COMPLEXES ARE ABUNDANT IN OXYGENATED WATERS AND STABILIZED BY HUMIC LIGANDS[3]

Abstract

Dissolved Mn (dMn_T) is thought to be dominated by metastable Mn(II) in the presence of oxygen, as the stable form is insoluble Mn(IV). We show, for the first time, that Mn(III) is also stable as a soluble species in the oxygenated water column, when stabilized by organic ligands as Mn(III)-L complexes. We measured Mn(III)-L complexes in the oxygenated waters of a coastal fjord and a hemipelagic system where they make up to 86 % of the dMn_T. Although Mn(III) forms similar complexes to Fe(III), unlike most of the analogous Fe(III)-L complexes, the Mn(III)-L complexes are not colloidal, as they pass through both 0.20 µm and 0.02 µm filters. Depending on the kinetic stability of the Mn(III) complexes and the microbial community of a given system, these Mn(III)-L complexes are capable of donating or accepting electrons and may therefore serve as both reductants or oxidants, can be biologically available, and can thus participate in a multitude of redox reactions and biogeochemical processes. Furthermore, sample acidification experiments revealed that Mn(III) binding to humic ligands is responsible for up to 100 % of this complexation, which can influence the formation of other metal complexes including Fe(III) and thus impact nutrient

---

[3] *Chapter 4 published in Geochimica et Cosmochimica Acta:* Oldham, V.E., Mucci, A., Tebo, B.M., Luther, G.W. (2017). Soluble Mn(III)-L complexes are abundant in oxygenated waters and stabilized by humic ligands. Geochim. Cosmochim. Acta. 199, 238-246.

availability and uptake. Hence, humic ligands may play a greater role in dissolved Mn transport from coastal areas to the ocean than previously thought.

4.1 Introduction

Manganese (Mn) is ubiquitous in the global ocean, where it is an essential trace nutrient in the electron transfer processes of several metallo-enzymes - notably in photosystem II for photosynthetic organisms. In its solid oxidized form, it serves as an electron acceptor in the bacterial decomposition of sedimentary organic matter and acts as an important scavenger for many trace elements and radionuclides. The chemical speciation of Mn in marine systems governs its diverse functions and is ultimately controlled by the redox conditions of the environment and the microbial community. The favorable oxidation state of Mn in oxic waters is Mn(IV), and thus Mn in oxygenated waters is primarily bound to oxygen as solid Mn(III/IV)-oxides (MnO_x). However, soluble Mn(II) is metastable in oxygenated waters because the oxidation of $Mn(H_2O)_6^{2+}$ to MnO_x by O_2 in an one electron transfer is thermodynamically unfavorable and the two electron transfer is kinetically slow (Luther 2010), unless facilitated by microbes, surface catalysis or superoxide-promotion (Stumm and Morgan, 1996).

In the last decade, soluble manganese (dMn_T) speciation has been re-evaluated to include soluble Mn(III) bound to ligands (Mn(III)-L complexes) in low oxygen environments. Mn(III)-L complexes have been measured in the suboxic porewaters of the St. Lawrence Estuary (Madison et al., 2013), the suboxic waters of the Black Sea (Yakushev et al., 2007, 2009; Trouwborst et al., 2006) and the Baltic Sea (Dellwig et

al., 2012) as well as the anoxic bottom waters of the Chesapeake Bay (Trouwborst et al., 2006; Oldham et al., 2015). Because Mn(III)-L complexes can donate or accept electrons, they can potentially have a profound impact on the redox chemistry of a given environment. In addition to their reactivity, Mn(III)-L complexes can affect the uptake of other metals due to metal-ligand competition reactions (Luther et al., 2015). For example, the siderophore pyoverdine from the Mn(II)-oxidizing Pseudomonas putida GB-1 has a higher affinity for Mn(III) than for Fe(III) (Parker et al., 2004). Likewise, kinetic experimentation, using known laboratory ligands (desferrioxamine-B, pyrophosphate, to name two) and suboxic porewater samples from the St. Lawrence Estuary also indicate that Mn(III) may bind more strongly than Fe(III) to the same ligands (Luther et al., 2015). These findings are important given that many microorganisms use Fe(III)-binding ligands for Fe uptake. However, the impact of this ligand competition is poorly described because the presence of Mn(III)-L has not yet been documented in oxygenated marine environments as dMn_T concentrations in these environments are typically lower than the detection limits of current speciation methods (50 nM, Madison et al., 2011). Consequently, thus far, dMn_T speciation in oxygenated systems has been thought to be dominated by Mn(II) (e.g. Landing and Bruland, 1986).

Using a modification of the UV-Vis method of Madison et al. (2011), we show for the first time that, like Fe(III)-L complexes which account for up to 99.9% of dFe_T (e.g. Gledhill and van den Berg, 1994) in oxygenated marine waters, Mn(III)-L complexes are present in the oxygenated waters of both a coastal fjord and in the hemipelagic waters of the St. Lawrence Estuary, the largest enclosed estuary in the world. These Mn(III)-L complexes account for most of the dMn_T, but, unlike most

Fe(III)-L complexes (Schlosser et al., 2013), are not colloidal (operational size class between 20 to 200 nm). Finally, our findings indicate that binding to humic ligands is responsible for up to 100 % of the Mn(III)-L in these waters.

4.2 Materials and Methods

4.2.1 Water Column Sample Processing

Water column samples were collected in September 2014 from two sites in the St. Lawrence Estuary (Figure 4.1; Station 23 [~350 m depth]: 48ºº42.29'N, 68ºº38.83'W; and Station SAG-30 [~260 m depth]: 48ºº21.72'N, 70ºº23.71'W) into 12 x 12 L Niskin PVC bottles mounted on the CTD-rosette. Contamination was avoided by sampling through a trace metal clean tube into clean 50 mL polypropylene centrifuge tubes (Falcon), which were overflowed three times before filling. Water samples were immediately filtered through 0.20 µm syringe filters (Nylon, Whatman), in a fume hood aboard the R/V Coriolis II, into new 50 mL centrifuge tubes, and were kept in the dark until analysis. Aliquots were frozen at -20 ºC in 50 mL centrifuge tubes for future analyses.

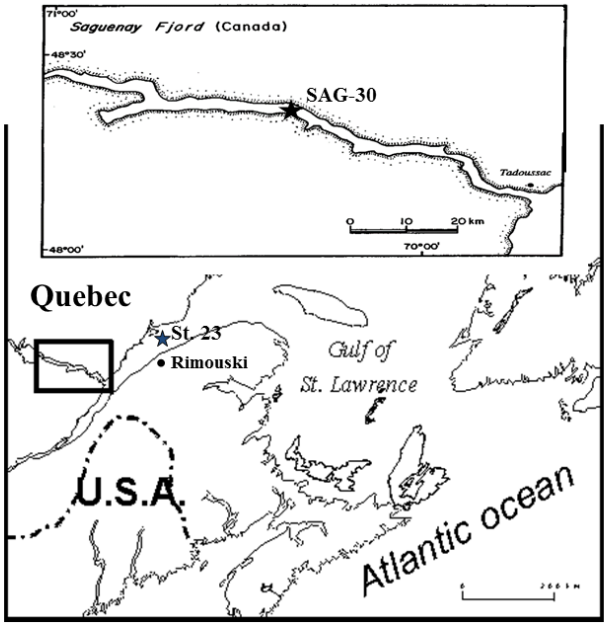

Figure 4.1 Map of the two study sites in the St. Lawrence Estuary.

To obtain true bottom-water samples, undisturbed sediment multi-cores were recovered at Station 23 using a Bowers & Connelly Multicorer and 10-cm diameter clear plastic barrels. The overlying water at the sediment-water interface was withdrawn from the barrels with a trace metal clean polypropylene syringe, filtered and handled as above. The water analyzed is termed overlying sediment-core water and its composition, relative to waters above it, provides insights on the direction and magnitude of the flux of chemical species across the sediment-water interface.

4.2.2 Dissolved Mn Speciation

All samples were analyzed for soluble Mn speciation within two hours of collection following the addition of a soluble porphyrin ligand [α, β, γ, δ-tetrakis(4-

carboxyphenyl)porphine (T(4-CP)P)] , according to the method described by Madison et al. (2011). The method allows for the subsequent spectrophotometric determination of both Mn(II) and Mn(III)-L_{weak} (Mn(III)-L_{weak} can be outcompeted by the added porphyrin ligand, and has $logK_{cond}$<13.2; Oldham et al., 2015; Luther et al., 2015) using the differential kinetics of the reaction between Mn and the added porphyrin which is initially complexed to Cd(II). The Mn(II) displaces the Cd(II) and reacts rapidly with the porphyrin, forming a Mn(III)-porphyrin complex as Mn(II) oxidizes in the presence of oxygen, whereas the Mn(III)-L_{weak} undergoes a ligand substitution reaction with the porphyrin to form the Mn(III)-porphyrin complex ($logK_{cond}$ <13.2, Oldham et al., 2015; Luther et al., 2015). The complex yields a sharp Soret band at 468 nm (ε = 94,600 mol^{-1} cm^{-1}), which can be measured by UV-Vis spectrophotometry. To measure Mn(III)-L_{strong} (cannot be outcompeted by the added porphyrin ligand, $logK_{cond}$ >13.2; Oldham et al., 2015), a reducing agent (hydroxylamine, 100-fold excess of expected dMn_T, does not dissociate the Mn-porphyrin complex at this concentration due to abundant O_2) is added to the filtered sample, converting all Mn(III)-L to Mn(II), and the sample is reanalyzed for dMn_T. The difference between the reduced (dMn_T) and non-reduced (dMn(II) + dMn(III)-L_{weak}) sample gives the concentration of Mn(III)-L_{strong}. Laboratory-synthesized colloidal MnO_2 does not react with the porphyrin (Madison et al., 2011). The detection limit for this method is 50 nM, which is sufficiently low for porewater analysis, but not low enough for water column samples.

We modified the method of Madison et al. (2011) for water column samples to achieve a detection limit of 0.3 nM (3 times the standard deviation of a blank) by using a 100-cm liquid waveguide capillary cell and the addition of a heating step as well as a

strong reducing agent for Mn speciation. All chemicals were A.C.S. reagent grade, and all solutions were prepared with deionized water (18.2 mΩ). As the absorbance is proportional to the cell pathlength, for low levels of Mn, the reagents described by Madison et al. (2011) were diluted 100-fold to fit into the analytical detection window. The [T(4-CP)P] stock solution was 2.00×10^{-4} M (final sample concentration of 2.33×10^{-7} M), the borate buffer was made up to pH 8.0-8.2 using trace metal clean NaOH (final sample buffer concentration 4.16×10^{-4} M), and the $CdCl_2$ stock solution was prepared to 1.20×10^{-4} M (final sample concentration 2.40×10^{-7} M). All samples were analyzed in triplicate following 12 to 30-fold dilution into the reagents to yield a total Mn concentration in the range of 10-100 nM.

The rate of reaction is proportional to the concentration of reactants, and at the low levels of the modified method, the reaction is slow. Hence, a heating step, prior to analysis, is employed to accelerate the reaction kinetics. Because the Cd(II) in the porphyrin reacts with chloride in seawater, seawater samples are diluted to ensure reaction of the porphyrin with Mn(II); thus, the practical detection limit of the method is 3.0 nM. Recovery tests with $MnCl_2$ standards were performed, and the most successful recovery in a reasonable time period was achieved by heating at 90 °C for 1 hour (98-106 % recovery, Table 4.1). A NASS-6 seawater standard was tested for recovery using this heating step, and a triplicate measurement was within 1 standard deviation of the known value of the standard [dMn_T] (Table 4.1). For Mn speciation, strong Mn(III)-L complexes are reduced by an excess of a strong reducing agent, hydroxylamine (at least 100-fold expected dMn_T concentration). Samples are analyzed first without hydroxylamine for dissolved Mn(II) and then with the addition of hydroxylamine for

dMn_T (Mn(II) + Mn(III)-L). This method does not allow for the independent kinetic assessment of weak Mn(III)-L complexes and can only determine the concentration of Mn(II) and strong Mn(III)-L complexes. Hence, the Mn(II) fraction reported in Table 4.2 likely includes weak Mn(III)-L complexes that react during the heating step.

Table 4.1 Recovery tests of dMn_T measured using a 100-cm cell coupled to a UV/Vis spectrophotometer following a heating step. Standard deviations for recovery were ± 5 % based on a standard calibration curve and the standard deviation for the NASS-6 seawater standard was based on triplicate analyses.

Treatment	dMnT(known) (nM)	dMnT(measured) (nM)	% Recovery
60 minutes	5	0.6 ± 0.03	*12.3*
in 60 ºC	10	2.3 ± 0.17	*23.4*
bath	25	12.6 ± 0.63	*50.3*
30 minutes	5	1.7 ± 0.09	*34.7*
in 80 ºC	10	5.0 ± 0.25	*50.0*
bath	25	19.8 ± 0.10	*79.4*
15 minutes	5	2.1 ± 0.1	*42.6*
in 90 ºC	10	8.6 ± 0.43	*86.4*
bath	25	17.3 ± 0.9	*69.4*
60 minutes	5	5.2 ± 0.25	*104.9*
in 90 ºC	10	9.8 ± 0.50	*98.0*
bath	25	26.6 ± 1.3	*106.4*
NASS-6 Seawater Standard	*6.1 ± 0.6*	*5.8 ± 0.7*	*95.1*

The liquid waveguide capillary cell (World Precision Instruments) was coupled to a UV-Vis spectrophotometer (Ocean Optics). In this spectrophotometric set up, a mini deuterium halogen light source (DT-Mini-2-GS) was coupled to a USB2000+ fiber

optic spectrometer controlled with SpectraSuite software. The Mn(III)-T(4-CP)P complex was measured at its absorbance maximum (468 nm) against a reagent and sample blank. For small peaks, peak height was determined using an algorithm adapted to resolve small peaks with the application of linear fit tangent baseline subtraction (ECDSOFT, which can be found at: https://mojoblak.irb.hr/index.php/s/dxB24S8m5H6fsZW?path=%2FProMCC).

4.2.3 MnO_x Measurements

Known volumes of sample (265 mL) were filtered through 47 mm diameter 0.20 µm Whatman Nucleopore track-etched polycarbonate filters. Using the method of Altmann (1972), filters were amended with 2 mL of 0.0032 % leucoberbelin blue dye (LBB, 65 % diluted, Sigma-Aldrich). The dye color, formed on oxidation by particulate manganese or MnO_x, was measured in a 100-cm liquid waveguide capillary cell at 620 nm using the Ocean Optics spectrophotometric set-up described above. The LBB (410.5 g mol^{-1}) stock solution is prepared by dissolution in Milli-Q water to 4 % w/w and the addition of 40 µL of 10 M sodium hydroxide (NaOH) per 10 mL of solution. Working solutions are made by diluting the stock into 1% acetic acid (made up in Milli-Q water), to 0.04 % w/w. A calibration curve was generated using potassium permanganate ($KMnO_4$). We expect that to produce an equivalent absorbance, 2.5 times more Mn(IV) is required than Mn(VII), since Mn(VII) oxidizes 5 LBB molecules, compared to 2 LBB molecules for Mn(IV). In a 100-cm pathlength cell, the limit of detection is 0.05 nM.

4.3 Results

At the hemipelagic site, Station 23 (Figure 4.2A), the water column is characterized by the presence of three water masses: (1) a 25 – 50 m thick surface layer of low salinity (27 – 32) that flows seaward, (2) an intermediate layer of cold water (−1° to 2°C with intermediate salinity; 32) that extends to about 150 m depth and flows landward from the Gulf, and (3) an underlying deep layer with warmer (4° to 6°C) and saltier (34 – 34.6) water (Figure 4.2B) that flows landward and originates in the northwestern Atlantic Ocean. Concentrations of dissolved O_2 (dO_2) decreased from the surface (339 μM) to the bottom (55 μM) (Figure 4.2B) whereas dMn_T increased almost monotonically with depth, reaching the highest concentrations in the deepest sample recovered by the CTD-rosette (289 nM ~5-10 m above bottom) and in the overlying sediment-core water (2.93 μM) (Figure 4.2A). The dMn_T speciation (Figure 4.2A) is dominated by Mn(III)-L between 150-300 m (52 – 86 % of dMn_T) whereas the % Mn(III)-L was lower in surface (17.6 %) and bottom waters (2.0 %). In the two deepest samples, dMn_T was dominated by Mn(II), indicating that dMn_T escapes from the sediment to the overlying waters as Mn(II).

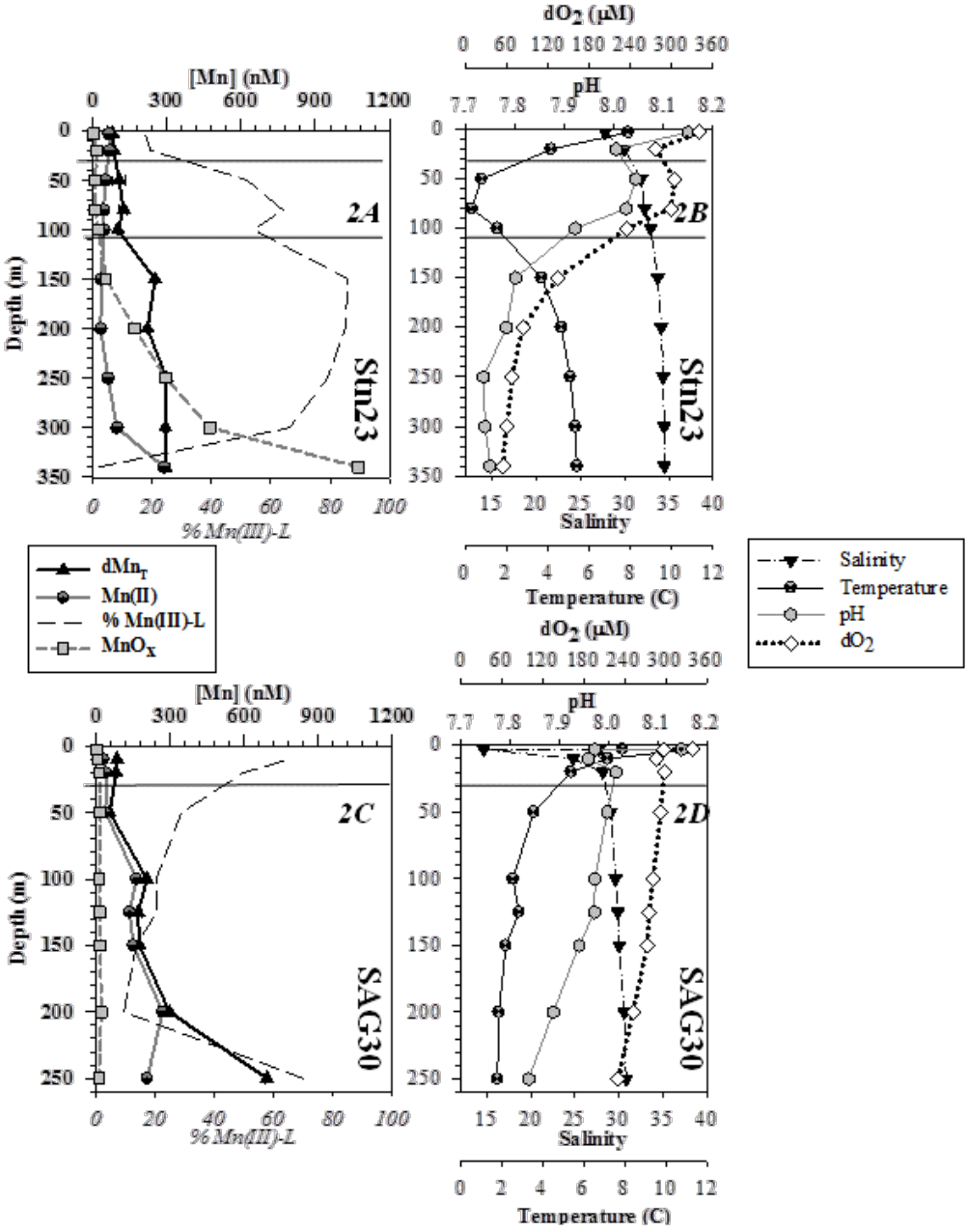

Figure 4.2 Water column Mn speciation data from Station 23 (2A) and SAG-30 (2C), with dMnT, Mn(II), and % Mn(III) determined by their difference, and MnOx measured by leucoberbelin blue (LBB) on solids collected onto a 0.20 µm filter. Physical parameters are given for Station 23 (2B) and for SAG-30 (2D) with salinity and temperature measured using the CTD-rosette system, pH measured spectrophotometrically or potentiometrically (NBS scale) on discrete samples and dO2 determined on discrete samples by Winkler titration. Standard deviations are given for Mn speciation measurements, and where not visible, are smaller than the symbols.

The water column in the Saguenay Fjord (SAG-30) is fully oxygenated (228-302 µM dO_2). The practical salinity (S_P) of the 3 to 10-m surface-water wedge was 14.6 – 24.8 at SAG-30 at the time of sampling, whereas more saline waters (S_P = 28.2 – 30.8) originating from the St. Lawrence Estuary are found below. Evidence of Mn(II) oxidation to Mn(III)-L (see eqs. 1 – 4 below) and to MnO_x in the water column is also observed here (Figure 4.2C). Like Station 23, the highest dMn_T concentrations were measured in the bottom waters. Mn(III)-L accounted for 9.5 - 70 % of dMn_T in the water column (Table 4.2), but the speciation profile was shaped differently than at Station 23. At SAG-30, the highest fractions of Mn(III)-L (65-70 %) are observed in the bottom and surface waters. Mn(II) accounted for 100% of the dMn_T speciation in the overlying sediment-core water, its concentration (2.28 µM) being higher than in the bottom waters at Station 23.

Table 4.2 Water column speciation results from both stations. Concentrations of Mn species are in nM. The dO_2 is from the recalibrated CTD probe (µM; Seabird SBE-43), and salinity by CTD probe (Seabird SBE-911). % Mn(III) represents the difference between measure dMn_T and Mn(II).

Station	Depth (m)	Mn (II)			dMn_T			*% Mn(III)-L*	MnO_x			dO_2	Salinity	Temperature (ºC)	pH
23	3	66.7	±	1.9	80.9	±	3.4	*17.6*	4.2	±	0.0	339	27.78	7.89	8.15
	20	69.1	±	2.5	86.0	±	0.6	*19.6*	18.1	±	0.2	277	29.96	4.15	8.00
	50	51.8	±	2.7	108.1	±	27.3	*52.1*	10.7	±	0.0	304	31.86	0.80	8.04
	80	45.2	±	0.6	125.8	±	15.8	*64.1*	9.2	±	0.2	299	32.25	0.32	8.02
	100	47.0	±	3.5	102.8	±	4.8	*54.3*	24.2	±	0.0	235	32.92	1.55	7.92
	150	35.2	±	5.5	253.0	±	5.5	*86.1*	55.1	±	0.2	134	33.73	3.69	7.80
	200	33.2	±	8.8	222.1	±	5.2	*85.0*	171.2	±	0.0	83.4	34.14	4.65	7.78
	250	62.5	±	3.3	299.5	±	13.7	*79.1*	295.9	±	2.4	68.5	34.34	5.08	7.74
	300	99.3	±	6.8	294.9	±	9.8	*66.3*	473.3	±	3.4	59.6	34.46	5.33	7.74
	340	289.2	±	15.4	295.1	±	16.5	*2.0*	1073	±	11.2	54.8	34.49	5.41	7.75
	Overlying	2930	±	25.0	2930	±	25.0	*0.0*							
SAG30	10	29.8	±	3.5	85.2	±	4.8	*65.0*	5.9	±	0.3	287	24.77	7.15	7.96
	20	41.4	±	2.6	82.3	±	2.8	*49.7*	13.7	±	0.3	298	28.16	5.38	8.02
	50	39.6	±	9.2	55.6	±	1.4	*28.8*	18.1	±	0.3	293	29.09	3.56	8.00
	100	164.3	±	2.2	206.2	±	2.2	*20.3*	13.3	±	0.3	281	29.60	2.55	7.97
	125	135.7	±	4.3	170.6	±	15.0	*20.5*	15.5	±	0.3	276	29.87	2.84	7.97
	150	152.0	±	5.2	175.7	±	8.6	*13.5*	18.3	±	0.3	272	30.03	2.20	7.94
	200	269.5	±	10.1	297.7	±	6.7	*9.5*	21.6	±	0.3	251	30.60	1.86	7.89
	250	207.8	±	7.7	691.9	±	7.6	*70.0*	12.8	±	0.3	230	30.83	1.79	7.84
	Overlying	2280	±	19.5	2280	±	19.5	*0.0*							

Previous studies may have neglected a fraction of the dMnT in natural waters since nearly all dissolved metal studies employ an acidification step for sample storage which would precipitate humic substances. To test this hypothesis, three frozen, filtered samples were thawed and amended with concentrated HCl (Optima) to pH < 1.5 to precipitate Mn(III)-humic complexes. After 1 hour, the acidified sample was centrifuged, to remove the humic precipitate, and the Mn speciation of the centrifuged supernatant was subsequently determined (Table 4.3). The % Mn(III)-humic is calculated as the difference between the original shipboard dMn_T and shore-based analysis after freezing, thawing and acidification (removal of precipitated humic material). The % Mn(III)-humic agreed with the original shipboard % Mn(III)-L,

indicating that the acidification step removed all of the Mn(III)-L and that the Mn(III)-L was in the form of humic complexes. In the bottom waters of the Saguenay Fjord, most of the Mn(III)-L complexes were also lost upon acidification, with ~75 % of the Mn(III)-L (53.4 % of dMn_T) lost in the 250-m sample (Table 4.3).

Table 4.3 A comparison of the original speciation results from the shipboard porphyrin method analysis ($dMn_{T(unacidified)}$ and $Mn(II)_{unacidified}$) to samples analyzed 13 months later, after freezing, thawing, acidification, and centrifuging ($dMn_{T\ (acidified)}$); all concentrations are reported in nM. The *% Mn(III)-L = 100*(original $dMn_{T(unacidified)}$ - $Mn(II)_{unacidified}$)* shipboard measurements. The *% Humic = 100*(original shipboard $dMn_{T(unacidified)}$ - $dMn_{T(acidified)}$)* analyzed 13 months later after freezing, thawing, and acidifying. The *%Mn(III)-L_{Humic}= 100*(% Mn(III)-L / % Humic)* and indicates what % of the Mn(III)-L is the result of humic complexation.

		Original, shipboard, unacidifed			*13 Months later, frozen, acidifed*		
Station	**Depth (m)**	**$dMn_{T(unacidified)}$**	**$Mn(II)_{(unacidified)}$**	***% Mn(III)-L***	**$dMn_{T(acidified)}$**	***% Humic***	**% Mn(III)-L_{Humic}**
23	3	80.9 ± 3.4	66.7 ± 1.9	*17.6*	66.7 ± 7.2	*17.6*	***99.9***
	100	102.8 ± 4.8	47.0 ± 3.5	*54.3*	49.7 ± 3.7	*51.6*	***95.1***
	300	294.9 ± 9.8	99.3 ± 6.8	*66.3*	99.6 ± 6.8	*66.2*	***99.8***
	340	295.1 ± 16.5	289.2 ± 15.4	*2.0*	288.1 ± 1.8	*2.4*	***120.2***
SAG30	250	691.9 ± 7.6	207.8 ± 7.7	*70.0*	322.6 ± 26.6	*53.4*	***76.3***

We additionally performed analysis on frozen samples and compared them to original shipboard measurements, to show that freezing filtered samples is suitable for Mn speciation preservation. Three frozen, filtered water column samples from Station 23 and two samples from SAG-30 were thawed in October 2015, filtered through 0.02 µm filters (Anatop), and the dMn speciation analyses repeated. The 0.02 µm filtered samples had the same concentrations and speciation at both sites as the original 0.20 µm filtered samples analyzed shipboard (Table 4.4), even at basal depths where particulate MnOx concentrations were high. Thus, we conclude that the measured Mn(III) is not

colloidal and that freezing filtered samples is suitable for storage of soluble Mn samples destined for total and speciation analyses.

4.4 Discussion

Mn(III)-L complexes were detected at both Station 23 in the Lower St. Lawrence Estuary (LSLE) and in the Saguenay Fjord, indicating for the first time that Mn(III)-L complexes are stable in oxic waters (Figure 4.2, Table 4.2). The concentration of dO2, the bacterial community and the abundance as well as the nature of Mn(III)-binding ligands at each site are responsible for the formation and stabilization of Mn(III)-L, via the following potential oxidative (eqs. 1-4) and reductive (eqs. 5-6) pathways (unbalanced):

$$Mn(II) + surface + L \xrightarrow{surface\ catalysis} Mn(III) - L \quad 4.1$$

$$Mn(II) + O_2 + L \xrightarrow{bacteria} Mn(III) - L \quad 4.2$$

$$L + oxidizer \rightarrow L_{ox}\ ;\ Mn(II) + L_{ox} \rightarrow Mn(III) - L \quad 4.3$$

$$Mn(II) + O_2^- + 2H^+ + L \xrightarrow{dark} Mn(III) - L + H_2O_2 \quad 4.4$$

$$MnO_2 + L \xrightarrow{bacteria} Mn(III) - L \quad 4.5$$

$$MnO_2 + L_{red} \rightarrow Mn(III) - L \quad 4.6$$

The high dMn_T in bottom waters was predominantly in the form of Mn(II) at both sites, indicating that dMn escapes mostly in the form of Mn(II) from the sediments to the overlying water. Madison et al., (2013) showed that the sediment porewaters in

the St. Lawrence Estuary are rich in Mn(III)-L complexes, which are concentrated at the oxic-suboxic interface, and that oxidation of Mn(II) by O_2 accounts for up to 100 % of the Mn(III) inventory. We propose that Mn(II) diffusing up from the sediment anoxic zone is responsible for the Mn(III)-L production in the suboxic porewaters, and that these complexes may be recycled to Mn(II) upon burial or oxidized to MnO_x in the oxic zone. Upward diffusion of porewater Mn(II) and/or advection of Mn(II)-bearing particles by bioturbation (Richard et al., 2013) likely supply Mn(II) to the overlying water column from the sediments. Associated with the flux of Mn(II) to the bottom waters at Station 23, we also observed a maximum [MnO_x] (1070 nM) in bottom waters (340 m, Figure 4.2A), indicating the oxidation of Mn(II) to MnO_x, is the dominant prominent sink of the soluble Mn. The large fraction of dMnT (66.3 %) in the form of Mn(III)-L at 300 m may result from the oxidation of Mn(II) escaping from the sediment (eqs. 4.1 – 4.4) or the reductive dissolution of sinking or advected authigenic Mn oxides (eqs. 4.5 and 4.6), but likely represents a residual species from the dominant oxidation of Mn(II) to MnO_x in bottom waters. The abiotic oxidation of Mn(II) by O_2 is slow, but can be accelerated by adsorption onto mineral surfaces (eq.4.1; Davies and Morgan, 1989), through bacterial mediation (eq.4.2; Tebo et al., 1997), and/or via in situ ligand-promoted oxidation by an oxidizing ligand such as photo-altered dissolved organic matter or a ligand in the presence of oxygen, such has been shown for the formation of Mn(III) with desferrioxamine-B (eq.4.3; Duckworth and Sposito, 2005; Parker et al., 2007). In the St. Lawrence Estuary, particle concentrations are greater in surface waters (2.5 – 2.7 mg L^{-1}) than in bottom waters (1.2 – 1.5 mg L^{-1}; Bourgoin and Tremblay, 2010), and we predict that surface-catalyzed oxidation (eq.4.1) is not the dominant oxidizing mechanism at this site, particularly as our highest MnO_x concentrations were

measured in bottom water samples. Bacterial oxidation rates of Mn(II) are ~5 times faster than surface-catalyzed oxidation rates in most seawater systems (Tebo et al., 2004), thus bacterial oxidation may dominate MnO_x formation at this site. As there is no light penetration at the depth of our deep samples, these measurements could also be a manifestation of dark production of reactive oxygen species, such as O_2^-, and their reaction with Mn(II) (eq.4.4; Hansard et al., 2011; Learman et al., 2011).

At station SAG-30, the abundance of Mn(II), coupled with the appearance of Mn(III)-L within 5 m above the sediment-water interface (our deepest Niskin bottle sample) is also interpreted as evidence of the oxidation of Mn(II) fluxing out of the sediment. Furthermore, the much lower MnO_x concentrations (5.9 – 21.6 nM) in the water column at SAG-30 than at Station 23 (Figure 4.2) may reflect the greater abundance of terrestrially-derived ligands, inhibiting the complete oxidation of Mn(II) to MnO_x or reductively dissolving MnO_x to produce Mn(III)-L complexes (eqs. 4.5 and 4.6) as shown in Oldham et al. (2015). It is also possible that the lower [MnO_x] in the Saguenay Fjord could be attributed to the greater particulate load of the Saguenay Fjord relative to Station 23 (Bourgoin and Tremblay, 2010) rendering MnO_x removal by scavenging more likely.

Given its dimensions and tributary inputs, the dissolved and particulate load in the Saguenay Fjord carries a greater terrestrial signature than the Lower St. Lawrence Estuary (LSLE). As in most estuaries, the humic substances originate from terrestrial runoff and humification of marine organic matter in the water column and sediments (Beck et al., 1974). Humic substances make up to 62 - 100% of the sedimentary organic matter at our study site in the Saguenay Fjord (Tremblay and Gagné, 2007), and these

are mostly terrigenous. Shiller et al., (2006) indicated that the presence of photofresh, riverine allochthonous dissolved organic matter promotes stronger metal complexation than photodegraded material found downstream, consistent with our surface water speciation data from SAG-30 relative to surface water at Station 23. Tremblay and Gagné (2007) report dissolved organic matter concentrations ([DOM]) in the water column at each of our study sites, and find that DOM concentrations are nearly three times larger in the surface waters of the Saguenay Fjord (~13.0 mg L^{-1}) than the surface waters of Station 23 (~2.6 mg L^{-1}). This is consistent with our observation of high % Mn(III)-L complexation in the surface waters of the Saguenay Fjord compared to Station 23. Accordingly, we propose that Mn(III)-binding terrigenous ligands enter the Saguenay Fjord from surface runoff and nearby wetlands, and ultimately accumulate in the sediments.

In Figure 4.3, we compare our dMn_T speciation results from 2014 at Station 23 to the extractable-dMn_T results (measured by sample acidification and subsequent ammonium pyrollidine dithiocarbamate (APDC) extraction) on samples collected in May of 1974 by Yeats et al (1979) at their Station 63, within 0.5 km from our Station 23. The salinities of our 2014 samples are within ± 1.0 of the salinities reported by Yeats et al (1979) for similar depth intervals, and thus we feel the water masses are comparable. The 2014 profile for Mn(II) follows the shape of the extractable-dMn_T obtained in 1974, with higher dMn_T measured at all depths in 2014. The accumulation of dMn_T in the water column since 1974 may have resulted from decreased dO_2 (Gilbert et al., 2005), but the 2014 dMn_T is significantly higher at all depths (irrespective of dO_2), except in the bottom waters where 2014 dMn_T is almost entirely Mn(II). We

attribute the difference to the presence of Mn(III)-L complexes, and propose that the extractable fraction of dMn_T analyzed in 1974 (Yeats et al., 1979) is missing most of the Mn(III)-L. We postulate that the acidification step (pH<2), employed in the APDC extraction applied by Yeats et al (1979), resulted in the precipitation of humic Mn(III)-L complexes. Furthermore, Yeats et al (1979) explicitly state that the APDC-extractable Mn is defined by the availability to the chelating agent and stability at storage pH. The loss of Mn(III)-L upon acidification is supported by our finding that our dMn_T(acidified) corresponds to Mn(II) in the 2014 samples as well as the shape of the 1974 acidified extractable Mn profile (Yeats et al., 1979).

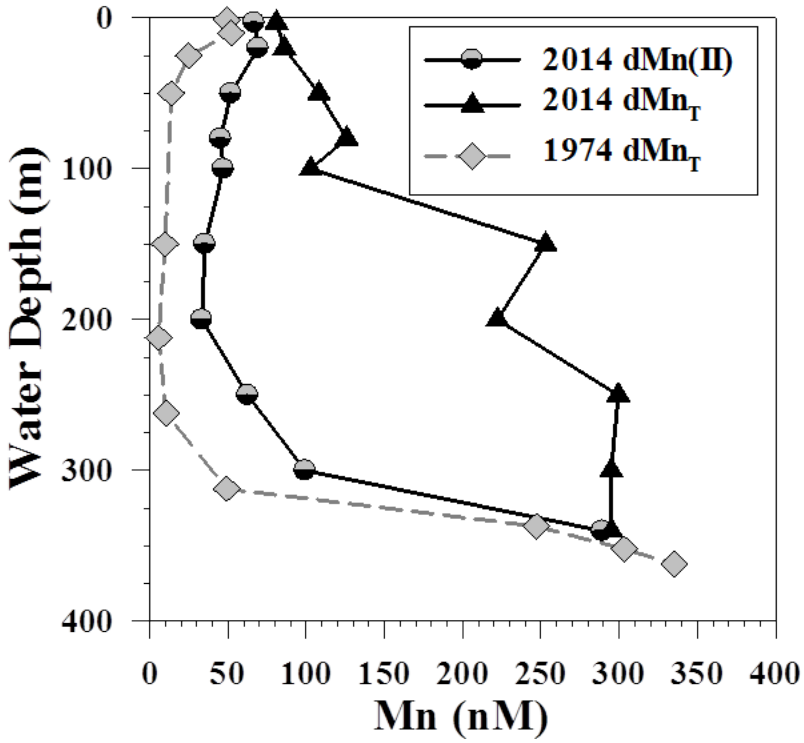

Figure 4.3 A comparison of dMnT from 1974 at Station 63 (Yeats et al., 1979) and the data from this study at Station 23. The Yeats et al. (1979) water samples were collected, filtered, acidified, and analyzed following an ammonium pyrollidine dithiocarbamate (APDC) extraction. Our samples were analyzed immediately after filtration using the porphyrin addition method.

Several research groups have shown that Fe(III)-humic complexation is also important in coastal environments (Laglera and van den Berg, 2009; Abualhaija et al., 2015; Krachler et al., 2015). Mn(III) binds to the same ligands as dissolved Fe(III) and their thermodynamic stability constants are greater or similar to Fe(III) complexes (Kostka et al., 1995; Klewicki and Morgan, 1998; Parker et al., 2004; Duckworth and Sposito, 2007; Luther et al., 2015). Because many microorganisms use complexed Fe(III) to facilitate Fe uptake (Goyne and Carpenter, 1974; Trick, 1989), the presence of

excess Mn(III) could affect Fe(III) bioavailability by competing for the same ligands, especially where Fe(III) may be a limiting nutrient for some microorganisms. Furthermore, because dMn_T is generally not limiting in surface waters compared to dFe_T (Morel and Price 2003), we anticipate that humic binding and competition for these ligands has been underestimated.

Aliquots of 5 samples (Table 4.4) were filtered shipboard, frozen and stored for future analyses. Figure 4.4 shows the linear correlation between samples analyzed shipboard (x-axis) and samples analyzed after preservation (y-axis, filtered, frozen and thawed 12 months later). Thawed samples (closed circles) were compared to thawed and further filtered samples (0.02 µm, open squares). Given the near 1:1 slope in relation to shipboard measurements, the excellent R^2 values, and the overlap between thawed 0.20 µm-filtered and thawed 0.02 µm-filtered samples, we conclude that freezing filtered samples is suitable for sample preservation. Moreover, the Mn(III)-L complexes we measured at this site are not operationally colloidal (size class between 20 to 200 nm), unlike Fe(III)-L species for which up to 90 % are found in the colloidal fraction (Schlosser et al., 2013). One possible interpretation of these results is that that Mn(III)-L species are more mobile and transported farther than their Fe(III)-L counterparts. Mn redox reactivity in a given system will vary pending the stability of the complex, which depends on many factors including ligand concentration, photochemical effects and microbial mediation. Mn(III)-L complexes formed at sites like the St. Lawrence Estuary are likely kinetically (meta)stable, and their long range transport may be sustained by high fluxes of Mn from the coast. Because Mn(III) can donate or accept electrons, upon transport from coastal to oceanic environments, these

Mn(III)-L complexes may eventually act as important redox active species in the cycling of other elements.

Table 4.4 Comparison of dMn_T (nM) from shipboard analyses (Sept. 2014) following filtration through a 0.20 µm membrane, laboratory analyses 13 months later after filtration through a 0.20 µm membrane, and laboratory analyses one year later following filtration through a 0.02 µm membrane.

Station	Depth (m)	dMn_T 0.2 µm	dMn_T 0.2 µm - Oct. 2015	dMn_T 0.02 µm - Oct. 2015
23	3	80.9 ± 3.4	71.2 ± 1.8	73.7 ± 9.6
	100	102.8 ± 4.8	99.9 1.7	92.7 ± 3.7
	340	295.1 ± 16.5	310.4 ± 5.6	306.9 ± 19.2
SAG30	50	55.6 ± 1.4	55.2 ± 13.2	59.0 ± 2.0
	250	691.9 ± 7.6	683.0 ± 4.5	635.2 ± 59.5

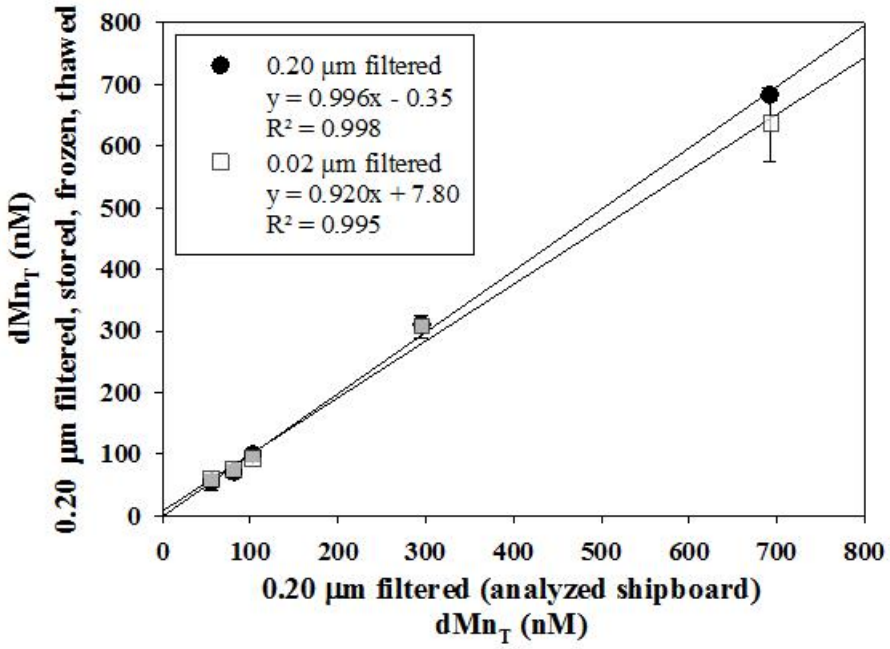

Figure 4.4 Linear correlation of total dissolved Mn from samples analyzed shipboard (x-axis) and samples analyzed 12 months after sampling, stored by filtering and freezing. Closed circles represent samples which were thawed and reanalyzed, open squares represent samples that were thawed, and filtered again through 0.02 µm filters. Standard deviations of triplicate measurements are shown as error bars.

4.5 Conclusions

Our findings have broad implications for understanding the cycling of Mn in the global ocean. We demonstrate that Mn(III)-L complexes are present in oxygenated waters, and are thus likely ubiquitous in the marine environment. The presence of Mn(III)-L in the marine environment can have a profound impact on the mobility and uptake of other nutrients (Kostka et al., 1995). In the Lower St. Lawrence Estuary (LSLE), the fate (oxidation and complexation to Mn(III)-L or oxidation to MnOx) of Mn(II) fluxing out of the sediments is critical in determining the transport and residence

time of dMn_T in the water column (Mucci et al., 2003). The rate of Mn(II) oxidation is a function of the flux of dMn_T out of the sediments, the nature of the ligand(s) in the water column, the abundance of particles in the water column, and the dO_2. Mn(II) escapes from the sediments to the overlying waters at both study sites, and the appearance of Mn oxides and Mn(III)-L in bottom waters is clear evidence of Mn(II) oxidation in the water column (Sundby et al., 1981; Richard et al., 2013). In the deep waters at Station 23, the Mn(II) is oxidized to MnO_x, whereas, in the Saguenay Fjord, [Mn(III)-L] >> [MnO_x]. We attribute this difference to the presence of stronger terrestrially-derived ligands that prevent the complete oxidation of Mn(II) to MnO_x in the Saguenay Fjord, and/or higher reductive dissolution rates of authigenic MnO_x. At Station 23, the initial fate of Mn(II) fluxing from sediments is its oxidation to MnO_x in bottom waters. Nevertheless, we still observe Mn(III)-L in the water column indicating that reduction of MnO_x and stabilization of Mn(III)-L may be an important formation pathway of Mn(III). It is also possible that Mn(III) is a residual product of the two-step oxidation of Mn(II) to Mn(IV), and stabilized as Mn(III)-L by ambient ligands. Our findings suggest that the development of hypoxic bottom waters in the LSLE may have led to increased dMn_T at Station 23, and that this additional dMn_T is stabilized as Mn(III)-L complexes in the presence of strong organic ligands (with $\log K_{cond}$ >13.2). Mn speciation studies need to include the measurement of Mn(III)-L complexes, which cannot be accomplished upon acidification for sample storage, as acidification precipitates Mn(III)-L humic complexes, a previously overlooked class of Mn species. Finally, our data highlight the importance of humic ligands to the coastal ocean, and provide evidence of a neglected potential pathway for the transport of dissolved metal-organic complexes to the global ocean.

4.6 Acknowledgments

This work was funded by grants from the Chemical Oceanography program of the National Science Foundation (OCE-1558738 and OCE-1155385 to GWL; OCE-1558692 and OCE-1154307 to BMT) and the National Sciences and Engineering Research Council of Canada (NSERC) through Discovery and Ship-time grants to AM. Véronique Oldham thanks the University of Delaware for receipt of a Marian R. Okie Fellowship and a University of Delaware Graduate Fellowship. Thanks also to the crew of the *R/V Coriolis II* who made sampling for this research possible, and Matthew R. Jones who carried out the MnO_x analyses.

REFERENCES

Abualhaija M.M., Whitby H. and van den Berg H. (2015) Competition between copper and iron for humic ligands in estuarine waters. *Mar. Chem.* 172, 46-56.

Altmann H.J. (1972) Determination of dissolved oxygen in water with Leukoberbelin-Blue I. A quick Winkler method. *Anal. Chem.* 262, 97-99.

Beck K.C., Reuter J.H. and Perdue E.M. (1974) Organic and inorganic geochemistry of some coastal plain rivers of the southeastern United States. *Geochim. Cosmochim. Acta.* 38, 341-364.

Bourgoin, L-H., Tremblay, L. (2010) Bacterial reworking of terrigenous and marine organic material in estuarine water columns and sediments. *Geochim. Cosmochim. Acta.* 74, 5593-5609.

Davies S.H.R. and Morgan J.J. (1989) Manganese(II) oxidation-kinetics on metal-oxide surfaces. J. *Colloid Interface Sci.* 129, 63-77.

Dellwig O., Schnetger B., Brumsack H., Grossart H. and Umlauf L. (2012) Dissolved reactive manganese at pelagic redoxclines (part II): Hydrodynamic conditions for accumulation. *J. Mar. Syst.* 90, 31-41.

Duckworth O.W. and Sposito G. (2005) Siderophore-manganese(III) interactions I. Manganite dissolution promoted by desferrioxamine-B. *Environ. Sci. Technol*. 39, 6045-6051.

Duckworth O.W. and Sposito G. (2007) Siderophore-promoted dissolution of synthetic and biogenic layer-type Mn oxides. *Chem. Geol*. 242, 497-508.

Gilbert D., Gobeil C., Sundby B., Mucci A. and Tremblay G.H. (2005) A seventy-two year record of diminishing deep-water oxygen levels in the St. Lawrence estuary: The northwest Atlantic connection. *Limnol. Oceanogr*. 50, 1654-1666.

Gledhill M. and van den Berg C.M.G. (1994) Determination of complexation of iron (III) with natural organic complexing ligands in seawater using cathodic stripping voltammetry. *Mar. Chem.* 47, 41-54.

Goyne E.R. and Carpenter E.J. (1974) Production of iron-binding compounds by marine microorganisms. *Limnol. Oceanogr.* 19, 840-842.

Hansard S.P., Easter H.D. and Voelker B.M. (2011) Rapid reaction of nanomolar Mn(II) with superoxide radical in seawater and simulated freshwater. *Environ. Sci. Technol.* 45, 2811-2817.

Klewicki J.K. and Morgan J.K. (1998) Kinetic behavior of Mn(III) complexes of pyrophosphate, EDTA and citrate. *Environ. Sci. Technol*. 32, 2916-2922.

Kostka J.E., Luther G.W. and Nealson G.W. (1995) Chemical and biological reduction of soluble Mn(III): potential importance as an environmental oxidant. *Geochim. Cosmochim. Acta.* 59, 885-894.

Krachler R., Krachler R.F., Wallner G., Hann S., Laux M., Recalde M.C.F., Jirsa F., Neubauer E., von der Kammer F., Hofmann T. and Keppler T. (2015) River-derived humic substances as iron chelators in seawater. *Mar. Chem*. 174, 85-93.

Laglera L.M. and van den Berg C.M.G. (2009) Evidence for geochemical control of iron by humic substances in seawater. *Limnol. Oceanogr.* 54, 610-619.

Landing W.M. and Bruland K.W. (1986) The contrasting biogeochemistry of iron and manganese in the Pacific Ocean. *Geochim. Cosmochim. Acta.* 51, 29-43.

Learman D.R., Voelker B.M., Vazquez-Rodrigues A.I. and Hansel C.M. (2011) Formation of manganese oxides by bacterially generated superoxide. *Nat. Geosci.* 4, 95 – 98.

Luther, G.W. (2010) The Role of One- and Two-Electron Transfer Reactions in Forming Thermodynamically Unstable Intermediates as Barriers in Multi-Electron Redox Reactions. *Aqu. Geochem.* 16, 395-420.

Luther G.W., Madison A.S., Mucci A., Sundby B. and Oldham V.E. (2015) A kinetic approach to assess the strengths of ligands bound to soluble Mn(III). *Mar. Chem.* 173, 93-99.

Madison A.S., Tebo B.M. and Luther G.W. (2011) Simultaneous determination of soluble manganese(III), manganese(II) and total manganese in natural (pore)waters. *Talanta*. 84, 374-382.

Madison A.S., Tebo B.M., Mucci A., Sundby B. and Luther G.W. (2013) Abundant porewater Mn(III) is a major component of the sedimentary redox system. *Science.* 341, 875-878.

Morel, F.M.M., and Price, N.M. 2003. The biogeochemical cycles of trace metals in the oceans. *Science.* 300, 944-947.

Mucci A., Boudreau B., and Guignard C. (2003) Diagenetic mobility of trace elements in sediments covered by a flash flood deposit: Mn, Fe and As. *Appl. Geochem.* 18, 1011-1026.

Oldham V.E., Owings S.M., Jones M.R., Tebo B.M and Luther G.W. (2015) Evidence for the presence of strong Mn(III)-binding ligands in the water column. *Mar. Chem.* 171, 58-66.

Parker D.L., Sposito G. and Tebo B.M. (2004) Manganese(III) Binding to a Pyoverdine Siderophore Produced by a manganese(II)-Oxidizing Bacterium. *Geochim. Cosmochim. Acta*. 68, 4809-4820.

Parker D.L., Takami M., Mylene L., Mozafarzadeh R.V., McCarthy J.K. and Tebo B.M. (2007) Inter-Relationships of MnO2 Precipitation, siderophore–Mn(III) Complex Formation, Siderophore Degradation, and Iron Limitation in Mn(II)-Oxidizing Bacterial Cultures. *Geochim. Cosmochim. Acta*. 71, 5672-83.

Richard D., Sundby B. and Mucci A. (2013) Kinetics of manganese adsorption, desorption, and oxidation in coastal marine sediments. *Limnol. Oceanogr*. 58, 987-996.

Schlosser C., Streu P. and Croot P.L. (2013) Vivaspin ultrafiltration: A new approach for high resolution measurements of colloidal and soluble iron species. *Limnol. Oceanog. Methods.* 11, 187-201.

Shiller A.M., Shuiwang D., van Erp P. and Bianchi T.S. (2006). Photo-oxidation of dissolved organic matter in river water and its effect on trace element speciation. *Limnol. Oceanogr.* 51, 1716-1728.

Stumm W. and Morgan J. J.. 1996. Aquatic Chemistry. John Wiley & Sons, Inc., pp1022.

Sundby B., Silverberg N. and Chesselet R. (1981) Pathways of manganese in an open estuarine system. *Geochim. Cosmochim. Acta* 45, 293-307.

Tebo B.M., Ghiorse W.C., vanWaasbergen L.G., Siering P.I. and Caspi R. (1997) Review in mineralogy. *Mineralog. Soc. Am.* 35, 225-266.

Tebo, B.M., Bargar, J.R., Clement, B.G., Dick, G.J., Murray, K.J., Parker, D., Verity, R., Webb, S.M. (2004). Biogenic manganese oxides: properties and mechanisms of formation. *Ann. Rev. Earth Planet. Sci.* 32, 287-328.

Tremblay L. and Gagné J.-P. (2007) Distribution and biogeochemistry of sedimentary humic substances in the St. Lawrence Estuary and the Saguenay Fjord, Québec. *Org. Geochem.* 38, 682-699.

Trick C.G. (1989) Hydroxamate-siderophore production and utilization by marine eubacteria. Curr. Microbiol. 18, 375-378.

Trouwborst R.E., Clement B.G., Tebo B.M., Glazer B.T. and Luther G.W. (2006) Soluble Mn(III) in suboxic zones. *Science.* 313, 1955-1957.

Yakushev E.V., Pollehne F., Jost G., Kuznetsov I., Schneider B. and Umlauf L. (2007) Analysis of the water column oxic/anoxic interface in the Black and Baltic seas with a numerical model. *Mar. Chem.* 107, 388-410.

Yakushev E.V., Pakhomova S., Sørenson K. and Skei J. (2009) Importance of the different manganese species in the formation of water column redox zones: Observations and modeling. *Mar. Chem.* 117, 59-70.

Yeats P.A., Sundby B. and Bewers J.M. (1979) Manganese recycling in coastal waters. *Mar. Chem.* 8, 43-55.

Chapter 5

THE CYCLING OF MANGANESE AND IRON: REVISITING METAL REMOVAL IN ESTUARIES[4]

Abstract

Metal removal by estuarine mixing has been studied for several decades, but few studies emphasize dissolved metal speciation and organic ligand complexation. Findings from the last decade indicate that metal-humic complexation can be significant for dissolved metals including Cu(II), Al(III) and Fe(III), but little consideration is given to the precipitation of these complexes with humic material at pH<2. Given that total soluble metal analysis involves an acidification step for sample preservation, we show that Mn and other metal concentrations may have been underestimated in estuaries, especially when humic substance concentrations are high. A competitive ligand assay of selected samples from our study site, a coastal waterway bordered by wetlands (Broadkill River, DE), showed that Mn(III)-humic complexation is significant, and that some Mn(III)-L complexes precipitate during acidification. In the oxygenated surface waters of the Broadkill River, total dissolved Mn (dMn_T) was up to 100 % complexed to ambient ligands as Mn(III)-L, and we present evidence for humic-type Mn(III)-L complexes. The Mn(III) complexes were kinetically stabilized against Fe(II) reduction, even when [Fe(II)] was 17 times higher than [dMn_T]. Unlike typical oceanic surface waters, [Fe(II)]>[Fe(III)-L] in surface waters, which may be attributed to high rates of

[4] *Chapter 5 submitted to Geochimica et Cosmochimica Acta.*

photoreduction of Fe(III)-L complexes. Total [Mn(III)-L] ranged from 0.22 – 8.4 μM, in excess of solid MnO_x (below 0.28 μM in all samples). Filtration of samples through 0.02 μm filters indicated that all Mn(III)-L complexes pass through the filters and were not colloidal species in contrast to dissolved Fe. Incubation experiments indicated that the reductive dissolution of solid MnO_x by ambient ligands may be responsible for Mn(III) formation in this system. Unlike previous studies of estuarine mixing, which demonstrated metal removal during mixing, we show significant export of dMn and dissolved Fe (dFe) in the summer and fall of 2015. Thus, we propose seasonal cycling of estuarine removal and export for dMn and dFe.

5.1 Introduction

Considerable attention has been given to the transformations of dissolved and particulate material during estuarine mixing because these transformations impact the transport of terrestrially derived organic matter (OM) to the ocean, and the cycling of important nutrients and trace elements. Estuarine environments, including coastal salt marshes and waterways, have high OM content because of high primary productivity and influx of terrestrial OM (Hedges et al, 1997). This OM is cycled such that only some is discharged to the ocean while the rest is precipitated to the sediment (Hedges et al, 1997). In particular, riverine OM can be rich in humic acids and negatively charged functional groups capable of binding metal ions. Thus, during estuarine mixing, riverine OM interacts with marine metal cations, including trace metals leading to flocculation/aggregation and the transformation of trace metals from the dissolved to particulate phase. It has been suggested that up to 50-95 % of total dissolved iron (dFe_T) and 25-45 % of total dissolved manganese (dMn_T) is transformed in this way in coastal riverine systems (Boyle et al, 1977; Sholkovitz et al, 1978).

Several studies have examined the cycling and removal of dFe_T (Coonley et al, 1971; Windom et al, 1971; Boyle et al, 1974, 1977; Moore et al, 1979; Eastman and Church, 1984) and dMn_T (Windom et al, 1971; Boyle et al, 1974; Graham et al, 1976; Moore et al, 1979; Eastman and Church, 1984) at sites of estuarine mixing, but considerably fewer studies have been conducted for dFe speciation (Batchelli et al, 2010; Buck et al, 2007; Gledhill and van den Berg, 1994; Rijkenberg, et al, 2006; Sander et al, 2015; van den Berg, 1995) and none, to our knowledge, on the speciation of dMn. In natural waters, Mn and Fe undergo a variety of redox transformations between soluble uncomplexed species ($Fe(H_2O)_6^{2+}$, $Mn(H_2O)_6^{2+}$), soluble complexed species (Fe(II)-L, Fe(III)-L, and Mn(III)-L) and insoluble metal (hydr)oxides. Historically, speciation studies of Mn in natural waters have focused on soluble Mn(II) (operationally defined as passed through a 0.20 µm filter) and solid Mn(III/IV) oxides (retained onto a 0.20 µm filter), neglecting the intermediate soluble Mn(III)-L complexes. However, speciation studies have shown that Mn(III)-L complexes can make up to 90 % of the dMn_T pool in the suboxic water column of Black Sea (Trouwborst et al, 2006; Yakushev et al, 2007, 2009) and Baltic Seas (Dellwig et al, 2012; Yakushev et al, 2007, 2009), the anoxic water column of the Chesapeake Bay (Oldham et al, 2015), and in suboxic pore-waters of the St. Lawrence (Madison et al, 2011, 2013). Whereas Mn(III) complexation has only recently been measured in oxygenated surface waters in the St. Lawrence Estuary (Oldham et al, 2017), dFe_T has been shown to be predominantly complexed to organic ligands as Fe(III)-L (Buck et al, 2007; Sander et al, 2015) with dFe_T transport and bioavailability linked to complexation. Laboratory studies have shown that Mn(III) is stabilized by the same

ligands binding Fe(III) in the presence of oxygen (Luther et al, 2015; Parker et al, 2004, 2007) and that Mn(III)-L can be formed by Mn(II) oxidation (Parker et al, 2004) or by MnO_2 reduction (Duckworth and Sposito, 2007; Oldham et al, 2015). Thus, we predict that Mn(III)-L complexes should be present in all coastal systems with high organic matter concentrations, including our study site, the Broadkill River estuary of the Delaware Bay. The coupled cycling of Mn and Fe in such environments is of interest because they may be competing for the same ligands, and the presence of excess Mn could affect the complexation of Fe. In this study, we show that Mn(III)-L complexes are present in oxygenated surface waters and that Mn(III)-L complexes likely bind the same ambient ligands as Fe(III). In particular, we show that Mn(III) binds to humic material, which is consistent with findings of humic Mn(III) complexation in the St. Lawrence Estuary (Oldham et al, 2017).

Our study site, the Broadkill River Estuary runs through the Great Marsh into the lower Delaware Bay (Fig. 5.1). The Great Marsh is a saline, high marsh site which undergoes complete inundation only during spring tides and storm surges (Stumpf, 1983). The site is dominated by the cord grass *Spartina alterniflora* which dominates many salt marshes of the East coast of the United States. *S. alterniflora* (and emergent vegetation in general) is the principle source of organic matter in the soils of salt marshes, releasing approximately 330 kg of *Spartina*-related humic substances per hectare annually (Filip and Alberts, 1989). Studies examining estuarine mixing of Mn and Fe have typically employed acidification (pH<1.5) to stabilize dissolved metals. However, *humic acids operationally precipitate at pH<2*. Thus, a primary goal of this study is to show that previous work may have underestimated the soluble fraction of

these metals due to precipitation of metals bound to humic acids during the acidification step prior to analyses. Here we present findings concerning the seasonal relationship between dissolved humic acids, dFe speciation, and dMn speciation in the Broadkill River.

5.2 Methods

Samples were collected over 9 sampling events from April 2015 to February 2016. The October 7th sampling occurred 2 days after severe coastal flooding from Hurricane Joaquin. For each sampling event, 4 or 8 sample sites (Fig. 5.1) were selected based on an increasing surface salinity gradient. A YSI (Model 350) probe was used to measure temperature and salinity. Water samples were collected from a small boat into acid-washed 500 mL PTFE bottles, by opening and filling bottles beneath the surface to avoid surface microfilm contamination. The samples were immediately filtered in the field using nylon luer-lock syringe filters (Millipore, 0.20 µm) into clean Falcon tubes. One aliquot of filtered water was amended immediately with 1 mM hydroxylamine hydrochloride, to reduce Mn(III)-L in order to determine total dissolved Mn. Filters were saved for MnO_x analysis, for each sample site, on June 23rd, July 7th, July 21st, and October 7th 2015.

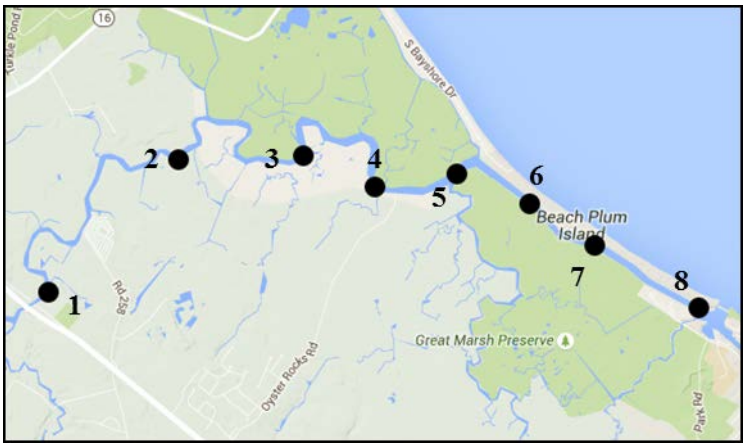

Figure 5.1 Site map from the June 23rd sampling event, which is representative of the locations for the 8 sampling sites for each sampling. Site #1 represents the fresh end-member and Site #8 is at the mouth of the Broadkill River within the Delaware Bay, the saline end-member.

In this work, all samples were filtered within 5 minutes of collection, and were analyzed for Mn speciation (no acidification step) within two hours of collection. Samples were taken for Fe speciation from June 2015 to February 2016, and these were acidified after filtration, in the field, with concentrated HCl (Fisher, Optima Grade) to a pH of 2; they were analyzed within 1 day of collection. On July 21st and October 7th additional samples were filtered on site, but not acidified to assess whether acidification resulted in a difference in Fe speciation.

On October 7th, all Mn speciation and unacidified Fe speciation samples were also filtered through 0.02 µm filters (Anatop) and reanalyzed for speciation to determine into which of three size fractions the metal species were found [<0.02 µm, or 0.02 - 0.20 µm, or >0.20 µm]. We operationally define the 0.02 - 0.20 µm class as colloidal to be consistent with recent Fe research (e.g. Fitzsimmons et al, 2015).

5.2.1 Dissolved Mn Analysis

Each sample was analyzed within two hours of collection, and 3-6 replicates were performed for each sample to determine dissolved Mn(II), Mn(III)L_{weak} and dMn_T. Samples were kept capped, and in the dark, between analyses to ensure no degradation. Samples were analyzed using the established method of a spectrophotometric ligand addition ([α, β, γ, δ-tetrakis(4-carboxyphenyl)porphine] or T(4-CP)P (ε= 95,400 M^{-1} cm^{-1})) previously developed by Ishii et al, (1982) and modified by Madison et al, (2011) to speciate dissolved Mn(II) and Mn(III)-L_{weak}. In this method, the kinetics of the reaction of Mn(II) + Mn(III)-L_{weak} with the added porphyrin allows for the speciation of the two species. Through differential kinetics, we obtain the kinetic dissociation constant, k_d, of the Mn(III)-L_{weak} complex (Luther et al, 2015). We then can estimate a conditional stability constant, K_{cond} for weak Mn(III)-L complexes, based on k_d and an estimated kinetic metal- ligand formation constant, k_f. The upper limit for the Mn(III)-L_{weak} complex in seawater is $\log K_{cond}$ = 13.2 (Luther et al, 2015). This K_{cond} is uncorrected for the side reaction coefficients for Mn(III) and the unknown ligand.

The addition of a strong reducing agent, such as hydroxylamine, prior to analysis, reduces any Mn(III)-L_{strong} complexes in solution so that total dissolved Mn can be determined. The difference between the sample treated with and without hydroxylamine is the concentration of the Mn(III)-L_{strong}. These strong complexes are not outcompeted by the added porphyrin ligand so their $\log K_{cond}$ exceeds 13.2 (Luther et al, 2015, Oldham et al, 2015). We therefore can operationally define two ligand classes (Mn(III)-L_{weak}, Mn(III)-L_{strong}).

A Hewlett Packard 8452B diode array spectrophotometer was coupled with Olis. Inc. Globalworks software for all UV/Vis measurements (2 nm wavelength resolution). All reagents were made according to Madison et al, (2011), and a standard calibration was performed prior to analysis with standards ranging from 50 nM to 10 μM, made from $MnCl_2$-$4H_2O$ (Fisher Scientific) into deionized water (18.2 mΩ).

5.2.2 MnO_x Analyses

Known volumes of sample (25 – 30 mL) were filtered through 0.20 μm Millipore nylon syringe filters in triplicate. Filters were amended with 20 μM of leucoberbelin blue dye (LBB, 65 %, Sigma-Aldrich) by pushing 3 mL of the LBB solution back and forth through the filter with two syringes. The filters sat overnight with the dye, before filtering the dye solution for analysis. The dye color, formed on oxidation by particulate manganese or MnO_x, was measured in a 1 cm cuvette at 620 nm using the spectrophotometric protocol described above (Altmann, 1972). The LBB (410.5 g mol^{-1}) stock solution was made by dissolving it in Milli-Q water to a concentration of 4 % and adding 40 μL of 10 M sodium hydroxide (NaOH) per 10 mL of LBB solution. Working solutions are made by diluting the stock into 1% acetic acid (made up in Mili-Q water), to 0.04 %. A calibration curve was generated using potassium permanganate (0.2 – 10 μM $KMnO_4$) and using a soluble MnO_2 made in the lab (Perez-Benito et al, 1996). To produce equivalent absorbance, 2.5 times more Mn(IV) is required than Mn(VII), as Mn(VII) oxidizes 5 LBB molecules, compared to 2 LBB molecules for Mn(IV). After this consideration, however, we find that MnO_2 produces ~10% higher molar absorptivity, likely due to the oxidation and destruction of some of the LBB dye by $KMnO_4$. The molar absorptivity of MnO_2, then, better

reproduces the molar absorptivity reported by Altman (1972) than $KMnO_4$ (ε = 110, 000 mol^{-1} at λ_{max} = 623 nm).

5.2.3 Dissolved Fe Analyses

Triplicate Fe(II) and dFe_T measurements were made on filtered acidified samples within 1 day of collection, and within 2 hours of collection for unacidified samples, using the method of Stookey (1970) and the UV-Vis system described above. Samples were buffered in 2.5 M ammonium acetate, prior to addition of the ferrozine reagent, which reacts with Fe(II) to produce an absorption at 562 nm. Hydroxylamine hydrochloride was added as a reducing agent to separate aliquots of samples in order to measure dFe_T. The difference between dFe_T and the Fe(II) measurements gives soluble Fe(III).

5.2.4 Characteristic Humic Absorbance Measurements

Characteristic humic acid absorption peaks in filtered samples were measured within one day of sample collection using the 1 cm spectrophotometric set-up described above. Triplicate scans of the sample were taken from 200 – 800 nm, and absorbances were recorded at 258 and 280 (characteristic of average humic and fulvic acids; the result of $\pi - \pi *$ electron transfer for a number of aromatic substances) as well as at 400 nm, which is characteristic of a Mn complex containing 1 Mn bound to 1 catechol (Sever and Wilker, 2004).

5.2.5 Competitive Ligand Assay

Experiments were performed on two samples, from the July 7th sampling event, to determine whether humic acids were responsible for binding Mn(III). Filtered samples from our sites with 0 ppt salinity and 15 ppt salinity were subsampled. For

each, one aliquot was amended with concentrated HCl (Fisher, Optima Grade), to pH<1.5 to precipitate humic material; the solution was then centrifuged, and decanted. The resulting supernatant was brought back up to pH=8 with trace metal grade 1 M NaOH (Luther et al, 2011). The second aliquot was untreated, thereby keeping the humic material in solution. Both treatments (with and without humic material) were then amended with Mn(III)-pyrophosphate (Mn(III)-PP, ε_{max}=484 nm), and allowed to react for 15 minutes. Any change in the Mn(III)-PP absorbance is due to ligand substitution with ambient ligands.

5.2.6 MnO_2 Reductive Dissolution

A sample was collected on July 28th from our low salinity site (1.8 ppt salinity) into a 1 L trace metal clean PTFE bottle, after triple rinsing with sample. The sample was filtered on site using a hand-syringe through a 0.20 µm Nylon filter (Millipore), into another clean 1 L PTFE bottle. The sample was analyzed in triplicate for initial Mn speciation using the porphyrin method in section 2.1 and LBB method in section 2.2. Afterwards, the sample was amended with 10 µM MnO_2 (prepared as in Perez-Benito et al, 1996). The sample was reanalyzed, in triplicate, for MnO_2 and dMn speciation at 4 subsequent time points (30 minutes, 1 hour, 3 hours and 21 hours) to observe any reductive dissolution of MnO_2 by ambient ligands in the water sample as previously shown in laboratory experiments by Oldham et al (2015).

5.3 Results

5.3.1 Soluble Mn Speciation Along a Salinity Gradient

The speciation of dMn along the salinity gradient in the Broadkill River (Figure 5.2, Table 5.1) changed seasonally from April 2015 to February 2016. However, dMn_T

did not follow expected conservative mixing nor estuarine removal, but rather it was exported in all sampling events. For example, Figure 5.2 shows the speciation of dMn_T from spring (Fig. 5.2A), summer (Fig. 5.2B), fall (Fig. 5.2C) and winter (Fig. 5.2D) samplings. In the spring, dMn_T was higher at mid-salinities, at sites corresponding to the presence of large creeks, which acts as a source of dMn_T, ligands and/or Mn(III)-L to the system. In all samplings, dMn_T was exported from the system to the Delaware Bay as Mn(III)-L, and this export was most pronounced in the summer and fall. Soluble Mn(II) concentrations were low during all sampling events, relative to Mn(III)-L concentrations. There were only two samples where % Mn(II) > % Mn(III)-L, throughout the entire sampling campaign, both at the site of maximum salinity.

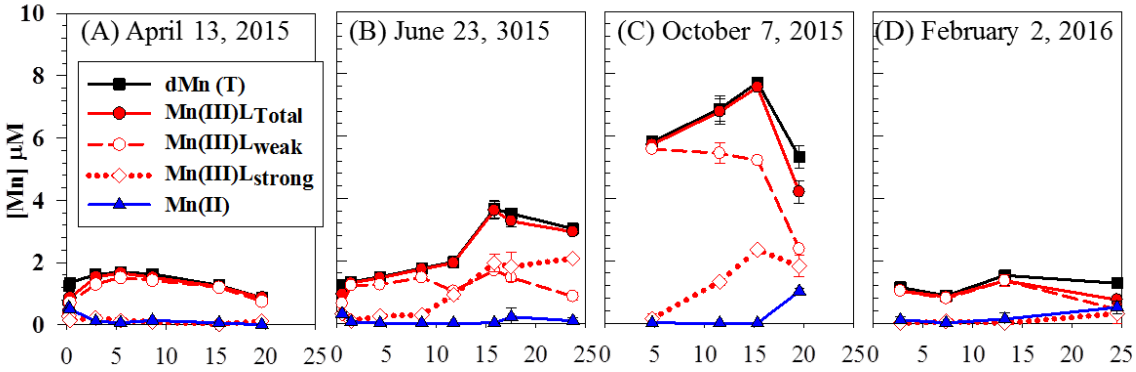

Figure 5.2 The speciation of dMn_T along the salinity gradient from (A) April 13th, 2015; (B) June 23rd, 2015; (C) October 7th, 2015; and (D) February 2nd, 2016. Mn(III)-L complexes are in red, with symbols and lines differing for Total, Strong and Weak complexes. The total dMn_T (Mn(II)+Mn(III)-L_{Total}) is in black. Where error bars are not visible, they are smaller than the symbols.

In October 2014, dMn_T was <50 nM in the surface waters of the Delaware Bay indicating that the Bay is not a Mn source. In all Broadkill River samples, dMn_T was predominantly in the form of Mn(III)-L complexes, with Mn(III)-L ranging from 57.1 % (0 ppt salinity) to 99.5 % (20 ppt salinity) in the spring sampling and from 76.7% (0 ppt salinity) to 100 % (1.4 ppt salinity) in the summer sampling. The highest dMn_T concentrations (5.32 – 7.72 µM) were measured on October 7th, two days after hurricane Joaquin hit the region, resulting in complete flooding of the Great Marsh. Additionally, maximum senescence occurs around October in this region, and higher release of OM from decaying plants may also contribute to the maximum values we

observed in October. In the winter, we observe lower dMn_T concentrations (0.88 – 1.53 µM) but Mn(III)-L complexation still dominated, with Mn(III)-L complexes making up 58.5 % (24.5 salinity) to 95.8 % (7.3 salinity) of the dMn_T.

Table 5.1 Sample salinity, dMn speciation and % for each ligand class. All speciation measurements were in 3-6 replicates.

Date	S (ppt)	Mn(T)	Mn(II)	Mn(III)-L_{weak}	%	Mn(III)-L_{strong}	%	Mn(III)-L_{total}	%
April 13	0.2	1.26 ± 0.08	0.56 ± 0.03	0.44 ± 0.01	***35***	0.28 ± 0.09	***22***	0.72 ± 0.09	***57***
2015	0.3	1.35 ± 0.06	0.51 ± 0.02	0.72 ± 0.03	***53***	0.15 ± 0.08	***11***	0.87 ± 0.09	***64***
	2.9	1.62 ± 0.07	0.12 ± 0.01	1.31 ± 0.03	***81***	0.23 ± 0.08	***14***	1.54 ± 0.09	***95***
	5.4	1.70 ± 0.08	0.07 ± 0.01	1.52 ± 0.05	***90***	0.15 ± 0.10	***9***	1.67 ± 0.11	***98***
	10	2.02 ± 0.04	0.45 ± 0.01	1.44 ± 0.02	***71***	0.13 ± 0.05	***7***	1.58 ± 0.05	***78***
	8.6	1.64 ± 0.01	0.14 ± 0.00	1.43 ± 0.00	***88***	0.10 ± 0.01	***6***	1.53 ± 0.02	***93***
	15	1.27 ± 0.06	0.07 ± 0.00	1.21 ± 0.06	***95***	0.03 ± 0.09	***2***	1.23 ± 0.11	***97***
	20	0.88 ± 0.02	0.00 ± 0.00	0.75 ± 0.01	***86***	0.12 ± 0.02	***14***	0.87 ± 0.02	***99***
May 27	0.2	0.28 ± 0.02	0.04 ± 0.02	0.23 ± 0.02	***83***	0.01 ± 0.02	***2***	0.24 ± 0.03	***85***
2015	0.5	0.22 ± 0.02	0.00 ± 0.02	0.21 ± 0.00	***98***	0.00 ± 0.02	***2***	0.22 ± 0.02	***100***
	1.2	0.43 ± 0.02	0.08 ± 0.02	0.34 ± 0.01	***79***	0.01 ± 0.02	***2***	0.35 ± 0.02	***81***
	5.6	0.92 ± 0.01	0.02 ± 0.01	0.88 ± 0.01	***95***	0.02 ± 0.01	***2***	0.89 ± 0.02	***97***
	10	0.96 ± 0.02	0.07 ± 0.12	0.87 ± 0.12	***91***	0.02 ± 0.12	***2***	0.89 ± 0.16	***93***
	14	0.97 ± 0.01	0.01 ± 0.02	0.96 ± 0.01	***99***	0.00 ± 0.02	***0***	0.96 ± 0.02	***99***
	18	0.94 ± 0.02	0.15 ± 0.08	0.77 ± 0.07	***82***	0.02 ± 0.08	***2***	0.79 ± 0.11	***84***
	21	0.80 ± 0.03	0.00 ± 0.02	0.78 ± 0.00	***98***	0.02 ± 0.03	***2***	0.80 ± 0.03	***100***
June 11	0.8	0.89 ± 0.01	0.37 ± 0.05	0.52 ± 0.06	***58***	0.03 ± 0.04	***4***	0.55 ± 0.07	***62***
2015	1.7	1.14 ± 0.15	0.35 ± 0.03	0.79 ± 0.13	***69***	0.21 ± 0.13	***18***	0.92 ± 0.19	***80***
	3.8	1.17 ± 0.00	0.03 ± 0.02	1.14 ± 0.02	***98***	0.19 ± 0.01	***16***	1.15 ± 0.03	***99***
	7.6	1.18 ± 0.00	0.00 ± 0.00	1.16 ± 0.00	***98***	0.00 ± 0.01	***0***	1.16 ± 0.01	***98***
	12	1.23 ± 0.00	0.16 ± 0.03	1.07 ± 0.04	***87***	0.38 ± 0.02	***31***	1.09 ± 0.04	***88***
	17	1.13 ± 0.07	0.04 ± 0.04	1.09 ± 0.09	***96***	0.00 ± 0.00	***0***	1.09 ± 0.09	***97***
	20	1.10 ± 0.05	0.19 ± 0.07	0.87 ± 0.02	***79***	0.01 ± 0.05	***1***	0.93 ± 0.06	***84***
	24	0.84 ± 0.02	0.18 ± 0.05	0.65 ± 0.07	***78***	0.15 ± 0.15	***18***	0.81 ± 0.17	***96***
June 23	0.5	1.21 ± 0.02	0.30 ± 0.06	0.62 ± 0.06	***52***	0.30 ± 0.03	***25***	0.93 ± 0.07	***77***
2015	1.4	1.33 ± 0.07	0.04 ± 0.04	1.21 ± 0.03	***91***	0.12 ± 0.00	***9***	1.33 ± 0.03	***100***
	4.3	1.48 ± 0.04	0.00 ± 0.00	1.23 ± 0.03	***83***	0.22 ± 0.02	***15***	1.45 ± 0.04	***98***
	8.5	1.76 ± 0.07	0.00 ± 0.00	1.46 ± 0.01	***83***	0.27 ± 0.07	***15***	1.73 ± 0.07	***98***
	12	1.96 ± 0.14	0.00 ± 0.00	1.02 ± 0.01	***52***	0.91 ± 0.13	***46***	1.93 ± 0.13	***99***
	16	3.66 ± 0.28	0.01 ± 0.01	1.69 ± 0.08	***46***	1.92 ± 0.29	***53***	3.61 ± 0.30	***99***
	18	3.51 ± 0.18	0.20 ± 0.28	1.46 ± 0.04	***42***	1.81 ± 0.46	***51***	3.27 ± 0.47	***93***
	24	3.03 ± 0.05	0.08 ± 0.09	0.86 ± 0.12	***28***	2.07 ± 0.05	***68***	2.93 ± 0.13	***97***
July 7	0.5	1.54 ± 0.19	0.50 ± 0.15	0.37 ± 0.15	***24***	0.68 ± 0.19	***44***	1.05 ± 0.24	***68***
2015	1.2	1.66 ± 0.19	0.04 ± 0.03	1.03 ± 0.02	***62***	0.62 ± 0.19	***37***	1.65 ± 0.19	***99***
	3.8	2.77 ± 0.45	0.00 ± 0.00	1.16 ± 0.01	***42***	1.57 ± 0.46	***57***	2.74 ± 0.47	***99***
	10	2.43 ± 0.02	0.00 ± 0.00	1.11 ± 0.02	***46***	1.31 ± 0.05	***54***	2.42 ± 0.05	***100***
	15	2.21 ± 0.05	0.00 ± 0.00	0.76 ± 0.05	***34***	1.49 ± 0.09	***67***	2.25 ± 0.11	***100***
	18	2.58 ± 0.35	0.02 ± 0.02	1.78 ± 0.04	***69***	0.76 ± 0.40	***29***	2.54 ± 0.40	***98***
	21	1.98 ± 0.08	0.07 ± 0.00	1.91 ± 0.05	***96***	0.00 ± 0.00	***0***	1.91 ± 0.05	***96***
	28	1.13 ± 0.07	0.10 ± 0.10	1.01 ± 0.15	***89***	0.00 ± 0.00	***0***	1.01 ± 0.15	***89***
July 21	1	0.93 ± 0.05	0.02 ± 0.03	0.93 ± 0.04	***100***			0.93 ± 0.04	***100***
2015	1.9	1.01 ± 0.05	0.00 ± 0.00	1.02 ± 0.06	***100***			1.02 ± 0.06	***100***
	4.5	1.06 ± 0.02	0.00 ± 0.00	1.05 ± 0.03	***99***			1.05 ± 0.03	***99***
	7	1.00 ± 0.05	0.00 ± 0.00	1.01 ± 0.03	***100***			1.01 ± 0.03	***100***
	9.8	1.11 ± 0.08	0.00 ± 0.00	1.08 ± 0.08	***97***			1.08 ± 0.08	***97***
	14.5	0.82 ± 0.03	0.04 ± 0.03	0.76 ± 0.04	***93***			0.76 ± 0.04	***93***
	19.2	2.27 ± 0.08	0.20 ± 0.12	2.05 ± 0.12	***90***			2.05 ± 0.12	***90***
	27.8	0.46 ± 0.29	0.23 ± 0.11	0.22 ± 0.39	***49***			0.22 ± 0.39	***49***
October 7	4.7	5.82 ± 0.16	0.00 ± 0.00	5.58 ± 0.06	***96***	0.15 ± 0.14	***3***	5.73 ± 0.11	***99***
2015	11.5	6.88 ± 0.41	0.00 ± 0.00	5.45 ± 0.33	***79***	1.33 ± 0.11	***19***	6.79 ± 0.24	***99***
	15.3	7.72 ± 0.10	0.00 ± 0.00	5.22 ± 0.11	***68***	2.35 ± 0.01	***30***	7.57 ± 0.08	***98***
	19.5	5.32 ± 0.37	1.02 ± 0.08	2.38 ± 0.06	***45***	1.83 ± 0.34	***34***	4.21 ± 0.24	***79***
Novembe	0.8	5.44 ± 0.37	0.38 ± 0.17	0.36 ± 0.06	***7***	4.67 ± 0.20	***86***	5.03 ± 0.15	***92***
2015	5.3	3.70 ±	0.33 ± 0.07	0.77 ± 0.05	***21***	2.50 ±	***68***	3.27 ± 0.04	***88***
	17.8	3.26 ± 0.06	0.04 ± 0.07	0.91 ± 0.11	***28***	2.38 ± 0.17	***73***	3.28 ± 0.14	***100***
	28.8	2.38 ± 0.37	1.48 ± 0.50	0.84 ± 0.30	***35***	0.00 ± 0.00	***0***	0.84 ± 0.21	***35***
February	2.7	1.15 ± 0.01	0.10 ± 0.10	1.04 ± 0.07	***90***	0.00 ± 0.00	***0***	1.04 ± 0.05	***90***
2016	7.3	0.88 ± 0.09	0.01 ± 0.02	0.79 ± 0.11	***90***	0.05 ± 0.06	***6***	0.84 ± 0.09	***96***
	13.2	1.53 ± 0.16	0.13 ± 0.21	1.36 ± 0.18	***89***	0.00 ± 0.00	***0***	1.36 ± 0.13	***89***
	24.5	1.28 ± 0.10	0.51 ± 0.19	0.44 ± 0.01	***34***	0.31 ± 0.31	***24***	0.75 ± 0.22	***58***

5.3.2 The Strength and Stability of Mn(III)-L Complexes

Weak Mn(III)-L complexes in this system had kinetic conditional stability constants (log K_{cond}) ranging from 11.23 – 11.88. This range is higher than the range reported in the sediment porewaters of the lower St. Lawrence Estuary (11.1 – 11.6; Madison et al, 2013; Luther et al, 2015). Additionally, these values are higher than the conditional stability constants (also uncorrected for the side reaction coefficients of M and L) reported by Abualhaija et al, (2015) for Fe(III)-humic complexes along a salinity gradient (4 – 35) in the Mersey Estuary (UK), which had an average log K_{cond} of 11.2.

We detected two Mn(III)-binding ligand classes present for all sampling events. Strong complexes, requiring reduction with NH_2OH before detection ($\log K_{cond} > 13.2$), made up to 22.4 % of the dMn_T in the first two spring sampling events, and up to 68.4 % of dMn_T in the summer and fall sampling events. Thus, there is an increase in strong binding ligands in the system as the summer and fall progress, resulting from the increased production of OM within the system, due to enhanced productivity and degradation of terrestrial plant and estuarine algal material.

5.3.3 Solid and Colloidal Species

Solid MnO_x was measured from samplings occurring on June 23rd, July 7th, July 21st and October 7th, 2015. The measured MnO_x was below 0.27 µM in June and July, decreasing from fresh to saline water, and below 0.04 µM in October. The MnO_x was significantly lower than dMn_T in all samples.

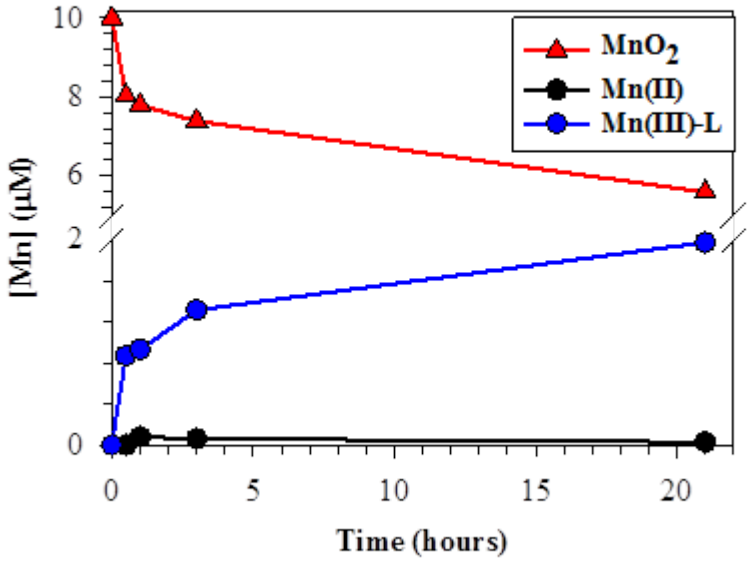

Figure 5.3 The results from an incubation of a fresh end-member sample (1.8 ppt salinity) taken on July 28th. This figure shows the change in Mn speciation after an amendment of 10 µM nanoparticulate MnO_2 to the filtered sample. Error bars for triplicate measurements were smaller than the data symbols.

To test for the reductive dissolution of Mn(IV) in MnO_x, a sample was taken on July 28th at a low salinity site (1.8 ppt salinity). The sample was filtered on site and brought back to the lab where 10 µM MnO_2 was amended to the sample. The sample was analyzed at 30 minutes, 1 hour, 3 hours, and 21 hours after the amendment to test whether ambient ligands were reductively dissolving the MnO_2 (Figure 5.3). Within 3 hours, the added MnO_2 concentration decreased to 80% of the original concentration (loss of 2 µM MnO_2) which corresponded to an increase in dMn_T of 2 µM (99.5 % as

Mn(III)-L). After 21 hours, MnO_2 had decreased to 60 % of the original concentration (loss of 4 µM), corresponding to an increase in dMn_T of 3 µM (99.5 % as Mn(III)-L). The 1 µM loss of total Mn after 21 hours (MnO_2 + dMn_T should be 10 µM) may be due to MnO_2 precipitation or absorption onto the container walls. Additionally, in the initial sample, there was no Mn(II), but after 1 hour, 0.08 µM Mn(II) was detected, indicating a minor amount of complete reduction of the MnO_2, as most Mn form MnO_2 was stabilized as Mn(III)-L, supporting the reductive dissolution of Mn(IV) in MnO_x by ambient ligands in this system.

Measurements of MnO_x on the 0.20 µm filters from samples collected in June and July, revealed detectable MnO_x (0.11-0.16 µM) but the MnO_x remained approximately constant at all salinities, and well below soluble Mn concentrations. We also performed experiments to ensure that the porphyrin analysis was not recovering colloidal MnO_x < 0.2 µm, as shown by Madison et al, (2011) where the porphyrin was unreactive towards MnO_2.

In Figure 5.4, we compare Mn and Fe speciation on samples collected October 7th after filtration through 0.2 µm and 0.02 µm filters. Panels 5.4A and 5.4B represent Mn speciation, and show that speciation was not significantly different after the second 0.02 µm filtration. The sample at ~10 ppt salinity showed the most significant decrease of dMn_T (~15 %), corresponding to loss of Mn(III)-L_{strong}. Additionally, the larger error bars on dMn_T for the 0.02 µm filtered samples is also related to the Mn(III)-L_{strong} complexes. It is possible that some Mn(III)-L complexes interacted with the alumina-based Anatop filters, or that some of the Mn(III)-L_{strong} is in a colloidal fraction

(perhaps bound to colloids). In contrast, dFe_T decreased from 80 – 95% after filtration through the 0.02 µm filter (panels 5.4C and 5.4D), indicating that the dFe_T in this system is largely colloidal, and that Fe(II) may be bound to Fe(III)-L complexes/colloids.

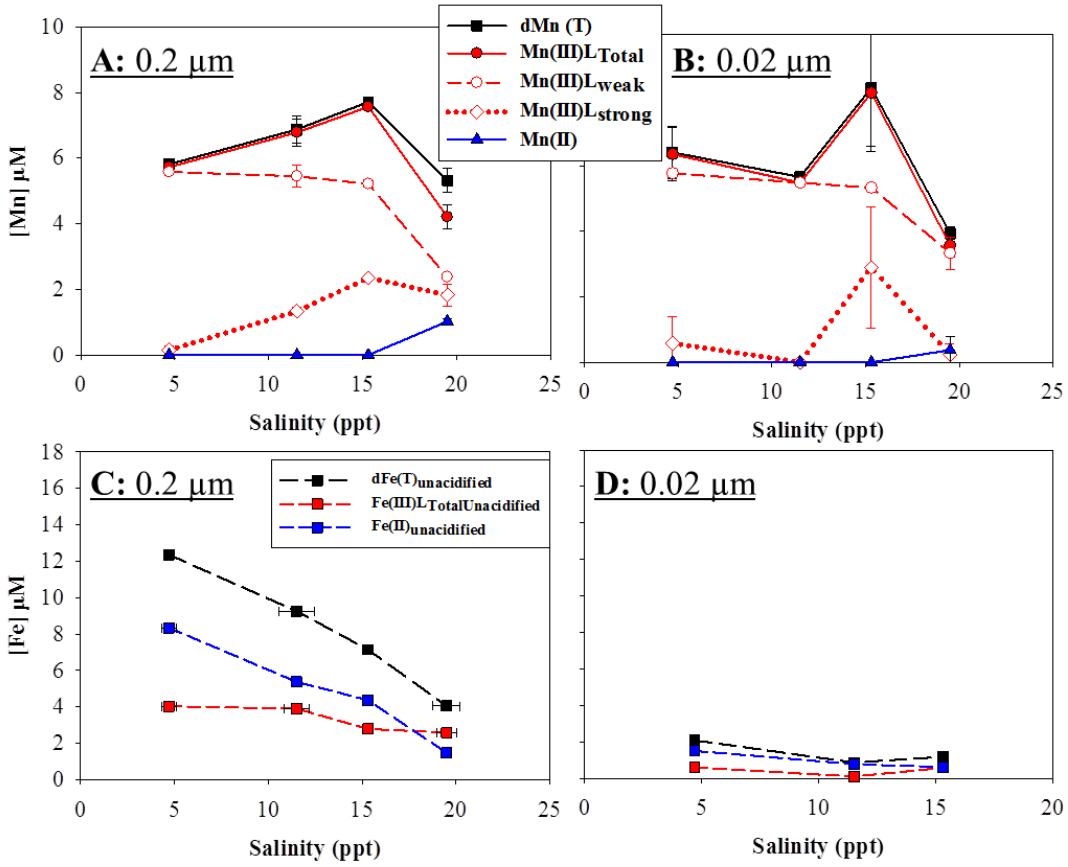

Figure 5.4 The speciation of dissolved Mn (top: A and B) and dissolved Fe (bottom: C and D) from October 8th, comparing filtration though 0.2 µm (left: A and C) with filtration through 0.02 µm (right: B and D). Fe results are from unacidified treatments.

5.3.4 Fe Speciation Along a Salinity Gradient

Dissolved Fe_T concentrations ranged from 0.4 – 18.8 µM (concentrations for sites 1, 5 and 8 given in Table 5.2), falling within the range of previous dFe_T concentrations in estuarine environments (Boyle et al, 1977). Figure 5.5 shows the speciation of dFe along the salinity gradient of the Broadkill River from 4 sampling dates. On June 23rd 2015, dFe_T decreased threefold from the first, freshwater site to the next site (salinity = 1.4), and then steadily decreased to the mouth of the river, exhibiting typical estuarine removal. However, on July 21st 2015, October 7th 2015 and February 2nd 2016, dFe_T does not follow estuarine removal but rather, export on July 21st and near-conservative mixing on October 7th and February 2nd.

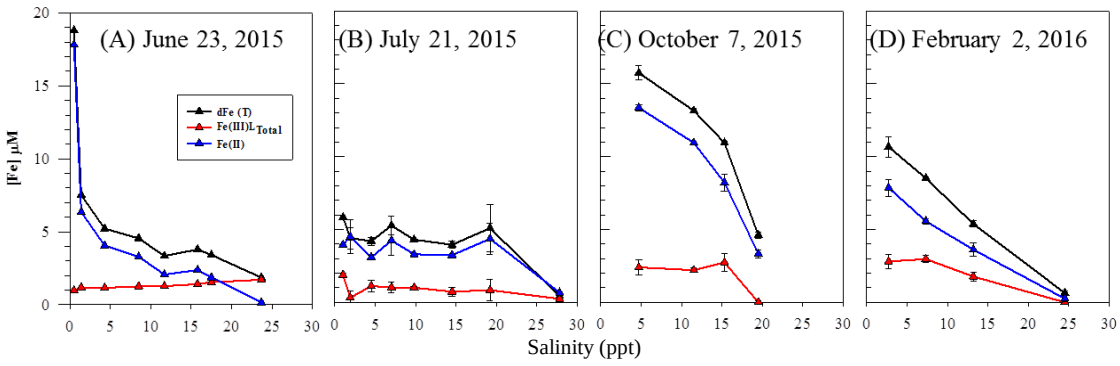

Figure 5.5 The speciation of dFe_T along the salinity gradient from (A) June 23rd, 2015; (B) July 21st, 2015; (C) October 7th, 2015; and (D) February 2nd, 2016. Where error bars are not visible, they are smaller than the symbols.

The speciation of dFe was dominated by Fe(II) for all sampling events, in contrast to previous estuarine work, where dFe_T was predominantly complexed as Fe(III)-L (Buck et al, 2007; Sander et al, 2015).

Table 5.2 Comparing dMn speciation to characteristic humic absorbances (258, 280 and 400 nm), % humic absorbance lost after acidification, dFe speciation and solid MnO_x. Where values are blank, no measurements were made.

Site #	Date	S (ppt)	Mn(T)	*% Mn(III)-L Total*	abs_{258}	% abs_{258} lost	abs_{280}	% abs_{280} lost	abs_{400}	% abs_{400} lost	Fe(T)	Fe(II)
1	13-Apr	0.2	1.26 ± 0.08	***57***	0.071		0.057		0.007			
	27-May	0.2	0.28 ± 0.02	***85***	0.071		0.057					
	11-Jun	0.8	0.89 ± 0.01	***62***			0.122	**0.0**				
	23-Jun	0.5	1.21 ± 0.02	***77***	0.173	**1.3**	0.126	**9.0**	0.021	**29.5**	18.8	17.8
	7-Jul	0.5	1.54 ± 0.19	***68***	0.162	**1.1**	0.126	**10.9**	0.016	**49.1**	15.1 ± 3.97	14.6 ± 3.83
	21-Jul	1	0.93 ± 0.05	***100***	0.146	**0.0**	0.114	**8.4**	0.012	**23.7**	5.8 ± 0.15	3.9 ± 0.03
	7-Oct	4.7	5.82 ± 0.16	***99***	0.208	**-0.6**	0.155	**9.2**	0.003	**27.7**	15.8 ± 0.50	13.4 ± 0.19
	17-Nov	0.8	5.44 ± 0.37	***92***	0.141		0.114		0.023		14.4 ± 0.15	11.2 ± 0.19
	2-Feb	2.7	1.15 ± 0.01	***90***	0.109		0.087		0.015		10.7 ± 0.70	7.9 ± 0.58
5	13-Apr	10.2	2.02 ± 0.04	***78***	0.119		0.093		0.011			
	27-May	10.1	0.96 ± 0.02	***93***	0.119		0.093					
	11-Jun	12.4	1.23 ± 0.00	***88***			0.121	**7.0**				
	23-Jun	11.7	1.96 ± 0.14	***99***	0.198	**2.8**	0.141	**10.1**	0.027	**42.5**	3.34	2.06
	7-Jul	15	2.21 ± 0.05	***102***	0.218	**22.5**	0.168	**30.5**	0.031	**85.5**	5.1 ± 0.56	5.1 ± 0.29
	21-Jul	9.8	1.11 ± 0.08	***97***	0.241	**1.7**	0.182	**11.1**	0.019	**28.4**	4.3 ± 0.04	3.3 ± 0.05
	7-Oct	15.3	7.72 ± 0.10	***98***	0.187	**-5.3**	0.135	**5.6**	0.000	**38.6**	10.9 ± 0.10	8.2 ± 0.58
	17-Nov	17.8	3.26 ± 0.06	***101***	0.133		0.100		0.018		4.4 ± 0.64	2.8 ± 0.20
	2-Feb	13.2	1.53 ± 0.16	***89***	0.144		0.117		0.025		5.37 ± 0.22	3.61 ± 0.46
8	13-Apr	19.6	0.88 ± 0.02	***99***	0.033		0.025		0.000			
	27-May	20.6	0.80 ± 0.03	***100***	0.033		0.025					
	11-Jun	23.9	0.84 ± 0.02	***96***			0.082	**3.2**				
	23-Jun	23.7	3.03 ± 0.05	***97***	0.114	**-5.9**	0.079	**1.9**	0.017	**35.1**	1.85	0.14
	7-Jul	27.6	1.13 ± 0.07	***89***	0.074	**35.2**	0.063	**53.2**	0.018	**100.0**	0.8 ± 0.43	0.3 ± 0.20
	21-Jul	27.8	0.46 ± 0.29	***49***	0.037	**0.0**	0.027	**0.0**	0.000		0.4 ± 0.26	1.5 ± 1.39
	7-Oct	19.5	5.32 ± 0.37	***79***	0.162	**-4.3**	0.115	**10.5**	0.002	**73.3**	4.6 ± 0.24	3.3 ± 0.27
	17-Nov	28.8	2.38 ± 0.37	***35***	0.012		0.007		0.000		0.43 ± 0.08	0.22 ± 0.18
	2-Feb	24.5	1.28 ± 0.10	***58***	0.055		0.042		0.006		0.64 ± 0.15	0.25 ± 0.22

5.3.5 Humic Absorbance and Metal Complexation

To test the positive correlation between humic material and Mn(III)-L complexation, we measured characteristic UV/Vis absorbances for humic substances at

254 nm, 280 nm and 400 nm (Rodriguez et al, 2016). Figure 5.6 examines Mn speciation and humic absorbance at 280 nm over the course of the 9 sampling events. Three sites are represented: low salinity (site #1), mid salinity (site #5) and the mouth of the river, into Delaware Bay, with high salinity (site #8). At all sites, humic absorbance increased over the summer and fall months, corresponding to an increase in the concentration of Mn(III)-L.

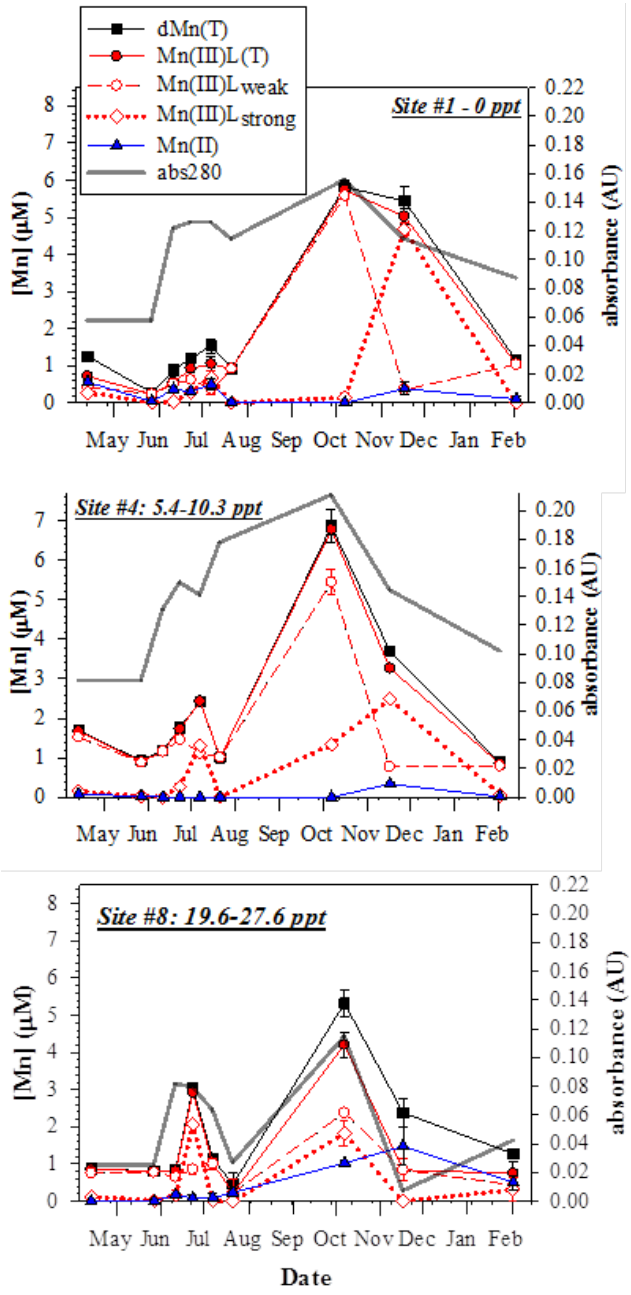

Figure 5.6 The seasonal change in Mn speciation and humic absorbance (280 nm) for three sampling sites: Site #1: low salinity, Site #5: mid-salinity, and Site #8: high salinity. Where error bars are not visible, they are smaller than the symbol.

To further examine the relationship between humic material and Mn(III), we performed a competitive ligand experiment on a sample collected on July 7th. A sample with low humic absorption (abs_{280}=0.126, 0 ppt salinity) and a sample with high humic absorption (abs_{280}=0.168, 15 ppt salinity) were compared. Each sample was filtered and separated into two aliquots (4 total tests, summarized in Table 5.3): *an acidified aliquot* to precipitate humic material (pH<1.5, centrifuged, decanted, brought back to pH=8 with NaOH) *and a non-acidified aliquot*. All 4 treatments were amended with 100 µM Mn(III)-pyrophosphate (a weak Mn(III)-L complex). The absorbance of this complex (484 nm) was observed for 15 minutes. The four tests showed the following types of reactivity:

Table 5.3 A matrix of Mn-humic complexation tests from July 7th, 2015. Two filtered samples were compared for a change in absorbance peak of added Mn(III)-pyrophosphate, each with and without acidification.

Salinity	Acid	No Acid
0 (low humics)	no change	no change
15 (high humics)	no change	peak change

Test #1 (low humic, acidified): Mn(III)-PP + $L_{non\text{-}humic}$ → no reaction

Test #2 (low humic, no acid): Mn(III)-PP + $L_{non\text{-}humic}$ → no reaction

Test #3 (high humic, acidified): Mn(III)-PP + $L_{non\text{-}humic}$ → no reaction

Test #4 (high humic, no acid): Mn(III)-PP + L_{humic} → Mn(III)-L_{humic} + PP

In three of the four tests (both acidified samples, and the non-acidified low-humic sample), there was no change in the absorbance of Mn(III)-pyrophosphate (484 nm) after 15 minutes. However, in the non-acidified sample with high humics, the

absorbance peak of Mn(III)-pyrophosphate decreased and was replaced by a broad peak at 400 nm where [Mn(catecholate)] complexes absorb (Sever and Wilker, 2004), and we observed a change in color from pale-pink (Mn(III)-pyrophosphate) to yellow.

Thus, the ambient excess humic ligands outcompeted the pyrophosphate for Mn(III). To the sample with the new broad peak at 400 nm ("Mn(III)-L_{humic}"), excess desferrioxamine-B (DFOB; 500 µM) was added. Within 1 minute, 86 % of the Mn added as Mn(III)-pyrophophate was recovered as Mn(III)-DFOB (based on the absorbance of Mn(III)-DFOB at 310 nm).

Test #4b (high humic, no acid): Mn(III)-L_{humic} + DFOB (excess) → Mn(III)-DFOB + L_{humic}

Because we were able to recover the originally added Mn in Mn(III)-PP by outcompeting the new Mn(III)-L_{humic} with excess DFOB, these data indicate that humic material is responsible for some metal complexes in this system.

Additionally, before any amendments were made to the acidified solution, the supernatant was decanted and re-analyzed for Mn speciation after pH re-adjustment to 8. We found that 62% of the dMn_T was recovered as Mn(III)L. The remaining humic precipitate, which was 38 % of the original dMn_T , was re-dissolved into pH 8 Milli-Q water (brought up with trace metal clean NaOH). We recovered all of the Mn in the precipitated humic material as Mn(III)L. These data indicate that there are diverse

ligands binding Mn(III), including both humic- and non-humic-type ligands, in this system.

On July 21st and October 7th we measured Fe speciation with and without acidification, to test whether the acidification step could be also precipitating Fe(III)-humic complexes. These results are summarized in Table 5.4, with bold values indicating higher dFe_T without acidification. Although dFe_T is higher in nearly all acidified samples, Fe(III) is often higher in unacidified samples. Additionally, the standard deviations for unacidified samples are generally better than for acidified samples. Given that we measured a significant amount of "colloidal Fe (0.02 – 0.20 µm)" in our October 7th assay, it is possible that acidification results in the partial dissolution of colloidal species, resulting in variable Fe results.

Table 5.4 The speciation of dissolved Fe from acidified and non-acidified samples. Bolded values are those where unacidified measurements were higher than acidified measurements.

Date	Salinity	abs280	Fe(T)$_{unacidified}$	Fe(II)$_{unacidified}$	Fe(III)$_{unacidified}$	Fe(T)$_{acidified}$	Fe(II)$_{acidified}$	Fe(III)$_{acidified}$
21-Jul	1.00	0.11	4.29 ± 0.40	3.89 ± 0.39	0.40 ± 0.56	5.83 ± 0.15	3.95 ± 0.03	1.88 ± 0.14
2015	1.90	0.17	**4.41** ± 0.15	3.78 ± 0.06	**0.62** ± 0.16	4.41 ± 0.73	4.50 ± 1.16	0.32 ± 0.45
	4.50	0.16	**4.37** ± 0.10	**3.65** ± 0.04	0.72 ± 0.11	4.19 ± 0.28	3.08 ± 0.14	1.11 ± 0.38
	7.00	0.18	5.20 ± 0.13	4.38 ± 0.18	0.82 ± 0.22	5.27 ± 0.65	4.24 ± 1.03	1.02 ± 0.38
	9.80	0.18	**5.65** ± 0.21	**3.94** ± 0.06	**1.71** ± 0.22	4.30 ± 0.04	3.30 ± 0.05	1.00 ± 0.09
	14.5	0.16	**4.93** ± 0.10	**3.52** ± 0.04	**1.41** ± 0.11	3.95 ± 0.27	3.23 ± 0.09	0.72 ± 0.30
	19.2	0.14	3.12 ± 0.05	2.96 ± 0.04	0.17 ± 0.06	5.08 ± 1.65	4.36 ± 1.08	0.84 ± 0.73
	27.8	0.03	**1.18** ± 0.05	**0.68** ± 0.08	**0.49** ± 0.09	0.43 ± 0.26	0.66 ± 0.03	0.23 ± 0.40
7-Oct	4.70	0.14	12.36 ± 0.12	8.34 ± 0.38	**4.02** ± 0.39	15.75 ± 0.50	13.35 ± 0.19	2.40 ± 0.38
2015	11.5	0.13	9.26 ± 0.93	5.37 ± 0.19	**3.89** ± 0.69	13.15 ± 0.16	10.95 ±	2.20 ± 0.11
	15.3	0.13	7.14 ± 0.22	4.36 ± 0.14	**2.78** ± 0.21	10.95 ± 0.10	8.22 ± 0.58	2.73 ± 0.42
	19.5	0.10	4.04 ± 0.72	1.46 ± 0.10	**2.57** ± 0.52	4.59 ± 0.24	3.32 ± 0.27	1.28 ± 0.25
17-Nov	0.80	0.11	7.81 ± 0.20	2.30 ± 0.07	**5.51** ± 0.15	14.37 ± 0.15	11.25 ± 0.19	3.12 ± 0.34
2015	5.30	0.14	6.43 ± 0.12	3.48 ± 0.25	2.96 ± 0.20	6.61 ± 2.85	3.24 ± 1.23	3.37 ± 1.61
	17.8	0.10	1.29 ± 0.06	0.67 ± 0.04	0.62 ± 0.05	4.44 ± 0.64	2.81 ± 0.20	1.64 ± 0.46
	28.8	0.01	0.00 ± 0.00	0.00 ± 0.00	0.00 ± 0.00	0.43 ± 0.08	0.22 ± 0.18	0.00 ± 0.10
2-Feb	2.70	0.09	4.39 ± 0.01	1.48 ± 0.10	**2.92** ± 0.07	10.67 ± 0.70	7.87 ± 0.58	2.80 ± 0.47
2016	7.30	0.10	1.45 ± 0.03	0.46 ± 0.10	0.99 ± 0.07	8.53 ± 0.09	5.56 ± 0.19	2.96 ± 0.26
	13.2	0.12	1.27 ± 0.05	1.27 ± 0.04	0.00 ± 0.05	5.37 ± 0.22	3.61 ± 0.46	1.76 ± 0.33
	24.5	0.04	0.00 ± 0.00	0.00 ± 0.00	0.00 ± 0.00	0.64 ± 0.15	0.25 ± 0.22	0.00 ± 0.09

5.4 Discussion

The reduced metal states of Fe and Mn, dissolved Fe(II) and Mn(II), enter estuarine systems via freshwater rock weathering processes (Chester, 1990). These species are not stable in the presence of O_2, and in oxic systems at seawater pH, Fe(III) and Mn(III/IV) oxides can dominate. However, Fe and Mn oxides are susceptible to reduction and their solubility is influenced by light, the pH, surface reactivity, and organic matter. Therefore, in systems where freshwater and seawater meet, many chemical species of both Fe and Mn can coexist and rapidly cycle. For the following discussion, we write 20 possible reactions or pathways for iron and manganese cycling in our given system. The schematic in Figure 5.7 describes the essence of the Fe and Mn cycles described herein, with equations 1-20 given and described in the text below.

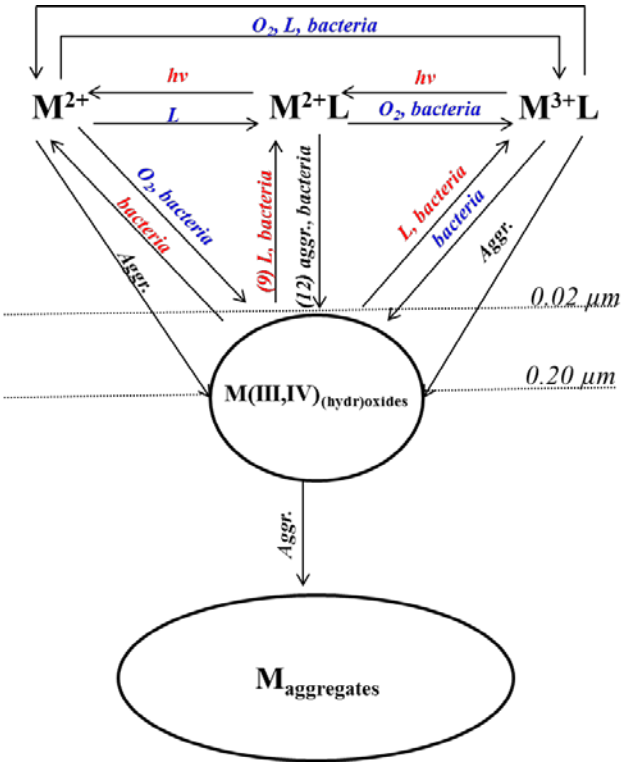

Figure 5.7 The proposed cycling mechanisms of Fe and Mn in the Broadkill River system. Pathways in blue represent oxidative pathways and those in red, reductive pathways.

5.4.1 Abiotic Oxidation

Equations 5.1 and 5.2 describe the abiotic formation of metal-ligand complexes with an ambient organic ligand. Equation 5.1 describes non-redox complexation of an organic ligand to a metal hexaaquo species, and this reaction could be followed by equation 5.2, where the formed M^{2+}-L complex is oxidized to a M^{3+}-L complex in the presence of dissolved oxygen. This mechanism is likely more important for Fe^{2+} than Mn^{2+} because Fe^{2+} bind ligands better than Mn^{2+} based on the $\log K_1$, which follows the charge to size ratio for the metal ion (Z/r).

$$M(H_2O)_6{}^{2+} + L \rightarrow M^{2+} - L \quad 5.1$$

$$M^{2+} - L \xrightarrow{O_2} M^{3+} - L \quad 5.2$$

The abiotic oxidation of Mn^{2+} with O_2 is several orders of magnitude slower than for Fe^{2+} at seawater pH (Stumm and Morgan, 1996) because the first electron transfer for $Mn(H_2O)_6{}^{2+}$ with O_2 (eq. 5.3) is thermodynamically unfavorable (Luther, 2010). The oxidation of Fe^{2+} proceeds via an outer sphere mechanism, whereas for Mn^{2+} is inner sphere, and at higher pH is autocatalytic (eq. 5.4). Thus, the abiotic oxidation of Mn^{2+} by O_2 to MnO_2 can be expressed by the following mechanism (unbalanced):

$$Mn^{2+} + O_2 \xrightarrow{slow} MnOOH(s) \quad 5.3$$

$$Mn^{2+} + MnOOH(s) + O_2 \xrightarrow{fast} MnOOH(s) \quad 5.4$$

$$MnOOH(s) + O_2 \xrightarrow{slow} 2MnO_2(s) \quad 5.5$$

5.4.2 Biological oxidation

The Mn oxidation mechanism above (eq. 5.3-5.5) is accelerated in the presence of abundant particles, but in most marine systems bacterial oxidation of Mn^{2+} dominates (Tebo et al, 2004). Microbial Fe^{2+} oxidation is also well documented (Weber et al, 2006), though abiotic oxidation likely dominates most surface waters for Fe. The reactions below summarize biotic oxidation pathways, including the formation of intermediate M^{3+}-L complexes, and solid phases.

$$M(H_2O)_6{}^{2+} + L \xrightarrow{O_2, bacteria} M^{3+} - L \quad 5.6$$

$$M(H_2O)_6{}^{2+} \xrightarrow{O_2, bacteria} M(III, IV)_{(hydr)oxide} \quad 5.7$$

Reaction 5.7 can proceed via a one-electron transfer for Mn(II) and Fe(II), forming FeOOH or MnOOH; via a two-electron transfer for Mn(II), forming MnO_2 (as in eqs. 5.3-5.5); or via a one electron transfer for Mn(III)-L, forming MnO_2 (eq. 5.8).

$$Mn^{3+} - L \xrightarrow{O_2, bacteria} MnO_2 \quad 5.8$$

5.4.3 Photochemical Reactions

In our Broadkill River system, we do not observe abundant MnO_x particles (Table 5.2), suggesting that they are not formed as Mn(III) is being trapped as a complex during oxidation, and/or that the rate of MnO_x reduction exceeds Mn(II) oxidation. Although we do not report Fe (hydr)oxide values, we do observe that Fe(II) concentrations generally exceed Fe(III)-L concentrations (Table 5.2), which is unusual for surface waters, and may also indicate that reductive processes are dominating Fe speciation. The abundance of soluble species may be the result of photochemical reactions in this system. Photochemical reactions can dissociate metal ligand complexes non-reductively (eq. 5.9) or reductively (eq. 5.10):

$$M^{2+} - L \xrightarrow{hv} M^{2+} + L \quad 5.9$$

$$M^{3+} - L \xrightarrow{hv} M^{2+} - L^{+} \quad 5.10$$

Fe(III)-L complexes are more readily photoreduced (eq. 5.10) than Mn(III)-L complexes because Mn(III)-L photoreduction involves L_{π}-M_{σ} or ligand π to metal σ electron transfer, whereas Fe(III)-L photoreduction involves L_{π}-M_{π} or ligand π to metal π electron transfer. In Fe(III)-L photoreduction, the ligand absorbs a photon which excites an electron to a higher energy state. As the π orbitals of Fe(III) have better overlap with the π orbitals of the donating ligand than the σ orbitals of Mn(III), photoreduction is more favorable. This would also help to explain the abundant Mn(III)-L in the presence of Fe(II) in our samples.

5.4.4 Chemical Reduction of Oxidized Mn by Fe(II)

The stabilized Fe(II) in the surface waters in the Broadkill River is particularly interesting in light of the abundance of Mn(III)-L complexes. We expect a negative correlation between Mn(III)-L and Fe(II) given the following possible one electron transfer reaction:

$$Mn^{3+} - L + Fe^{2+} \xrightarrow{fast} Mn^{2+} + Fe^{3+} - L \qquad 5.11$$

Dissolved Fe(II) is a strong reducing agent, and has been shown to rapidly reduce Mn oxides in an inner sphere redox process as Fe(II) and Mn(III,IV) species have an orbital symmetry mismatch (Siebecker et al, 2015), and should also reduce Mn(III)-L complexes. However, there are two plausible explanations for the inhibition of Mn(III)-L reduction by Fe(II), which could be occurring simultaneously in the Broadkill River system. The first involves kinetic inhibition due to a ligand binding Fe(II), and the second involves kinetic inhibition due to a ligand binding Mn(III). In the first scenario, Fe(II) does not reduce Mn(III)-L because it is complexed. Complexed

Fe(II)-L is not as good a reducing agent as Fe(II) because the organic complexation sterically prevents it from reducing Mn(III)-L complexes, even when Fe(II)-L is in excess of Mn(III)-L. Thus, equation 5.10 and the discussion in section 5.3 may explain why high concentrations of Mn(III)-L_{Total} (Mn(III)-L_{weak} + Mn(III)-L_{strong}) complexes were found in all samples despite the presence of Fe(II) (often in excess), and still made up 76.7% of the dMn_T on June 23rd, in the presence of 17.8 µM Fe(II) (~17 x excess of dMn_T).

The second possibility is that the complexed Mn(III) is kinetically inhibiting reduction by Fe(II). The strong complexes in the surface waters of the Broadkill River compare with those found in the anoxic waters of the Chesapeake Bay (Oldham et al, 2015), another system with high productivity and terrestrially influenced OM from nearby wetlands. In the Chesapeake Bay, Mn(III)-L_{strong} made up to 54 % of the dMn_T and were formed by the reductive dissolution of MnO_x (Oldham et al, 2015). In the Chesapeake Bay, strong Mn(III)-L complexes were kinetically stabilized against reduction by equimolar HS^-, and could only be titrated out of the system when HS^- was >10-fold in excess of the Mn(III)-L concentration.

5.4.5 Bacterially Catalyzed and Ligand-promoted Reduction and Dissolution of MnO_x

The stability of Fe and Mn oxides in the water column is governed by reduction and by surface-catalyzed reactions. In systems such as the Broadkill River, with high biological activity and organic matter concentrations, the stability of Fe and Mn oxides may be greatly influenced not only by photoreductive processes, but also by biologically- and/or ligand-promoted reductive dissolution (Stone and Morgan, 1984;

Zinder et al, 1986). Given that MnO_x concentrations were << dMn_T concentrations at all salinities, it is likely that as Mn oxides form, they react rapidly such that they do not accumulate in the Broadkill River system.

Bacterially catalyzed reduction has been documented for both Mn and Fe (reviewed by Nealson and Myers, 1992). This reduction can proceed via a 1 electron mechanism for MnOOH and FeOOH or via a two electron mechanism for MnO_2, as summarized by equation 5.12:

$$M(III,IV)_{(hydr)oxide} \xrightarrow{bacteria} M(H_2O)_6{}^{2+} \quad 5.12$$

The mineral-oxide reduction can also be catalyzed by organic ligands, with or without bacterial mediation, for both Mn (i.e. Duckworth and Sposito, 2005) and for Fe (Arnold et al, 1988). Equations 5.13 and 5.14 below can therefore proceed as written, or be bacterially catalyzed.

$$M(III)_{(hydr)oxide} + L \rightarrow M^{2+} - L \quad 5.13$$

$$MnO_2 + L \rightarrow Mn^{3+} - L \quad 5.14$$

There is also the potential for non-reductive dissolution of mineral oxides by ambient ligands. In this case, the ligand is adsorbed to an Fe(III) or Mn(III) at the mineral oxide, and the complex subsequently dissociates. This mechanism is given in equations 5.15-5.16 below, where ">" denotes a particle:

$$> M(III,IV)_{hydr(oxide)} - M^{3+} + L \xrightarrow{adsorbtion} > M(III,IV)_{hydr(oxide)} - M^{3+} - L$$ 5.15

$$> M(III,IV)_{hydr(oxide)} - M^{3+} - L \xrightarrow{dissociation} > M(III,IV)_{hydr(oxide)} + M^{3+} - L$$ 5.16

When we added 10 μM MnO_2 to a filtered freshwater sample from our system, we observed the loss of 4 μM MnO_2, after 21 hours, and formation of Mn(III)-L, indicating rapid cycling of MnO_x with Mn(III)-L complexes as the preferred product (eq. 5.14). The reductive dissolution of Mn oxides by humic and fulvic acids is well documented, in the context of organic matter degradation (Sunda et al, 1983; Waite et al, 1988; Sunda and Kieber, 1994); however, less is understood about the manganese products in the reaction. Based on data from figure 5.3, Mn(III)-humic complexes are a likely intermediate, if not a (meta)stable product, in the oxidative degradation of humic material by Mn oxides.

5.4.6 Aggregation and Removal of Soluble Fe and Mn

The principle removal mechanism of soluble Fe and Mn species when freshwater encounters seawater has been shown to be precipitation upon flocculation onto organic matter and solid metal oxides (Sholkovitz, 1978). Although biological oxidation of Fe(II) and Mn(II) is ubiquitous in natural waters (Fig. 5.7, eqns. 5.6-5.8), physical aggregation processes are particularly important in estuarine mixing zones, some of these are described in equations 5.17-5.20. The zero point of charge (ZPC) for a metal surface indicates the point at which that half the surface sites are protonated, and the surface is neutral. This can be expressed as pH_{ZPC}, as the pH where the solid surface is neutral. When the pH of a solution is greater than the pH_{ZPC} for a solid, that

solid surface is negatively charged and acts as a base. In estuarine mixing, flocculation will occur when the divalent cations in seawater aggregate on negatively charged metal surfaces, inducing flocculation of positively charged soluble Fe and Mn. Given that the pH_{ZPC} of MnO_2 is 4.6, compared to that of FeOOH at 9.7 (Xu and Schoonen, 2000), Mn oxides are more basic in estuarine systems, and thus more reactive to dissolved metal ions. Thus, equations 5.17-5.20 are likely more dominant for MnO_2 surfaces, but adsorption to Fe oxides is also possible (Fe_3O_4 has pH_{ZPC} = 6.5, for example; Xu and Schoonen, 2000). In equation 5.17, redox occurs between both metal centers at the surface, and if M^{2+} is Mn, this is known as a comproportionation reaction.

$$> Mn(IV)O_2 + M^{2+} \rightarrow > Mn(III)O_2 - M^{3+} \qquad 5.17$$

Adsorption can also occur non-reductively, shown in equation 5.18, which is essentially the reverse of the process in equations 5.15 and 5.16:

$$> M(III,IV)_{hydr(oxide)} + M^{2+} \rightarrow > M(III,IV)_{hydr(oxide)} - M^{2+} \qquad 5.18$$

Metal ligand complexes may also be adsorbed to surfaces, which may or may not be hindered by the ligand, depending on the ligand charge. The adsorption could thus occur via the metal centers (redox at the metal centers is also possible here, but not shown) as in equation 5.19, or via a bridging ligand as in equation 5.20. Note that equations 5.19 and 5.20 are also possible for M^{2+}-L, and again, represent the reverse of the process described in equations 5.15 and 5.16.

$$> Mn(IV)O_2 + M^{3+} - L \rightarrow > MnO_2 - M^{3+} - L \quad 5.19$$

$$> Mn(IV)O_2 + M^{3+} - L \rightarrow > MnO_2 - L - M^{3+} \quad 5.20$$

Additionally, in our system, we observed a greater loss or removal of dissolved Fe from the freshwater end-member to the Delaware Bay than for dissolved Mn, for all sampling events. The abiotic reaction of $Fe(H_2O)_6^{2+}$ with O_2 to form Fe oxides is at least 10^6 times faster than $Mn(H_2O)_6^{2+}$ with oxygen (Grassian, 2005); thus, we predict that Fe solids will precipitate more rapidly than Mn solids. Additionally, given that the Mn we measure in the Broadkill River is largely non-colloidal (Section 5.3, Fig. 5.4), it seems that aggregation processes (eqs 5.17-5.20) are less important for soluble Mn than for soluble Fe, which was predominantly in the colloidal fraction (0.02 to 0.20 μm).

Our observations in the Broadkill River indicate that soluble Mn and Fe loss mechanisms (eqs. 5.17-5.20) occur predominantly in the absence of high organic matter concentrations, as in winter and spring sampling events. Under summer and fall conditions, it is likely that processes like equations 5.15-5.16 dominate, in the presence of abundant organic ligands.

5.4.7 Revisiting Estuarine Removal

In our system, we observe high concentrations of soluble Mn(III)-L complexes and Fe(II) species, both of which appear to be seasonally exported from the Broadkill marsh system to the Delaware Bay in summer and fall months. These observations are in contrast to previous observations of estuarine mixing where metal removal processes (eqs. 5.17-5.20) have been shown to dominate (Coonley et al, 1971; Windom et al,

1971; Boyle et al, 1974, 1977; Graham et al, 1976; Moore et al, 1979; Eastman and Church, 1984).

Unlike earlier work that showed removal behavior in property-property plots of dissolved Fe and Mn along the estuarine freshwater and saltwater transects; in some months, we observe export of dMn rather than conservative mixing, and conservative mixing of dFe rather than removal. This is particularly evident for dMn in the summer and fall months, where dMn, in the form of Mn(III)-L complexes, is higher at salinities >10 than at salinities <10 (Fig. 5.2). Dissolved Fe also does not show typical estuarine removal as it shows conservative behavior in some samplings (Fig. 5.5). A source of dFe appears at mid-salinities in all sampling events (Fig. 5.5). We propose that organic matter production form marshes and metal-organic complexation (eqs. 5.1, 5.2, 5.6, 5.13-5.15) in the Broadkill River explains the high Mn(III)-L complexation and export along the salinity gradient, and the non-conservative mixing of dFe.

The dMn_T and dFe_T profiles from this study indicate that Mn(III) binds ambient ligands more strongly than Fe(III). Although Fe(II) decreased with increasing salinity on June 23rd, [~100-fold decrease from 0 ppt to mouth (~25-30 ppt)], Fe(III) increased 1.7-fold from 0 ppt salinity to the mouth of the river. Since both Fe(III) and Mn(III) increase along the salinity gradient on this day, similar ligands may be binding both metals. However, it seems that the Mn(III)-L complexes are more stable than the Fe(III)-L complexes, because [Mn(III)-L] >> [Fe(III)-L] and Mn(III)-L are less susceptible to photoreduction (eq. 5.10). This finding suggests that Mn(III) may have a

higher affinity for the ambient humic-type ligands in coastal mixing zones such as the Broadkill River.

Additionally, the dissolved organic compounds found in coastal waters such as the Broadkill River are higher in overall concentration than in oceanic environments, and are present as a complicated mixture with varied composition (Morel and Hering, 1993). Also, coastal organic matter contains a range of functional groups that may interact differently with Fe and Mn. This organic matter is both variable in origin, and can be transformed by biology, redox chemistry and photochemistry. Thus, given the variable inputs and transformations of organic matter in coastal systems, changes in organic matter reactivity and composition may occur faster than complexation reactions and therefore equilibrium may not be reached (Rose and Waite, 2003). Both soluble Mn and Fe can interact with oxygen and/or organic matter to form metal-organic complexes (Fig. 5.7, eqs. 5.1-5.2), which can prevent formation of crystalline Mn and Fe oxides.

5.4.8 Humic Complexation of Dissolved Mn

Although previous studies of estuarine removal have noted the correlation between metal removal and humic material removal (Sholkovitz, 1976), none have clearly shown that metal complexation to humic material occurs and may be important for transport and removal processes. In this study, high % Mn(III)-L corresponded to locations where the intersection of large creeks with the Broadkill river occurred, indicating that the wetland is acting as a source of ligands to the system through the degradation of plant material and release of humic material. Figure 6 examines Mn speciation and humic absorbance at 280 nm over the course of the 9 sampling events. Three sites are represented: low salinity (site #1), mid salinity (site #5) and the mouth of

the river, into Delaware Bay, with high salinity (site #8). At all sites, humic absorbance and Mn(III)-L_{Total} increased over the summer and fall months. Humic absorbance was generally highest at mid-salinities where we observe the highest density of small salt marsh creeks and a high abundance of *S. alterniflora*. Figure 5.6 also shows that the Broadkill River likely acts as a source of Mn(III)-L to the Delaware Bay, as the total dMn at the mouth of the river increases through the summer and into the fall. Our sampling on October 7th represents speciation after hurricane Joaquin, where the marsh was completely flooded. This corresponded to exceptionally high dMn_T and humic material. In the acid precipitation experiment detailed in section 5.3.3, we confirm that humic complexes are important in the Broadkill system by comparing an aliquot of a sample where humic acids were acid precipitated to another aliquot where excess humic materials were left in the sample. We recovered 38 % of the total dissolved Mn as Mn(III) from precipitated humic material, thereby indicating that humic complexation of Mn(III) is important in this system. We also showed that the ambient humic ligand was able to outcompete added pyrophosphate for Mn(III), only when the sample was not acidified. In particular, this finding may have implications for previous metal studies in coastal areas with high humic matter concentrations, which employed an acidification step for soluble metal preservation.

Previous studies have also found that humic type ligands can complex metals in natural waters. For example, Mantoura et al, (1978) found that Cu and Hg were 99.97 % and 100 % complexed as metal-humic species in a freshwater system. Although copper is likely the most thoroughly researched metal binding to humic substances (e.g. Alberts and Filip, 1998), more recently, Fe(III) has been shown to complex well to humic

material in fresh and saline samples (Abualhaija et al, 2015; Batchelli et al, 2010; Rijkenberg, et al, 2006). In a study examining the competition for copper binding sites by Fe(III) and Al(III), Alberts and Filip (1998) used the copper binding capacity (CuBC) to assess the effect of other elements on the CuBC of estuarine fulvic and humic acids. They found that Al and Fe decreased the CuBC of humic acids by 43%. Abualhaija et al, (2015) also found that Fe(III) competed for the same ligands as Cu(II), and that Fe(III)-humic complexes had similar conditional stability constants to Cu-humic complexes. Since we know that Mn(III) and Fe(III) can have similar binding strengths for the same known ligands, it is likely that humic binding is significant for both these elements, and that Mn(III) is competing for the same humic binding sites as Fe(III).

5.5 Conclusions

Mass balances in oceanic environments have been given considerable attention, and input from continental weathering by river and ocean mixing has been the best characterized. For many trace metals, including Fe and Mn, estuarine removal and/or conservative mixing during estuarine mixing is now assumed (Windom et al, 1971; Holiday and Liss, 1976; Sholkovitz, 1976; Boyle et al, 1977; Moore et al, 1979; Eastman and Church, 1984). The classic examples of estuarine removal of dFe_T are the summer and fall values reported by Boyle et al, (1977) where about 90 % of dFe_T was removed, as measured by the Ferrozine assay, 4 days after sample collection and acidification. However, river water DOM is largely composed of humic substances (Lamar, 1968; Beck et al, 1974), and these precipitate at pH<2. Because humic binding of many trace metals (Mn, Co, Ni, Cu, Zn, Cd, Hg, Fe, Al) has been shown to be significant (Mantoura et al, 1978), acidification may lead to an underestimate of total

dissolved metals. Our findings indicate that acidification precipitates Mn(III)-humic complexes in the Broadkill river. Thus, previous measurements may have missed dissolved trace metal export from estuaries to the coastal ocean, because acidification was used to preserve the soluble metal fraction.

We show that the metal-organic matter interactions in estuarine mixing are more important and complicated than previously shown, in particular, metal interactions with humic acids. Wetlands analogous to our Great Marsh system are the predominant feature of both the East and Gulf coasts of the United States. The decomposition of *S. alterniflora*, the dominant plant species along the entire East and Gulf coast of the United States produces humic acids; thus, humification is enriched during decomposition periods (Filip and Alberts, 1988, 1989). When decomposition is high in the summer and fall, and organic matter concentrations are high, we predict export of metal-organic complexes. When productivity is low in the winter, and there is little organic matter available for complexation, metal removal processes likely dominate in estuarine systems. Thus, seasonal changes in plant growth and decay determine whether estuarine systems show net removal or export of metal-organic complexes. This can be seen by our finding that organic Mn(III)-L complexes increased in concentration from April to October, and were notably higher at the mouth of the river, suggesting export. Our findings in the Broadkill River are likely representative of other similar wetland sites, which dominate the East and Gulf Coasts of the U.S., and indicate that coastal metal removal processes need to be revisited. Metal complexation may be an important factor in not only the export of dissolved metals to the coastal ocean, but also organic

matter, and thus our findings have significant implications for nutrient delivery from the coast to the ocean.

5.6 Acknowledgements

This work was supported by research grants from the chemical oceanography program of the National Science Foundation (OCE-1558738 and OCE-1155385 to GWL). Véronique Oldham thanks University of Delaware for receipt of a Marian R. Okie Fellowship and a University of Delaware Graduate Fellowship. Thanks to Dan MacDonald, Kristin Burk, Kevin Beam and Kristin Yoshimura for sampling assistance.

REFERENCES

Abualhaija, M.M., Whitby, H., and van den Berg, C.M.G. (2015). Competition between copper and iron for humic ligands in estuarine waters. *Mar. Chem*. 172, 46-56.

Alberts, J.J and Filip, Z. (1998). Metal binding in estuarine humic and fulvic acids: FTIR analysis of humic acid-metal complexes. *Environ. Tech.* 19, 923-931.

Altmann, H.J. (1972) Determination of dissolved oxygen in water with Leukoberbelin-Blue I. A quick Winkler method. *Anal. Chem.* 262, 97-99.

Arnold, R.G., Dichristina, R., and Hoffman, M.R. (1988). Reductive dissolution of Fe(III) oxides by Pseudomonas Sp. 200. *Biotech. Bioeng.* 32, 1081-1096.

Batchelli, S., Muller, F.L.L., Chang, K.C., and Lee, C.I., (2010). Evidence for strong but dynamic iron-humic colloidal associations in humic rich coastal waters. *Environ. Sci. Technol.* 44, 8485-8490.

Beck, K.C., Reuter, J.H., and Perdue, E.M. (1974). Organic and inorganic geochemistry of some coastal plain rivers of the southeastern United States. *Geochim. Cosmochim. Acta.* 38, 341-364.

Boyle E. A., Collier, R., Dengler, A.T., Edmond, J.M., Ng, A.C., and Stallard, R.F. (1974). On the chemical mass-balance in estuaries. *Geochim. Cosmochim. Acta.* 38, 1719-1728.

Boyle, E. A., Edmond, J.M., and Sholkovitz, E.R. (1977). The mechanism of iron removal in estuaries. *Geochim. Cosmochim. Acta.* 41, 1313-1324.

Buck, K. N., Lohan, M.C., Berger, C.J.M., and Bruland, K.W. (2007). Dissolved iron speciation in two distinct river plumes and an estuary: implications for riverine iron supply. *Limnol. Oceanogr.* 52, 843-855.

Chester, R. (1990). Marine Geochemistry. London, Unwin Hyman Ltd. 698 pp.

Coonley, L.S., Jr., Naker, E.B., and Holland, H.D., (1971). Iron in the Mullica River and Great Bay, New Jersey. *Chem. Geol.* 7, 51-63.

Dellwig, O., Schnetger, B., Brumsack, H., Grossart, H., and Umlauf, L. (2012). Dissolved reactive manganese at pelagic redoxclines (part II): Hydrodynamic conditions for accumulation. *J. Mar. Syst.* 90, 31-41.

Duckworth O. W., and Sposito, G. (2005). Siderophore-manganese(III) interactions I. Manganite dissolution promoted by desferrioxamine-B. *Environ. Sci. Technol.* 39, 6045-6051

Duckworth, O.W., and Sposito, G. (2007) Siderophore-promoted dissolution of synthetic and biogenic layer type Mn oxides. *Chem. Geol.* 242, 497-508.

Eastman, K.W., and Church, T.M. (1984). Behavior of iron, manganese, phosphate and humic acid during mixing in a Delaware salt marsh creek. *Est. Coast. Shelf Sci.* 18, 447-458.

Filip, Z., and Alberts, J.J., (1988). The release of humic substances from *Spartina alterniflora* (Loisel.) into sea water as influenced by salt marsh indigenous microorganism. *Sci. Total Environ.* 73, 143-157.

Filip, Z., and Alberts, J.J. (1989). Humic substances isolated from *Spartina alterniflora* (Loisel.) following long term decomposition in sea water. *Sci. Total Environ.* 83, 273-285.

Fitzsimmons, J.N., Carrasco, G.G., Wu, J., Roshan, S., Hatta, M., Measures, C.M., Conway, T.M., John, S.G., Boyle, E.A. (2015). Partitioning of dissolved iron and iron isotopes into soluble and colloidal phases along the GA03 GEOTRACES North Atlantic Transect, *Deep Sea Res. Pt. II: Topical Stud. Oceanogr.* 116, 130-151.

Gledhill, M., and van den Berg, C.M.G. (1994). Determination of complexation of iron(III) with natural organic complexing ligands in seawater using cathodic stripping voltammetry. *Mar. Chem.* 47, 41-54.

Graham, W.F., Bender, M.L., and Klinkhammer, G.P. (1976). Manganese in Narragansett Bay. *Limnol. Oceanogr.* 21, 65-73.

Grassian, V. (2005). Environmental Catalysis. CRC Press, pp 64-76.

Hedges, J.I., Keil, R.G., Benner, R. (1997). What happens to terrestrial organic matter in the ocean? *Org Geochem.* 27, 195-212.

Lamar, W.L., (1968). Evaluation of color and iron in natural surface waters. *U.S. Geol. Survey. Prof. Paper 600-D.* D24-D29.

Luther, III, G. W. 2010. The role of one and two electron transfer reactions in forming thermodynamically unstable intermediates as barriers in multi-electron redox reactions. *Aqu.Geochem.*16, 395-420.

Luther, III G. W., Findlay, A.J., MacDonald, D. J., Owings, S. M., Hanson, T. E., Beinart, R. A., Girguis, P. R. (2011). Thermodynamics and Kinetics of sulfide oxidation by oxygen: a look at inorganically controlled reactions and biologically mediated processes in the environment. *Front. Microbiol.* 62, 1-9.

Luther, G.W. III, Madison, A.S., Mucci, A., Sundby, B., and Oldham, V. E. (2015). A kinetic approach to assess the strengths of ligands bound to soluble Mn(III). *Mar. Chem.* 173, 93-99.

Madison, A.S., Tebo, B.M., Luther, G.W. (2011) Simultaneous determination of soluble manganese(III), manganese(II) and total manganese in natural (pore)waters. *Talanta.* 84, 374-381.

Madison, A. S., Tebo, B.M., Mucci, A., Sundby, B., and Luther, III, G.W. (2013). Abundant porewater Mn(III) is a major component of the sedimentary redox system. *Science*. 341, 875-878.

Mantoura, R.F.C., Dickson A., and Riley, J.P. (1978). The complexation of metals with humic materials in natural waters. *Est. Coast. Mar. Sci*. 6, 387-408.

Moore, R. M., Burton, J. D., Williams, J. B. and Young, M. L. (1979). The behavior of dissolved organic material, iron, and manganese in estuarine mixing. *Geochim. Cosmochim. Acta.* 43, 919-926.

Morel, F.M.M. and Hering, J.G. (1993). Principles and Applications of Aquatic Chemistry, Wiley, New York.

Nealson, K.H., and Myers, C.R. (1992). Microbial reduction of manganese and iron: New approaches to carbon cycling. *Appl. Environ. Microbiol.* 58, 439 – 443.

Oldham, V.E., Owings, S. M., Jones, M., Tebo, B.M., and Luther, G.W. 2015. Evidence for the presence of strong Mn(III)-binding ligands in the water column of the Chesapeake Bay. *Mar. Chem.* 171, 58-66.

Oldham, V.E., Mucci, A., Tebo, B.M., Luther, G.W. (2017). Soluble Mn(III)-L complexes are abundant in oxygenated waters and stabilized by humic ligands. *Geochim. Cosmochim. Acta.* 199, 238-246.

Parker D.L., Sposito G. and Tebo B.M. (2004) Manganese(III) Binding to a Pyoverdine Siderophore Produced by a manganese(II)-Oxidizing Bacterium. *Geochim. Cosmochim. Acta.* 68, 4809-4820.

Parker D.L., Takami M., Mylene L., Mozafarzadeh R.V., McCarthy J.K. and Tebo B.M. (2007) Inter-Relationships of MnO2 Precipitation, siderophore–Mn(III) Complex Formation, Siderophore Degradation, and Iron Limitation in Mn(II)-Oxidizing Bacterial Cultures. *Geochim. Cosmochim. Acta.* 71, 5672-83.

Perez-Benito, J.F., Arias, C., and Amat, E. (1996). A kinetic study of the reduction of colloidal manganese dioxide by oxalic acid. *J. Coll. Interface Sci.* 177, 288-297.

Rijkenberg, M.J.A., Gerringa, L.J.A., Velzeboer, I., Timmermans, K.R., Buma, A.G.J., and de Baar, H.J.W. (2006). Iron-binding ligands in Dutch estuaries are not affected by UV induced photochemical degradation. *Mar. Chem*. 100, 11-23.

Rodríguez, F.J., Schlenger, P., and García-Valverde, M. (2016). Monitoring changes in the structure and properties of humic substances following ozonation using UV–Vis, FTIR and 1H NMR techniques. *Sci.Tot. Environ.* 541, 623-637.

Rose, A.L. and Waite, D.T. (2003). Kinetics of iron complexation by dissolved natural organic matter in coastal waters. *Mar. Chem.* 84, 85-103.

Sander, S.G., Buck, K.N., and Wells, M. (2015). The effect of natural organic ligands on trace metal speciation in San Francisco Bay: implications for water quality. *Mar. Chem.* 173, 269-281.

Sever, M.J., and Wilker, J.J. (2004). Visible absorption spectra of metal-catecholate and metal-tironate complexes. *Daltron Trans.* 1061-1072.

Sholkovitz, E.E., (1976). Flocculation of dissolved organic and inorganic matter during the mixing of river water and seawater. *Geochim. Cosmochim. Acta.* 40, 831-845.

Sholkovitz, E.E. (1978). The flocculation of dissolved Fe, Mn, Al, Cu, Ni, Co and Cd during estuarine mixing. *Sci. Lett.* 41, 77-86.

Siebecker, M. G., Madison, A. S. and Luther, G. W. (2015). Reduction Kinetics of Polymeric (Soluble) Manganese (IV) Oxide (MnO_2) by Ferrous Iron (Fe^{2+}). *Aqu. Geochem.* 21, 143–158.

Stone, A. T., and Morgan, J.J. (1984). Reduction and dissolution of manganese (III) and manganese (IV) oxides by organics: Survey of the reactivity of organics. *Environ. Sci. Technol.* 18, 617-624.

Stookey, L. L. (1970). Ferrozine. A new spectrophotometric reagent for iron. *Anal. Chem.* 42, 770-781.

Stumpf, R.P. (1983). The process of sedimentation on the surface of a salt marsh. *Estuar. Coast. Shelf Sci*. 17, 495-508.

Stumm, W. and Morgan, J.J. (1996). Aquatic Chemistry. Wiley-Interscience, New York: 1022 pp.

Sunda, W.G., Huntsman, S.A., and Harvey, G.R. (1983). Photoreduction of manganese oxides in seawater and its geochemical and biological implications. *Nature.* 301, 234-237.

Sunda, W.G., and Kieber, D.J. (1994). Oxidation of humic substances by manganese oxides yields low-molecular-weight organic substrates. *Nature.* 367, 61-63.

Tebo, B.M., Bargar, J.R., Clement, B.G., Dick, G.J., Murray, K.J., Parker, D., Verity, R., and Webb. S.M. (2004). Biogenic Manganese Oxides: Properties and mechanisms of formation. *Annu. Rev. Planet. Sci.* 33, 287-328.

Trouwborst, R. E., Clement, B. G., Tebo, B. M., Glazer, B. T., and Luther, G. W. (2006). Soluble Mn(III) in suboxic zones. *Science.* 313, 1955-1957.

van den Berg, C.M.G. (1995) Evidence for organic complexation of iron in seawater. *Mar. Chem.* 50, 139-157.

Waite, D., Wrigley, I.C. and Szymczak, R. (1988). Photoassisted dissolution of a colloidal manganese oxide in the presence of fulvic acid. *Environ. Sci. Technol.* 22, 778-785.

Weber, K.A., Achenbach, L.A., and Coates, J.D. (2006). Microorganisms pumping iron: anaerobic microbial iron oxidation and reduction. *Nat. Rev. Microbiol*. 4, 752 - 764.

Windom, H., Beck K.C., and Smith, R. (1971). Southeast. Geol. 1109-1181.

Yakushev,E., Pakhomova, S., Sørenson, K., and Skei, J. (2009). Importance of the different manganese species in the formation of water column redox zones: Observations and modeling. *Mar. Chem.* 117, 59-70.

Yakushev, E.V., F. Pollehne, G. Jost, I. Kuznetsov, B. Schneider and L. Umlauf. (2007). Analysis of the water column oxic/anoxic interface in the Black and Baltic seas with a numerical model. *Mar. Chem.* 107, 388-410.

Zinder, B., Furrer, G., and Stumm, W. (1986). The coordination chemistry of weathering: Dissolution of Fe(III) oxides. *Geochim. Cosmochim. Acta.* 50, 1861-1869.

Xu Y., and Schoonen M.A.A. (2000) The absolute energy positions of conduction and valence bands of selected semiconducting minerals. *Am. Mineralog.* 85, 543–556.

Chapter 6

CONCLUDING REMARKS AND FUTURE DIRECTIONS

Soluble Mn(III) species have been detected in several suboxic marine environments (Trouwborst et al., 2006; Yakushev et al., 2009; Dellwig et al., 2012; Madison et al., 2013), and in this work, Mn(III) was detected in sulfidic waters and oxic waters. Thus, it is likely that soluble Mn(III) is ubiquitous in the marine environment. This dissertation describes the distribution of Mn(III)-L complexes in three distinct systems: the Chesapeake Bay- a seasonally anoxic basin; the St. Lawrence Estuary – a hemipelagic system with hypoxia developing in its bottom waters, and a fjord; as well as the Broadkill River – a tributary to the Delaware Bay bordered by a salt marsh. In each system, the objective was to describe Mn(III)-L formation and removal pathways and to shed light on the biogeochemical implications of Mn(III)-L. The results presented in this dissertation provide evidence for diverse formation pathways for Mn(III)-L complexes based on: (1) the concentration and nature of ambient ligands; (2) the oxygen content and gradient; and (3) the presence of reducing agents.

In the sections below, I highlight the major results and conclusions from this dissertation and indicate several areas for potential future research on dissolved Mn(III) in seawater. Given the rapid pace human-induced global climate change, it is important to provide a baseline for the state of Mn speciation in the global ocean. In particular, the distribution and speciation of Mn affects not only Mn bioavailability, but also the cycles and bioavailability of other essential nutrients. Thus, a complete understanding of Mn

cycling is essential for our understanding of changing primary productivity in the global ocean.

6.1 The impact of manganese speciation on iron bioavailability

Luther et al (2015) demonstrated that the thermodynamic conditional formation constants of Mn(III)-L and Fe(III)-L (uncorrected for side reaction coefficients) are similar in organic matter decomposition zones. In Chapter 2, I addressed the stability of several known Mn(III)-L complexes, and compared them to the strong ligands in the anoxic bottom waters of the Chesapeake Bay. The complexes stabilized in the Chesapeake Bay were found to be stronger ($\log K_{cond}$>13.2) than known laboratory Mn(III)-L complexes, such as desferrioxamine-B ($\log K_{cond}$<13.2). Known Mn(III)-L complexes have been shown to have similar (or larger) thermodynamic stability constants (K_{therm}) as the same Fe(III)-L complexes (Harrington et al., 2012). Therefore, it is likely that in most marine systems, Mn(III) and Fe(III) will compete for the same ambient ligands.

Competition between Fe(III) and Mn(III) for the same ligands is important in the context of oceanic primary productivity. Like Mn, Fe is a necessary nutrient for phytoplankton growth, and many other biological processes; but unlike Mn, Fe is the limiting nutrient in large regions of the global ocean. Phytoplankton make up the base of the marine food web and are principle drivers in the global carbon cycling and play a crucial role in the mediation of human-induced global climate change (Martin, 1990). The primary source of Fe to the ocean is dust deposition, and ~30% of the global ocean does not receive significant dust inputs, resulting in extremely low concentrations of Fe (Moore et al., 2013). The concentration of Fe is so low in these regions that phytoplankton productivity is limited and the regions are known as high nitrate-low

chlorophyll (HNLC) waters. It has been argued that Fe is the most limiting nutrient in the ocean due to its critical role in phytoplankton growth processes, but also due to the decreasing abundance of Fe as a result of oxygenic photosynthesis over geological timescales (Sunda and Huntsman, 2015). Sunda and Huntsman (2015) also argue that on shorter timescales, Fe will not only be limiting in HNLC regions of the ocean, but also in the deep chlorophyll maximum (DCM; usually near the base of the photic zone, > 50 m) of thermally stratified regions of the ocean such as subtropical mid-ocean gyres that occupy most of the remaining ~70 % of non-HNLC oceanic waters. The DCM of many regions is predicted to increase in size with increased temperatures, and Sunda and Huntsman (2015) point out that by affecting the community structure of phytoplankton in these regions, Fe will have a significant impact on primary productivity.

Organic complexation enhances Fe(III) solubility in seawater, as in the absence of complexation, Fe(III) hydrolyzes and precipitates rapidly. Some phytoplankton are adapted to low-Fe regions of the ocean via the production of unknown organic ligands to increase the bioavailable Fe pool (Maldonado and Price, 2001). Thus, if Mn(III) binds the organic ligands intended for Fe(III) the uptake, Fe(III) uptake may be inhibited, which may decrease oceanic primary productivity.

The results from this dissertation raise several questions with respect to Mn(III)-binding ligands, and the competition between Mn(III) and Fe(III) for the same ligands: What is the composition and reactivity of these organic ligands? Can organisms produce ligands specific to Fe(III) that do not bind Mn(III)? Can organisms respond to [Mn(III)]>>[Fe(III)]?

We know little on the speciation of Fe in ambient seawater and even less on the speciation of Mn. Moreover, the complexation of Fe(II) and Mn(II) by organic ligands has yet to be ruled out. Sensitive methods to discern the redox state of metal complexes, as well as their size and reactivity, need to be developed. In particular, the nature of the unknown ligands in seawater needs to be investigated. The work from this dissertation, on the precipitation of Mn with humic material, may provide a starting point for assays on humic-type ligands. If the precipitate is isolated, its composition could be determined via HPLC methods, to tell about the humic-type ligands that bind Mn(III) in coastal systems.

Experiments with Mn(III) and Fe(III) competing for the same biologically-produced ligands have not yet been conducted. Such experiments would be useful in monitoring the speciation of each respective metal, and on the growth of specific organisms known to produce ligands in response to Fe-stress. It would also be useful to enrich naturally Fe-limited samples with Mn(III) [as a weak Mn(III)-L complex, since adding Mn(III) hexaaquo is not trivial (Luther et al, 2015)], especially since Mn is known to replace Fe in some enzymes. This would serve to indicate whether increased levels of Mn(III) have an impact on already Fe-limited systems.

6.2 The Influence of Changing Oxygen Content of Seawater on Manganese Speciation

Under current global climate change conditions, regions of low dissolved oxygen (dO_2) at mid-depths in the ocean (oxygen minimum zones = OMZs) are predicted to increase, resulting in an overall decline in oceanic dO_2 (Stramma et al., 2010). Despite the importance of redox chemistry on trace metal speciation, investigations into the influence of decreasing oceanic dO_2 on marine processes and

studies on trace metal biogeochemistry still appear as isolated disciplines. Given that the reduction potential of the ocean (pε), driven by dO_2 is a master variable in determining which chemical species exist in a given environment, it is surprising that trace metal speciation in the context of OMZ formation has not been given much attention. For the purpose of this discussion, the speciation of Fe and Mn in oxic systems can be simplified by the following unbalanced pathways:

Fe: Fe (hydr)oxides (s) $\leftrightarrow$ Fe(III)-L complexes (aq) $\leftrightarrow$ $Fe(H_2O)_6^{2+}$ (aq)

Mn : Mn oxides (s) $\leftrightarrow$ Mn(III)-L complexes (aq) $\leftrightarrow$ $Mn(H_2O)_6^{2+}$ (aq)

These pathways shift to the left as seawater gets saturated with dO_2 and to the right as dO_2 decreases. In the absence of sulfide, decreasing dO_2 serves to increase the solubility of Fe and Mn mineral oxide phases, which consequently solubilizes other metals, trapped within their metal lattices.

In Chapters 2, 3 and 4, I characterized the speciation of Mn in different dO_2 regimes. Based on the findings in Chapter 4, I concluded that lower dO_2 in the bottom waters of the St. Lawrence was likely contributing to higher total dissolved Mn (dMn_T) concentrations in 2014 than in 1974. In particular, up to 86 % of this dMn_T was stabilized as Mn(III)-L complexes, indicating that lower dO_2 regimes may provide more formation pathways for Mn(III)-L complexes. Chapters 2 and 3 indicated that Mn(III)-L complexes were stable in the absence of detectable oxygen. Chapter 2 focused on the anoxic waters of the Chesapeake Bay and indicated that Mn(III)-L complexes could be stabilized in the absence of detectable dO_2, and that these complexes were kinetically stabilized against reduction by H_2S. Given these findings, it is likely that in OMZs such as the Arabian Sea and the eastern Equatorial Pacific Ocean, Mn(III)-L complexes should be stable if Mn(III)-binding ligands are present.

For future work, simple laboratory experiments that aim to trap Mn(III)-L during incubations of known microbial Mn oxidizers and reducers would be useful in evaluating the rates of these processes in changing dO_2 regimes, and in the presence or absence of H_2S. The information gained in these laboratory studies could be applied to predicted changes in oceanic dO_2 levels and used to determine the corresponding change in metal speciation. It would also be useful to produce a time-course of Mn speciation in a system like the Chesapeake Bay, over a full seasonal cycle. This could lend insight into how Mn speciation changes in natural systems as dO_2 decreases.

6.3 Rethinking terrestrial inputs of dissolved metals

Chapter 5 of this dissertation examined the impact of estuarine mixing on the speciation of Mn and Fe in the Broadkill River, a tributary to the Delaware Bay. I showed that soluble Mn and Fe were not completely removed during estuarine mixing, as previously thought. Instead, due to organic complexation, soluble Mn and Fe were seasonally exported in the late summer and fall. In particular, soluble Mn(III) export and complexation was much more pronounced than for Fe(III), indicating that the ligands in the Broadkill River may complex Mn(III) more strongly than Fe(III). The complexation arises predominantly due to the influx of organic exudates during the degradation of plant material in the late summer and fall. Some of the Mn complexation in the St. Lawrence Estuary and Broadkill River was shown to be humic. Given that many previous soluble metal assays involved an acidification step for sample preservation, and that humic material precipitates at pH<2 (Chapter 4), it is likely that a significant fraction of soluble metals remains unaccounted for in coastal systems where humic concentrations are high. In particular, seasonal export of many metals is possible, given that organic metal complexation is not exclusive to Mn and Fe.

Coastal transport of dissolved metals to the open ocean was considered to be a well-understood process, but may in fact be more complicated than previously thought. It is important to provide a baseline of metal transport from the terrestrial systems in estuaries, then to the coastal and the open ocean, particularly in light of human-induced global climate change. Many aspects of oceanic chemistry in coastal systems are predicted to change, including increased surface temperatures and vertical stratification, decreased oxygen content, sea level rise and changing circulation patterns – to name a few. In particular, the predicted increase in sea level rise and changing circulation patterns may lead to greater terrestrial inputs due to a greater surface area of seawater in contact with wetland sediments, which could lead to further intensification of coastal oxygen minimum zones due to increased primary productivity.

Klinkhammer et al (2009) examined increased dissolved terrestrial inputs to the coastal ocean during the last deglaciation, as a result of sea-level rise. Because Mn has a high crustal abundance and a short residence time in seawater (~50 years), it can be used as a sensitive tracer of terrestrial inputs to the ocean, by looking at the Mn/Ca ratios of planktonic and benthic foraminiferal calcite. Using Mn/Ca ratios, Klinkhammer et al (2009) observed that terrestrial inputs were ~1.5 times higher than they are today during the last deglaciation due to sea-level rise. These results were interpreted to mean greater productivity during this time, because enhanced terrestrial input of Mn means enhanced inputs of other important terrestrially derived nutrients like Fe; and indeed, this is consistent with widespread observations of increased denitrification during the interglacial period (e.g. Robinson et al, 2007). This process may be mimicked today on a much shorter timescale due to human-induced sea-level rise. Because increased productivity leads to intensification of oceanic OMZs, enhanced

terrestrial input of dissolved metals due to sea-level rise may act as a negative feedback mechanism: higher sea level will lead to greater fluxes of dissolved metals, which will enhance primary productivity, consequently expanding ocean OMZs. Moreover, decreasing dissolved oxygen content of seawater will act to solubilize many trace elements including Fe and Mn, leading to greater primary productivity, further expanding oceanic OMZs. To understand the extent of this possible scenario, it is imperative to obtain current "baseline" or near-baseline fluxes of metals from coastal systems to the global ocean, and to assess how these fluxes will change in in response to varying levels of dO_2.

6.4 The Role of Mn(III) in the Redox Cycles of Other Elements

Throughout this dissertation, a principle role of soluble Mn(III) in seawater has been as a redox active species in the coupled cycling of many other elements. In particular, I examined the relationship of Mn with sulfur as sulfide (H_2S), dissolved oxygen (dO_2), carbon in the form of organic ligands and humic material, and iron (Fe).

In Chapter 2, I discussed the kinetic stability of natural strong Mn(III)-L complexes against reduction with H_2S in the anoxic bottom waters of the Chesapeake Bay. I also show that Mn(III)-DFOB can be stabilized in the presence of equimolar H_2S in the laboratory. Thus, Mn(III)-L may play an important role in anoxic systems as an electron acceptor where other electron acceptors like oxygen and MnO_x are not present.

In Chapter 3, I discussed the oxidation of Mn(II) to Mn(III)-L and MnO_x in the suboxic zone of the Chesapeake Bay at non-detectable dissolved oxygen (dO_2) levels. Given a predicted decrease in oceanic dO_2, it would be useful to discern the limiting concentration of dO_2 at which Mn-oxidizing bacteria are capable of oxidizing Mn, and whether this oxidation process derives energy or breaks down organic matter. This

could be achieved with simple incubations of known Mn-oxidizers at set dO_2 conditions with Mn(II) and Mn(III)-L additions as well as diverse organic carbon sources. It would also be useful to measure Mn oxidation rates over the course of a seasonal cycle of anoxia in a system like the Chesapeake Bay.

Chapter 5 examined potential reactions between dissolved Mn and Fe in the Broadkill River, DE. I proposed that the Mn(III)-L complexes in the Broadkill River were stabilized against reduction by excess dissolved Fe(II) because Fe(II) was complexed, and thus sterically hindered against oxidation. In addition, I observed that soluble Fe was removed more readily during estuarine mixing than dissolved Mn. This is because reaction of $Fe(H_2O)_6^{2+}$ with O_2 to form Fe oxides is at least 10^6 times faster than $Mn(H_2O)_6^{2+}$ with oxygen (Grassian, 2005); thus, Fe solids precipitate more rapidly than Mn solids. Another important finding in Chapters 4 and 5 was that the dissolved Mn was non-colloidal (< 20 nm), unlike many "dissolved" Fe species, which can be up to 90 % colloidal (size fraction between 20 and 200 nm; Shlosser et al., 2009). Therefore, aggregation processes may be less important for Mn than for Fe.

There are many coupled cycles of Mn with other biologically relevant elements aside from the coupled cycles of Mn described in this dissertation. These include Mn reactivity with nitrogen (N), chromium (Cr), cobalt (Co), and zinc (Zn), to name a few. The importance of Mn(III)-L in the context of Mn cycling with these other elements warrants further study. For example, the reactions of many Mn species with N species are thermodynamically favorable (Luther et al, 1997), including the oxidation of NH_3 and organic-N to N_2 in sediments by MnO_2 in the presence of O_2. This effectively would sidestep the traditional nitrification/denitrification process in the nitrogen cycle and could explain the formation of N_2 in oxic sediments (Luther et al, 1997). Hulth et al

(1999) also investigated coupled nitrification and manganese reduction, showing that NO_3^- can be produced during Mn oxide reduction in anoxic sediments. The coupling of the Mn and N cycles was also suggested by Tebo et al (1991), who proposed that Mn(II) oxidation by bacteria in the Black Sea may be mediated by NO_3^-. However, these studies do not account for intermediate Mn(III)-L species, and have not been directly studied in seawater.

6.5 Final Thoughts

The work in this dissertation expands our knowledge of the widespread environmental occurrence of soluble Mn(III), and the importance of abiotic and biotic Mn redox cycling for the cycling of carbon, as well as the fate of nutrients. However, there is a paucity in knowledge regarding the mechanisms and pathways of electron transfer from Mn(II) $\leftrightarrow$Mn(III) $\leftrightarrow$Mn(IV). This dissertation lends insight into the potential mechanisms of Mn(III)-L formation as an intermediate in oxidative and reductive pathways. These pathways can be microbially or chemically mediated, but the rates and magnitudes of these pathways are still unknown. In particular, these pathways are undoubtedly occurring concurrently and at different rates in diverse systems and in changing oceanic conditions. Thus, understanding the relative magnitude and importance of each mechanism in seawater is not trivial.

One clear, current challenge is to discern abiotic from microbially-mediated Mn redox cycling. Future experimental design should emphasize not only sterile treatments as a control, but also the potential for microbial products to participate in abiotic reactions. For example, the biotic formation of H_2S followed by the abiotic reduction of MnO_2.

Field sampling of different redox species concurrently is also crucial in understanding redox processes of a given system. For example, studies examining Mn speciation, Fe speciation and reactive oxygen species in surface waters at one site would provide much more insight than studies examining one of these three things and many sites - which finally, emphasizes the importance of process oriented field studies. Given the heterogeneity of metal-organic interactions in seawater, process-based approaches are imperative because studies examining only elemental distributions cannot tell about reactivity and therefore they cannot truly tell about biogeochemical changes in a changing ocean.

REFERENCES

Dellwig O., Schnetger B., Brumsack H., Grossart H. and Umlauf L. (2012) Dissolved reactive manganese at pelagic redoxclines (part II): Hydrodynamic conditions for accumulation. *J. Mar. Syst.* 90, 31-41.

Grassian, V. (2005). Environmental Catalysis. CRC Press, pp.64-76.

Harrington,J. M., Parker, D. L., Bargar, J. R., Jarzecki, A. A., Tebo, B. M., Sposito, G., and Duckworth, O. W. (2012). Structural dependence of Mn complexation by siderophores: Donor group dependence on complex stability and reactivity. *Geochim. Cosmochim. Acta* 88, 106-119.

Hulth,S., Aller, R.C., Gilbert, F. (1999). Coupled anoxic nitrification/manganese reduction in marine sediments. *Geochim. Cosmochim. Acta*. 63, 49-66.

Klinkhammer, G. P., Mix, A. C. and Haley, B. A. (2009). Increased dissolved terrestrial input to the coastal ocean during the last deglaciation, *Geochem. Geophys. Geosyst.* 10, 1-11.

Luther, G. W., Sundby, B., Lewis, B. L., Brendel, P., J., and Silverberg, N. (1997).Interactions of manganese with the nitrogen cycle: alternative pathways to dinitrogen. *Geochim. Cosmochim. Acta.* 61, 4043–4052

Luther, G.W. III, Madison, A.S., Mucci, A., Sundby, B., and Oldham, V.E. (2015). A kinetic approach to assess the strengths of ligands bound to soluble Mn(III). *Mar. Chem.* 173, 93-99.

Madison, A.S., Tebo, B.M., Mucci, A., Sundby, B., and Luther, G.W. (2013). Abundant porewater Mn(III) is a major component of the sedimentary redox system. *Science*. 341, 875-878.

Maldonado, M.T., and Price, N.M. (2001). Reduction and transport of organically bound iron by *Thalassiosira oceanica* (Bacillariophyceae). *J Phycol* 37, 298–310.

Martin, J.H.(1990).Glacial-interglacial CO_2 change: the iron hypothesis. *Paleoceanogr.* 5, 1–13.

Moore, C.M., Mills, M.M., Arrigo, K.R., Berman-Frank, I., Bopp, L., Boyd, P.W., et al.(2013). Processes and patterns of oceanic nutrient limitation. *Nat. Geosci.* 6, 701–710.

Robinson, R. S., Mix, A. and Martinez, P. (2007), Southern Ocean control on the extent of denitrification in the southeast Pacific over the last 70 ka. *Quat. Sci. Rev*. 26, 201–212.

Schlosser C., Streu P. and Croot P.L. (2013) Vivaspin ultrafiltration: A new approach for high resolution measurements of colloidal and soluble iron species. *Limnol. Oceanog. Methods.* 11, 187-201.

Stramma, L., Schmidtko S., Levin, L.A., and Johnson, G.C., (2010). Ocean oxygen minima expansions and their biological impacts. *Deep-Sea Res. I*, 57, 587-595.

Sunda, W.G., and Huntsman, S.A. (2015). High iron requirement for growth, photosynthesis, and low-light acclimation in the coastal cyanobacterium *Synechococcus bacillaris*. *Frontiers microbial*. 6, 1-13.

Trouwborst, R.E., Clement, B.G., Tebo, B.M., Glazer, B.T. and Luther, G.W. (2006). Soluble Mn(III) in suboxic zones. *Science.* 313, 1955-7.

Yakushev, E., Pakhomova, S., Sørenson, K., and Skei, J. (2009). Importance of the different manganese species in the formation of water column redox zones: Observations and modeling. *Mar. Chem.* 117, 59-70.

Appendix

PERMISSIONS

ELSEVIER LICENSE

TERMS AND CONDITIONS

Feb 22, 2017

This Agreement between Veronique E Oldham ("You") and Elsevier ("Elsevier") consists of your license details and the terms and conditions provided by Elsevier and Copyright Clearance Center.

License Number: 4054320076289

License date

Licensed Content Publisher: Elsevier

Licensed Content Publication: Marine Chemistry

Licensed Content Title: Evidence for the presence of strong Mn(III)-binding ligands in the water column of the Chesapeake Bay

Licensed Content Author: Véronique E. Oldham, Shannon M. Owings, Matthew R. Jones, Bradley M. Tebo, George W. Luther

Licensed Content Date: 20 April 2015

Licensed Content Volume: 171

Licensed Content Issue: n/a

Licensed Content Pages : 9

Start Page: 58

End Page: 66

Type of Use: reuse in a thesis/dissertation

Portion: full article

Format: electronic

Are you the author of this Elsevier article?

Yes

Will you be translating?

No

Order reference number

Title of your thesis/dissertation

THE COMPLEXATION CHEMISTRY OF DISSOLVED MANGANESE(III) IN THE OCEAN AND ITS ROLE IN THE COUPLED CYCLES OF CARBON, IRON AND SULFUR

Expected completion date: May 2017

Estimated size (number of pages): 210

Elsevier VAT number

GB 494 6272 12

Requestor Location

Veronique E Oldham

16044-2 Bowman Drive

LEWES, DE 19958

United States

Attn: Veronique E Oldham

Publisher Tax ID

98-0397604

Total

0.00 USD

Terms and Conditions

INTRODUCTION

1. The publisher for this copyrighted material is Elsevier. By clicking "accept" in connection with completing this licensing transaction, you agree that the following terms and conditions apply to this transaction (along with the Billing and Payment terms and conditions established by Copyright Clearance Center, Inc. ("CCC"), at the time that you opened your Rightslink account and that are available at any time at http://myaccount.copyright.com).

GENERAL TERMS

2. Elsevier hereby grants you permission to reproduce the aforementioned material subject to the terms and conditions indicated.

3. Acknowledgement: If any part of the material to be used (for example, figures) has appeared in our publication with credit or acknowledgement to another source, permission must also be sought from that source. If such permission is not obtained then that material may not be included in your publication/copies. Suitable acknowledgement to the source must be made, either as a footnote or in a reference list at the end of your publication, as follows:

"Reprinted from Publication title, Vol /edition number, Author(s), Title of article / title of chapter, Pages No., Copyright (Year), with permission from Elsevier [OR APPLICABLE SOCIETY COPYRIGHT OWNER]." Also Lancet special credit -

"Reprinted from The Lancet, Vol. number, Author(s), Title of article, Pages No., Copyright (Year), with permission from Elsevier."

4. Reproduction of this material is confined to the purpose and/or media for which permission is hereby given.

5. Altering/Modifying Material: Not Permitted. However figures and illustrations may be altered/adapted minimally to serve your work. Any other abbreviations, additions, deletions and/or any other alterations shall be made only with prior written authorization of Elsevier Ltd. (Please contact Elsevier at permissions@elsevier.com). No modifications can be made to any Lancet figures/tables and they must be reproduced in full.

6. If the permission fee for the requested use of our material is waived in this instance, please be advised that your future requests for Elsevier materials may attract a fee.

7. Reservation of Rights: Publisher reserves all rights not specifically granted in the combination of (i) the license details provided by you and accepted in the course of this licensing transaction, (ii) these terms and conditions and (iii) CCC's Billing and Payment terms and conditions.

8. License Contingent Upon Payment: While you may exercise the rights licensed immediately upon issuance of the license at the end of the licensing process for the transaction, provided that you have disclosed complete and accurate details of your proposed use, no license is finally effective unless and until full payment is received from you (either by publisher or by CCC) as provided in CCC's Billing and Payment terms and conditions. If full payment is not received on a timely basis, then any license preliminarily granted shall be deemed automatically revoked and shall be void as if

never granted. Further, in the event that you breach any of these terms and conditions or any of CCC's Billing and Payment terms and conditions, the license is automatically revoked and shall be void as if never granted. Use of materials as described in a revoked license, as well as any use of the materials beyond the scope of an unrevoked license, may constitute copyright infringement and publisher reserves the right to take any and all action to protect its copyright in the materials.

9. Warranties: Publisher makes no representations or warranties with respect to the licensed material.

10. Indemnity: You hereby indemnify and agree to hold harmless publisher and CCC, and their respective officers, directors, employees and agents, from and against any and all claims arising out of your use of the licensed material other than as specifically authorized pursuant to this license.

11. No Transfer of License: This license is personal to you and may not be sublicensed, assigned, or transferred by you to any other person without publisher's written permission.

12. No Amendment Except in Writing: This license may not be amended except in a writing signed by both parties (or, in the case of publisher, by CCC on publisher's behalf).

13. Objection to Contrary Terms: Publisher hereby objects to any terms contained in any purchase order, acknowledgment, check endorsement or other writing prepared by you, which terms are inconsistent with these terms and conditions or CCC's Billing and Payment terms and conditions. These terms and conditions, together with CCC's Billing and Payment terms and conditions (which are incorporated herein), comprise the entire agreement between you and publisher (and CCC) concerning this

licensing transaction. In the event of any conflict between your obligations established by these terms and conditions and those established by CCC's Billing and Payment terms and conditions, these terms and conditions shall control.

14. Revocation: Elsevier or Copyright Clearance Center may deny the permissions described in this License at their sole discretion, for any reason or no reason, with a full refund payable to you. Notice of such denial will be made using the contact information provided by you. Failure to receive such notice will not alter or invalidate the denial. In no event will Elsevier or Copyright Clearance Center be responsible or liable for any costs, expenses or damage incurred by you as a result of a denial of your permission request, other than a refund of the amount(s) paid by you to Elsevier and/or Copyright Clearance Center for denied permissions.

LIMITED LICENSE

The following terms and conditions apply only to specific license types:

15. Translation: This permission is granted for non-exclusive world English rights only unless your license was granted for translation rights. If you licensed translation rights you may only translate this content into the languages you requested. A professional translator must perform all translations and reproduce the content word for word preserving the integrity of the article.

16. Posting licensed content on any Website: The following terms and conditions apply as follows: Licensing material from an Elsevier journal: All content posted to the web site must maintain the copyright information line on the bottom of each image; A hyper-text must be included to the Homepage of the journal from which you are licensing at http://www.sciencedirect.com/science/journal/xxxxx or the Elsevier homepage for books at http://www.elsevier.com; Central Storage: This license does not

include permission for a scanned version of the material to be stored in a central repository such as that provided by Heron/XanEdu.

Licensing material from an Elsevier book: A hyper-text link must be included to the Elsevier homepage at http://www.elsevier.com . All content posted to the web site must maintain the copyright information line on the bottom of each image.

Posting licensed content on Electronic reserve: In addition to the above the following clauses are applicable: The web site must be password-protected and made available only to bona fide students registered on a relevant course. This permission is granted for 1 year only. You may obtain a new license for future website posting.

17. For journal authors: the following clauses are applicable in addition to the above:

Preprints:

A preprint is an author's own write-up of research results and analysis, it has not been peer-reviewed, nor has it had any other value added to it by a publisher (such as formatting, copyright, technical enhancement etc.).

Authors can share their preprints anywhere at any time. Preprints should not be added to or enhanced in any way in order to appear more like, or to substitute for, the final versions of articles however authors can update their preprints on arXiv or RePEc with their Accepted Author Manuscript (see below).

If accepted for publication, we encourage authors to link from the preprint to their formal publication via its DOI. Millions of researchers have access to the formal publications on ScienceDirect, and so links will help users to find, access, cite and use the best available version. Please note that Cell Press, The Lancet and some society-

owned have different preprint policies. Information on these policies is available on the journal homepage.

Accepted Author Manuscripts: An accepted author manuscript is the manuscript of an article that has been accepted for publication and which typically includes author-incorporated changes suggested during submission, peer review and editor-author communications.

Authors can share their accepted author manuscript:

- immediately

via their non-commercial person homepage or blog

by updating a preprint in arXiv or RePEc with the accepted manuscript

via their research institute or institutional repository for internal institutional uses or as part of an invitation-only research collaboration work-group

directly by providing copies to their students or to research collaborators for their personal use

for private scholarly sharing as part of an invitation-only work group on commercial sites with which Elsevier has an agreement

- after the embargo period

via non-commercial hosting platforms such as their institutional repository

via commercial sites with which Elsevier has an agreement

In all cases accepted manuscripts should:

- link to the formal publication via its DOI
- bear a CC-BY-NC-ND license - this is easy to do

- if aggregated with other manuscripts, for example in a repository or other site, be shared in alignment with our hosting policy not be added to or enhanced in any way to appear more like, or to substitute for, the published journal article.

Published journal article (JPA): A published journal article (PJA) is the definitive final record of published research that appears or will appear in the journal and embodies all value-adding publishing activities including peer review co-ordination, copy-editing, formatting, (if relevant) pagination and online enrichment.

Policies for sharing publishing journal articles differ for subscription and gold open access articles:

Subscription Articles: If you are an author, please share a link to your article rather than the full-text. Millions of researchers have access to the formal publications on ScienceDirect, and so links will help your users to find, access, cite, and use the best available version.

Theses and dissertations which contain embedded PJAs as part of the formal submission can be posted publicly by the awarding institution with DOI links back to the formal publications on ScienceDirect.

If you are affiliated with a library that subscribes to ScienceDirect you have additional private sharing rights for others' research accessed under that agreement. This includes use for classroom teaching and internal training at the institution (including use in course packs and courseware programs), and inclusion of the article for grant funding purposes.

Gold Open Access Articles: May be shared according to the author-selected end-user license and should contain a CrossMark logo, the end user license, and a DOI link to the formal publication on ScienceDirect.

Please refer to Elsevier's posting policy for further information.

18. For book authors the following clauses are applicable in addition to the above: Authors are permitted to place a brief summary of their work online only. You are not allowed to download and post the published electronic version of your chapter, nor may you scan the printed edition to create an electronic version. Posting to a repository: Authors are permitted to post a summary of their chapter only in their institution's repository.

19. Thesis/Dissertation: If your license is for use in a thesis/dissertation your thesis may be submitted to your institution in either print or electronic form. Should your thesis be published commercially, please reapply for permission. These requirements include permission for the Library and Archives of Canada to supply single copies, on demand, of the complete thesis and include permission for Proquest/UMI to supply single copies, on demand, of the complete thesis. Should your thesis be published commercially, please reapply for permission. Theses and dissertations which contain embedded PJAs as part of the formal submission can be posted publicly by the awarding institution with DOI links back to the formal publications on ScienceDirect.

Elsevier Open Access Terms and Conditions

You can publish open access with Elsevier in hundreds of open access journals or in nearly 2000 established subscription journals that support open access publishing. Permitted third party re-use of these open access articles is defined by the author's choice of Creative Commons user license. See our open access license policy for more information.

credit (with a link to the formal publication through the relevant DOI), provides a link to the license, indicates if changes were made and the licensor is not represented as endorsing the use made of the work. Further, any new works must be made available on the same conditions. The full details of the license are available at http://creativecommons.org/licenses/by-nc-sa/4.0.

CC BY NC ND: The CC BY-NC-ND license allows users to copy and distribute the Article, provided this is not done for commercial purposes and further does not permit distribution of the Article if it is changed or edited in any way, and provided the user gives appropriate credit (with a link to the formal publication through the relevant DOI), provides a link to the license, and that the licensor is not represented as endorsing the use made of the work. The full details of the license are available at http://creativecommons.org/licenses/by-nc-nd/4.0. Any commercial reuse of Open Access articles published with a CC BY NC SA or CC BY NC ND license requires permission from Elsevier and will be subject to a fee.

Commercial reuse includes:

- Associating advertising with the full text of the Article
- Charging fees for document delivery or access
- Article aggregation
- Systematic distribution via e-mail lists or share buttons

Posting or linking by commercial companies for use by customers of those companies.

20. Other Conditions:

v1.9

ELSEVIER LICENSE

TERMS AND CONDITIONS

Feb 22, 2017

This Agreement between Veronique E Oldham ("You") and Elsevier ("Elsevier") consists of your license details and the terms and conditions provided by Elsevier and Copyright Clearance Center.

License Number

4054320370010

License date

Licensed Content Publisher: Elsevier

Licensed Content Publication: Geochimica et Cosmochimica Acta

Licensed Content Title: Soluble Mn(III)–L complexes are abundant in oxygenated waters and stabilized by humic ligands

Licensed Content Author: Véronique E. Oldham, Alfonso Mucci, Bradley M. Tebo, George W. Luther

Licensed Content Date: 15 February 2017

Licensed Content Volume: 199

Licensed Content Issue: n/a

Licensed Content Pages: 9

Start Page: 238

End Page: 246

Type of Use: reuse in a thesis/dissertation

Intended publisher of new work

other

Portion: full article

Format: electronic

Are you the author of this Elsevier article?

Yes

Will you be translating?

No

Order reference number

Title of your thesis/dissertation

THE COMPLEXATION CHEMISTRY OF DISSOLVED MANGANESE(III) IN THE OCEAN AND ITS ROLE IN THE COUPLED CYCLES OF CARBON, IRON AND SULFUR

Expected completion date: May 2017

Estimated size (number of pages): 210

Elsevier VAT number

GB 494 6272 12

Requestor Location

Veronique E Oldham

16044-2 Bowman Drive

LEWES, DE 19958

United States

Attn: Veronique E Oldham

Publisher Tax ID

98-0397604

Total

0.00 USD

Terms and Conditions

INTRODUCTION

1. The publisher for this copyrighted material is Elsevier. By clicking "accept" in connection with completing this licensing transaction, you agree that the following terms and conditions apply to this transaction (along with the Billing and Payment terms and conditions established by Copyright Clearance Center, Inc. ("CCC"), at the time that you opened your Rightslink account and that are available at any time at http://myaccount.copyright.com).

GENERAL TERMS

2. Elsevier hereby grants you permission to reproduce the aforementioned material subject to the terms and conditions indicated.

3. Acknowledgement: If any part of the material to be used (for example, figures) has appeared in our publication with credit or acknowledgement to another source, permission must also be sought from that source. If such permission is not obtained then that material may not be included in your publication/copies. Suitable acknowledgement to the source must be made, either as a footnote or in a reference list at the end of your publication, as follows:

"Reprinted from Publication title, Vol /edition number, Author(s), Title of article / title of chapter, Pages No., Copyright (Year), with permission from Elsevier [OR APPLICABLE SOCIETY COPYRIGHT OWNER]." Also Lancet special credit - "Reprinted from The Lancet, Vol. number, Author(s), Title of article, Pages No., Copyright (Year), with permission from Elsevier."

4. Reproduction of this material is confined to the purpose and/or media for which permission is hereby given.

5. Altering/Modifying Material: Not Permitted. However figures and illustrations may be altered/adapted minimally to serve your work. Any other abbreviations, additions, deletions and/or any other alterations shall be made only with prior written authorization of Elsevier Ltd. (Please contact Elsevier at permissions@elsevier.com). No modifications can be made to any Lancet figures/tables and they must be reproduced in full.

6. If the permission fee for the requested use of our material is waived in this instance, please be advised that your future requests for Elsevier materials may attract a fee.

7. Reservation of Rights: Publisher reserves all rights not specifically granted in the combination of (i) the license details provided by you and accepted in the course of this licensing transaction, (ii) these terms and conditions and (iii) CCC's Billing and Payment terms and conditions.

8. License Contingent Upon Payment: While you may exercise the rights licensed immediately upon issuance of the license at the end of the licensing process for the transaction, provided that you have disclosed complete and accurate details of your proposed use, no license is finally effective unless and until full payment is received from you (either by publisher or by CCC) as provided in CCC's Billing and Payment terms and conditions. If full payment is not received on a timely basis, then any license preliminarily granted shall be deemed automatically revoked and shall be void as if never granted. Further, in the event that you breach any of these terms and conditions or any of CCC's Billing and Payment terms and conditions, the license is automatically

revoked and shall be void as if never granted. Use of materials as described in a revoked license, as well as any use of the materials beyond the scope of an unrevoked license, may constitute copyright infringement and publisher reserves the right to take any and all action to protect its copyright in the materials.

9. Warranties: Publisher makes no representations or warranties with respect to the licensed material.

10. Indemnity: You hereby indemnify and agree to hold harmless publisher and CCC, and their respective officers, directors, employees and agents, from and against any and all claims arising out of your use of the licensed material other than as specifically authorized pursuant to this license.

11. No Transfer of License: This license is personal to you and may not be sublicensed, assigned, or transferred by you to any other person without publisher's written permission.

12. No Amendment Except in Writing: This license may not be amended except in a writing signed by both parties (or, in the case of publisher, by CCC on publisher's behalf).

13. Objection to Contrary Terms: Publisher hereby objects to any terms contained in any purchase order, acknowledgment, check endorsement or other writing prepared by you, which terms are inconsistent with these terms and conditions or CCC's Billing and Payment terms and conditions. These terms and conditions, together with CCC's Billing and Payment terms and conditions (which are incorporated herein), comprise the entire agreement between you and publisher (and CCC) concerning this licensing transaction. In the event of any conflict between your obligations established

by these terms and conditions and those established by CCC's Billing and Payment terms and conditions, these terms and conditions shall control.

14. Revocation: Elsevier or Copyright Clearance Center may deny the permissions described in this License at their sole discretion, for any reason or no reason, with a full refund payable to you. Notice of such denial will be made using the contact information provided by you. Failure to receive such notice will not alter or invalidate the denial. In no event will Elsevier or Copyright Clearance Center be responsible or liable for any costs, expenses or damage incurred by you as a result of a denial of your permission request, other than a refund of the amount(s) paid by you to Elsevier and/or Copyright Clearance Center for denied permissions.

LIMITED LICENSE

The following terms and conditions apply only to specific license types:

15. Translation: This permission is granted for non-exclusive world English rights only unless your license was granted for translation rights. If you licensed translation rights you may only translate this content into the languages you requested. A professional translator must perform all translations and reproduce the content word for word preserving the integrity of the article.

16. Posting licensed content on any Website: The following terms and conditions apply as follows: Licensing material from an Elsevier journal: All content posted to the web site must maintain the copyright information line on the bottom of each image; A hyper-text must be included to the Homepage of the journal from which you are licensing at http://www.sciencedirect.com/science/journal/xxxxx or the Elsevier homepage for books at http://www.elsevier.com; Central Storage: This license does not

include permission for a scanned version of the material to be stored in a central repository such as that provided by Heron/XanEdu.

Licensing material from an Elsevier book: A hyper-text link must be included to the Elsevier homepage at http://www.elsevier.com . All content posted to the web site must maintain the copyright information line on the bottom of each image.

Posting licensed content on Electronic reserve: In addition to the above the following clauses are applicable: The web site must be password-protected and made available only to bona fide students registered on a relevant course. This permission is granted for 1 year only. You may obtain a new license for future website posting.

17. For journal authors: the following clauses are applicable in addition to the above:

Preprints:

A preprint is an author's own write-up of research results and analysis, it has not been peer-reviewed, nor has it had any other value added to it by a publisher (such as formatting, copyright, technical enhancement etc.).

Authors can share their preprints anywhere at any time. Preprints should not be added to or enhanced in any way in order to appear more like, or to substitute for, the final versions of articles however authors can update their preprints on arXiv or RePEc with their Accepted Author Manuscript (see below).

If accepted for publication, we encourage authors to link from the preprint to their formal publication via its DOI. Millions of researchers have access to the formal publications on ScienceDirect, and so links will help users to find, access, cite and use the best available version. Please note that Cell Press, The Lancet and some society-

owned have different preprint policies. Information on these policies is available on the journal homepage.

Accepted Author Manuscripts: An accepted author manuscript is the manuscript of an article that has been accepted for publication and which typically includes author-incorporated changes suggested during submission, peer review and editor-author communications.

Authors can share their accepted author manuscript:

- immediately

via their non-commercial person homepage or blog

by updating a preprint in arXiv or RePEc with the accepted manuscript

via their research institute or institutional repository for internal institutional uses or as part of an invitation-only research collaboration work-group

directly by providing copies to their students or to research collaborators for their personal use

for private scholarly sharing as part of an invitation-only work group on commercial sites with which Elsevier has an agreement

- after the embargo period

via non-commercial hosting platforms such as their institutional repository

via commercial sites with which Elsevier has an agreement

In all cases accepted manuscripts should:

- link to the formal publication via its DOI
- bear a CC-BY-NC-ND license - this is easy to do

- if aggregated with other manuscripts, for example in a repository or other site, be shared in alignment with our hosting policy not be added to or enhanced in any way to appear more like, or to substitute for, the published journal article.

Published journal article (JPA): A published journal article (PJA) is the definitive final record of published research that appears or will appear in the journal and embodies all value-adding publishing activities including peer review co-ordination, copy-editing, formatting, (if relevant) pagination and online enrichment.

Policies for sharing publishing journal articles differ for subscription and gold open access articles:

Subscription Articles: If you are an author, please share a link to your article rather than the full-text. Millions of researchers have access to the formal publications on ScienceDirect, and so links will help your users to find, access, cite, and use the best available version.

Theses and dissertations which contain embedded PJAs as part of the formal submission can be posted publicly by the awarding institution with DOI links back to the formal publications on ScienceDirect.

If you are affiliated with a library that subscribes to ScienceDirect you have additional private sharing rights for others' research accessed under that agreement. This includes use for classroom teaching and internal training at the institution (including use in course packs and courseware programs), and inclusion of the article for grant funding purposes.

Gold Open Access Articles: May be shared according to the author-selected end-user license and should contain a CrossMark logo, the end user license, and a DOI link to the formal publication on ScienceDirect.

Please refer to Elsevier's posting policy for further information.

18. For book authors the following clauses are applicable in addition to the above: Authors are permitted to place a brief summary of their work online only. You are not allowed to download and post the published electronic version of your chapter, nor may you scan the printed edition to create an electronic version. Posting to a repository: Authors are permitted to post a summary of their chapter only in their institution's repository.

19. Thesis/Dissertation: If your license is for use in a thesis/dissertation your thesis may be submitted to your institution in either print or electronic form. Should your thesis be published commercially, please reapply for permission. These requirements include permission for the Library and Archives of Canada to supply single copies, on demand, of the complete thesis and include permission for Proquest/UMI to supply single copies, on demand, of the complete thesis. Should your thesis be published commercially, please reapply for permission. Theses and dissertations which contain embedded PJAs as part of the formal submission can be posted publicly by the awarding institution with DOI links back to the formal publications on ScienceDirect.

Elsevier Open Access Terms and Conditions

You can publish open access with Elsevier in hundreds of open access journals or in nearly 2000 established subscription journals that support open access publishing. Permitted third party re-use of these open access articles is defined by the author's choice of Creative Commons user license. See our open access license policy for more information.

credit (with a link to the formal publication through the relevant DOI), provides a link to the license, indicates if changes were made and the licensor is not represented as endorsing the use made of the work. Further, any new works must be made available on the same conditions. The full details of the license are available at http://creativecommons.org/licenses/by-nc-sa/4.0.

CC BY NC ND: The CC BY-NC-ND license allows users to copy and distribute the Article, provided this is not done for commercial purposes and further does not permit distribution of the Article if it is changed or edited in any way, and provided the user gives appropriate credit (with a link to the formal publication through the relevant DOI), provides a link to the license, and that the licensor is not represented as endorsing the use made of the work. The full details of the license are available at http://creativecommons.org/licenses/by-nc-nd/4.0. Any commercial reuse of Open Access articles published with a CC BY NC SA or CC BY NC ND license requires permission from Elsevier and will be subject to a fee.

Commercial reuse includes:

- Associating advertising with the full text of the Article
- Charging fees for document delivery or access
- Article aggregation
- Systematic distribution via e-mail lists or share buttons

Posting or linking by commercial companies for use by customers of those companies.

20. Other Conditions:

v1.9